2015

Stream microbial communities along an agricultural gradient

Cristine McIntyre Schucker
Eastern Washington University

STREAM MICROBIAL COMMUNITIES ALONG AN AGRICULTURAL GRADIENT

A Thesis

Presented to

Eastern Washington University

Cheney, Washington

In Partial Fulfillment of the Requirements

for the Degree

Master of Science

in

Biology

By

Cristine McIntyre Schucker

Fall 2015

THESIS OF

CRISTINE McINTYRE SCHUCKER

APPROVED BY:

_____	_____
Dr. Camille McNeely, Graduate Study Committee	Date
_____	_____
Dr. Robin L. O'Quinn, Graduate Study Committee	Date
_____	_____
Dr. Andrea Castillo, Graduate Study Committee	Date
_____	_____
Dr. Carmen Nezat, Graduate Study Committee	Date

MASTER'S THESIS

In presenting this thesis in partial fulfillment of the requirements for a master's degree at Eastern Washington University, I agree that the library shall make copies freely available for inspection. I further agree that copying of this project in whole or in part is allowable only for scholarly purposes. It is understood, however, that any copying or publication of this thesis for commercial purposes, or for financial gain, shall not be allowed without my written permission.

Signature _____

Date _____

Abstract

Although sediment microbes play key roles in decomposition and nitrogen (N) cycling, responses of microbial communities to N additions within watersheds is not well understood. Agriculture contributes excess N into stream systems, predominantly as ammonia, which is transformed through nitrification into nitrate by prokaryotes that produce the ammonia monooxygenase enzyme (AMO). The Latah Creek watershed in WA State (USA) drains approximately 1178 km^2, of which half is agricultural. Because the tributary streams reside in forested, agricultural and mixed use drainages, samples from these stream sediments capture microbial communities at different spatial gradients of land use. My research aimed to answer: to what extent does the percentage of agriculture within a drainage affect microbial community compositions?, and more specifically, how does it affect the abundance of nitrifying bacteria? Water and sediment samples were collected from ten locations along the watershed in spring and fall 2012. Two PCR techniques were used on the extracted sediment and pore-water DNA: terminal restriction fragment length polymorphism (T-RFLP) on the small ribosomal subunit *16S rRNA* assessed microbial diversity; and quantitative PCR (qPCR) on *amoA*, a subunit of the nitrifying gene ammonia monooxygenase, measured nitrifier abundance. A geographic information system (ArcGIS) was used to determine the percentage of agricultural land within each of the ten sampled tributary drainages; these percentages ranged from 0% at the headwaters to 96% along the Palouse. pH, temperature, conductivity and dissolved oxygen were measured *in situ*. Water samples were tested for nitrite, nitrate, ammonia, dissolved inorganic nitrogen (DIN) and soluble reactive phosphorus (SRP). The General Linear Model was used to assess relationships between physical and chemical variables, with and without molecular data. Season had a significant effect on SRP, temperature, pH, # of taxa, and % taxa dominance. Watershed area had a significant effect on % taxa dominance. % agriculture had a significant effect on conductivity and nitrifier abundance. Across the watershed, the abundance of nitrifying bacteria was positively correlated with an increase in agriculture. This study helps to better relate microbial communities and nitrification to patterns of land use and water quality.

Acknowledgements

I would like to thank my committee for all of their time and dedication, especially my co-advisors, Dr. Camille McNeely and Dr. Robin O'Quinn, for sharing their expertise and assisting me with field and lab work. Thank you to Dr. Andrea Castillo for letting me invade her lab for a few years and providing a sterile environment for me to work in. Thank you to Dr. Carmen Nezat for providing valuable feedback on my final document. Thank you to Dr. Prakash Bhuta for his assistance and lab use, and Dr. Peter Bilous for use of his qPCR equipment. I would also like to thank: my husband, Michael Schucker; my sister, Laura Smith; and former graduate student, Denise Davis for all of their field assistance. Thank you to John VanVeen for his undying enthusiasm for all things scientific and for helping me fashion the perfect sediment core-removal tool. Thank you to the Biology stock room crew, David French and John Shields, for always helping me find what I needed to keep going. For financial assistance I would like to thank: my mother, Cristine M. Perkins; American Water Resources Association; J. Herman and Jean Swartz Biotechnology Fellowship; Dr. Camille McNeely; and EWU Biology Department Travel Grant Committee. My research could not have been completed without their financial support. Finally, thank you to fellow graduate student Brittany Morlin for encouraging me to pursue a graduate degree.

Table of Contents

List of Tables

Table of Figures

Table of Maps

Introduction

Agriculture covers nearly 40% of the earth's land surface and has been identified as a primary contributor of pollutants and excess nutrients to aquatic ecosystems (Alexander *et al*., 2007; Food and Agriculture Organization of the United Nations, 2013; Kirk *et al*., 2004; McCrackin *et al*., 2013; USDA, 2012; Williams *et al*., 2015). These systems are important pathways for nutrient transport and processing, the latter of which is mediated by prokaryotes (bacteria and archaea). And while much is understood about aquatic and riparian ecosystem macro-organisms (i.e. terrestrial and benthic invertebrates, birds, bats, fish, and amphibians), less is understood about the function and ecology of sediment microbes. Organic matter decomposition and the cycling of carbon (C), nitrogen (N), phosphorus (P) and sulfur(S) are some key processes that require a wide range of microbial taxa, and represent significant primary and secondary production (Findlay and Sinsabaugh, 1999). Subsequently, microbial biomass acts as a substantial trophic catalyst in aquatic systems and it is critical that we understand not only how microbes release nutrients via organic matter decomposition, but also how they immobilize and transform nutrients, and what environmental parameters affect these processes.

As with other organisms, biotic and abiotic factors such as salinity, pH, dissolved oxygen (DO), temperature, the presence of heavy metals and nutrient concentrations can impact the biogeographic patterns of microbes (Altmann *et al*., 2003; Zhang *et al*., 2007). However, precise knowledge of how these factors affect microbial community structures, distribution and abundance is lacking (Findlay and Sinsabaugh, 1999). Most research on these microbially mediated functions has focused on marine environments, both open ocean and estuaries (Sinsabaugh and Findlay, 1995; Venter *et al*., 2004; Wankel *et al*., 2009; Wankel *et al*., 2011), however, the importance of understanding these processes in freshwater aquatic systems such as streams, aquifers and rivers is relevant to the understanding of the global system (Kemp and Dodds, 2002; Paerl and Pinckney, 1996). My research provides much needed information on the relationship between freshwater microbial communities and their distributions relative to land use, particularly agriculture. These relationships help to link microbial functions with ecosystem services and provide a more holistic account of how land use can modify nutrient dynamics.

Research on biotic uptake and transformation of nitrogen in streams is of particular importance as it is often a limiting nutrient, and excess N in an aquatic system can be detrimental to an entire ecosystem (Bernot and Dodds, 2005; Starry *et al*., 2005). Agriculture is an important source of N to surface waters, and understanding how microbial functions vary in response to N additions within many watersheds is unknown (Craig and Weil, 1993; Starry *et al*., 2005; Tesoriero *et al*., 2000; Williams *et al*., 2015). The majority of nitrogen in fertilizer, usually in the form of ammonia (NH_3), is not retained where it is applied and can enter watersheds via surface runoff, groundwater seepage, or wind deposition (Robertson and Vitousek, 2009; Starry *et al*., 2005). If not mitigated locally, it is transported downstream, remaining mobile until transformed, retained or dumped into terminal reservoirs such as lakes or oceans, where it can produce hypoxic zones (Abell *et al*., 2011; Kowalchuk and Stephen, 2001; Robertson and Vitousek, 2009). My study site resides within multiple land use categories and contains tributaries with varying percent agriculture in their drainages. As such, it offers an ideal platform for examining the relationship between land use and microbial community dynamics.

The Nitrogen Cycle

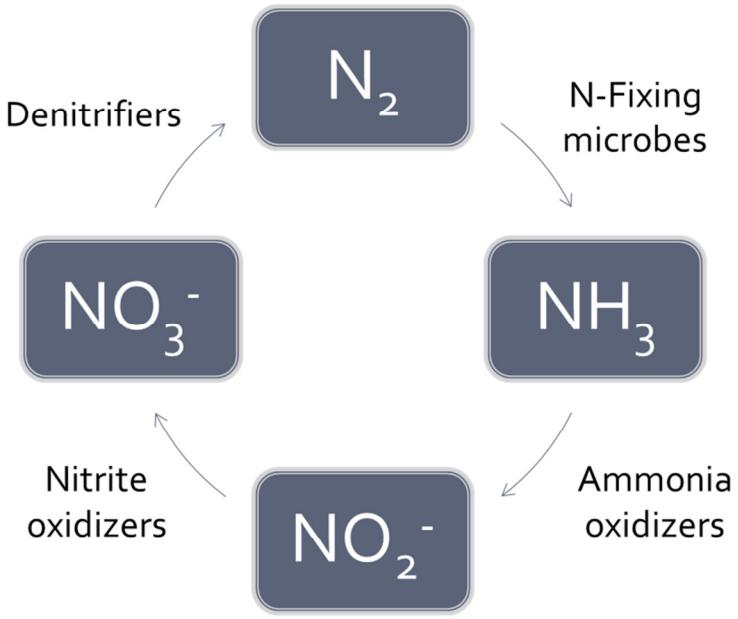

Figure 1. Simplified nitrogen cycle.

Nitrogen Fixation

The properties of the nitrogen atom allow it to easily participate in chemical reactions; nitrogen compounds exhibit a wide range of oxidation states (-3 to +5), and while the N_2 bond dissociation energy is one of the highest (945 kJ/mol), the N-N single bond is one of the lowest (160 kJ/mol). These chemical properties dictate the differential mobility of various nitrogen molecules. Approximately 78% of our atmosphere is unreactive nitrogen gas (N_2) (Figure 1); a form of N that is not biologically available to an ecosystem until it is transformed via nitrogen fixing bacteria and archaea into reactive ammonia (NH_3) through a reductive process called nitrogen fixation. These microbes, collectively known as diazotrophs, are highly diverse in their environmental requirements and yet all produce nitrogenase, the catalytic enzyme that facilitates the process of converting N_2 to NH_3 at soil temperatures between 13 – 26°C and normal atmospheric pressure (1 atm). It is,

however, energetically costly (16-30 ATP's) to break the N-N triple bond and therefore these microbes "turn off" N-fixation when NH_3 is available. Subsequently, this limits the over production of NH_3. That which is produced is quickly protonated to ammonium (NH_4^+), a biologically available form that can be taken up by organisms (a reversible pH driven process).

$$N_2 + 8H^+ + 8e^- \rightarrow 2NH_3 + H_2.$$

Chemical equation for N-fixation.

The unit of measurement for analyzing global nitrogen fixation is the teragram (Tg), which is 10^{12} g. Natural rates of N-fixation are estimated to be between 130-180 N Tg yr^{-1} (< 10 for lightning; < 30 - > 300 for marine environments; and ~ 90-140 for terrestrial ecosystems) (Galloway *et al*., 1995). Anthropogenic N-fixation accelerated in 1905 with the invention of the Haber-Bosch process which directly transforms N_2 into NH_3, and allows for the production of agricultural fertilizer.

$$N_2 + 3\ H_2 \rightarrow 2\ NH_3$$

Haber-Bosch chemical equation.

This chemical production of NH_3 now surpasses the rate of natural terrestrial N-fixation (Robertson and Vitousek, 2009). Overall, anthropogenic activity is estimated to add 140 Tg N yr^{-1} through: ammonia fertilizers (~ 80 Tg N yr^{-1}); burning fossil fuels (> 20 Tg N yr^{-1}), which releases geologically stored fixed N; and through the cultivation of leguminous crops (~ 40 Tg N yr^{-1}) (Galloway *et al*., 1995). The Haber-Bosch process is energetically costly, requiring conditions of extremely high temperature and pressure (400-650°C and 200-400 atms). Despite these high energetic costs, this anthropogenic source of ammonia is critical for maximizing global crop yields to feed the increasing human population. However, it bypasses the natural N-fixing process mediated by diazotrophs that provides limited biologically available N into a system. These anthropogenic inputs create an abundance of available N on a global scale. High N concentrations can be detrimental to ecosystems since it is usually a limiting nutrient and

the addition of excessive N into a system can decrease biodiversity if a limited number of species take it up faster and out-compete other species. Eutrophication can result from this increased biological growth and subsequent decay (McCaig *et al*., 1999). Additional sources of N loading are wastewater treatment plants, power plants, septic tanks and urban development, and the degradation of riparian zones and wetlands also acts to slow the mobility and increase the retention of fixed N (Vitousek *et al*., 1997). Common N-fixing bacteria and their associated environments include: Cyanobacteria - including *Anabaena* (freshwater), *Nostoc* and *Trichodesmium* (marine waters); Alphaproteobacteria - *Rhizobium* (soils), *Azospirillum* (soils); Gammaproteobacteria - *Azotobacter* (soils); Firmicutes - *Clostridium* (various); and *Chlorobium* (freshwater).

Nitrification

NH_3 that is not taken up by organisms (as NH_4^+), or released into the atmosphere as gas, is transformed through nitrification, a two-step oxidative process that converts NH_3 into nitrite (NO_2^-) and then nitrate (NO_3^-). The first step (ammonia oxidation) is considered the rate-limiting step and is carried out by chemotrophic ammonia-oxidizing bacteria (AOB) and archaea (AOA) that produce the ammonia monooxygenase enzyme (AMO). My research focuses on these nitrifying AOB, since many studies found them to be more common in freshwater systems and they are key contributors of cycling N through an ecosystem. AOB include *Nitrosomonas europaea*, *Nitrosomonas eutrophus*, *Nitrococcus oceanus*, *Nitrospira briensis*, and *Nitrosolobus multiformis*. In *N. europaea*, the chemical reaction begins when the membrane bound ammonia monooxygenase enzyme (AMO) catalyzes the conversion of NH_3 to hydroxylamine (NH_2OH) (Hofman and Lees, 1953; Yamanaka, 2008), followed by the oxidation of the NH_2OH to nitrous acid (HNO_2), which is mediated by periplasmic hydroxylamine oxidoreductase (HAO). Nitrite is toxic to most organisms, including ammonia-oxidizers. To avoid toxication, *N. europaea* have an invagination in the cell membrane that allows the cell to bring in ammonia as an electron donor and immediately flush the resultant nitrate out without it entering the cytoplasmic space (Figure 2). The invagination also increases surface area to accommodate the membrane bound ammonia monooxygenase.

$$NH_3 + 1.5O_2 \rightarrow NO_2^- + H^+ (+H_2O)$$

Overall reaction equation for the first step of nitrification.

The resultant NO_2^- is oxidatively transformed into nitrate (NO_3^-), which is also biologically available to most organisms. This second step of nitrification is also carried out by chemotrophic bacteria - including *Nitrobacter winogradsky*, *Nitrobacter hamburgensis*, *Nitrobacter mobilis* and *Nitrospira gracilis*. In *N.winogradsky*, the chemical reaction occurs when the nitrite oxidoreductase enzyme catalyzes the conversion of NO_2^- to NO_3^- (Yamanaka, 2008). Both nitrification steps are aerobic processes that result in the synthesis of cellular matter from carbon dioxide (CO_2) (Yamanaka, 2008). Possible fates of NH_4^+, in addition to biotic uptake and nitrification, are adsorption and volatilization.

$$NO_2^- + 0.5\ O_2 \rightarrow NO_3^-$$

Overall reaction equation for the second step of nitrification.

Figure 2. The photo on the left is of a *Nitrosomonas* cell membrane invagination. The photo on the right is *Nitrosomonas*. SEM photo credit: Woods Hole Oceanographic Institute.

Denitrification

Finally, through the stepwise reductive process of denitrification, NO_3^- is transformed back into N_2 through an anaerobic process facilitated by heterotrophic and autotrophic microbes that produce reductase enzymes (nitrate reductase, nitrite reductase, nitric oxide reductase, and nitrous oxide reductase). Common denitrifiers include: *Paracoccus denitrificans*, *Thiobacillus denitrificans*, *Pseudomonas spp.*, *Blastobacter denitrificans*, *Alkaligenes* and *Spirillum*. These microbes compete for NO_3^- with plants and ultimately control the rate of biologically available N lost from an aquatic system (Yamanaka, 2008). The only possible fate of NO_3^-, in addition to biotic uptake and denitrification, is adsorption (Kemp and Dodds, 2002b). Assimilation, also referred to as immobilization, is the uptake of NH_4^+ or NO_3^- and subsequent conversion into biomass. The reverse process is mineralization, also known as ammonification, by which organic molecules are converted to inorganic NH_4^+.

$$2\ NO_3^- + 10\ e- + 12\ H^+ \rightarrow N_2 + 6\ H_2O$$

Overall reaction equation for denitrification.

While nitrification and denitrification are critical in cycling NH_3/NH_4^+ and NO_3^-, harmful intermediate products - nitrous oxide (N_2O) and nitric oxide (NO) - are created in the process. N_2O is a significant greenhouse gas, approximately 296 times more potent than CO_2 (Petersen *et al*., 2012). During nitrification, microbes increase their production of N_2O when O_2 concentration is low (Yamanaka, 2008). An environment with high N and low O_2 concentrations can result in high N_2O production, although it may be offset by slower nitrification rates at low O_2 concentrations (Kemp and Dodds, 2002b). NO is an important biological molecule, but can react with sunlight and ozone to produce nitric acid (HNO_3), a component of acid rain. Anthropogenic NH_3 production has changed the ratio of stored N to active N, and increased the rate of N_2O and NO formation, further driving the importance of understanding the impact these reactions may have on microbial communities, and ultimately the ecosystem.

$$NO_3^- \rightarrow NO_2^- \rightarrow (NO) \rightarrow (N_2O) \rightarrow N_2$$

Formation of intermediate gaseous compounds during denitrification.

While aquatic N-fixing organisms generally dwell in the water column, nitrifiers and denitrifiers reside in the streambed sediments at the oxic / anoxic interface, although their precise stratification is not completely understood (Butturini *et al*., 2000).

Rates of Nitrification

Anthropogenic activities, such as agriculture, have altered the natural nitrogen cycle and understanding the role of microbes in this process has become increasingly important. Ultimately, nitrifying communities control the conversion of ammonia and the production of nitrate, which is one of the most abundant N compounds on earth (Kirchman, 2012). Key factors that control the rate of nitrification include the availability of NH_3, biotic uptake of N by heterotrophic assimilation, and physical and chemical properties of the ecosystem. In the next several paragraphs I will discuss previous research addressing these factors.

Previous studies on NH_3 availability and nitrification show that NH_3 concentrations can dictate the distribution and abundance of nitrifying microbes. Wang *et al*. (2011) studied AOB in sediments from four wetlands containing varying concentrations of ammonium and found wetlands with higher ammonium had a higher abundance of nitrifiers. Ammonia was also found to be a primary driver of AOB distribution in a eutrophic urban lake (Qiu *et al*., 2010). AOB abundance was directly correlated with NH_3 levels in the water column, and their data showed that specific *Nitrosomonas* species are inhibited at high concentrations. Cebron *et al*. (2003) studied the AOB community compositions in an estuary impacted by wastewater effluent, a significant source of NH_3, and found that the AOB sorted along a distance gradient from the inflow. In another stream study, Wakelin *et al*. (2008) measured the effect of wastewater treatment plant effluent on nitrogen cycling microbes by comparing microbial diversity along a spatial gradient from the effluent discharge. They found the highest diversity at 400 m downstream of the discharge, with a progressive decrease in diversity as they sampled downstream from that

point. They found the highest biomass at the furthest point away from the discharge. Overall, their study showed a strong correlation of NH_3 on the distribution and abundance of microbes.

Biotic uptake of NH_4^+ can significantly affect rates of nitrification as a result of competition among AOB and other organisms (Butturini *et al*., 2000; Strauss and Lamberti, 2000). Heterotrophic uptake of NH_4^+ is linked with concentrations of dissolved organic carbon (DOC) availability (Bernhardt *et al*., 2002). Carbon triggers heterotrophic growth and requires nitrifiers to compete for NH_4^+, often unsuccessfully. Starry *et al*. (2005) found that elevated levels of DOC inhibit nitrification, while high levels of NH_4^+ accelerate it, and that heterotrophic assimilation surpasses uptake of N by nitrifiers at a stream reach scale. A primary reservoir of C, as well as N and P, are stored in FBOM and released by microorganisms (Fierer *et al*., 2007). Research by Kemp and Dodds (2002b) also showed that a high C:N ratio results in reduced NH_4^+. Furthermore, vegetation takes up N-species differentially; all plants utilize NO_3^-, trees prefer NH_4^+, while weeds prefer NO_3^- (Kowalchuk and Stephen, 2001), suggesting that rates can be impacted by the abundance and type of vegetation.

In addition to NH_3 concentrations and biotic uptake of NH_4^+, physical and chemical factors of the ecosystem, such as DO, salinity, pH, season, temperature, heavy metals, and flow rate, can affect rates of nitrification. Kemp and Dodds (2002b) found that nitrification rates decreased with a decrease in DO and that the decrease in DO was linked to heterotrophic uptake in a high C:N ratio environment. The subsequent decay of biomass by microorganisms also requires oxygen and further adds to the reduction of DO. The location, diversity and abundance of AOA was also studied by Park *et al*. (2008) from four marine sites in which they compared the location and abundance of the AOA to that of ammonia-oxidizing bacteria (AOB) and found that the AOA outnumbered the AOB and occupied the sediment to a greater depth, which they correlated with oxygen availability. Similarly, in a lab experiment using estuarine sediments, Abell *et al*. (2011) found that ammonia-oxidizing communities show a rapid niche-partitioning response to changes in oxygen conditions. This is important information for understanding microbial

dynamics in hypoxic zones (Robertson and Vitousek, 2009). Francis *et al*. (2005) sampled sediments from four different marine locations - coastal and estuarine - and found that there were four distinct nitrifying microbial communities among the sites. These communities were made up of ammonia-oxidizing archaea (AOA) of different species and in different abundance, which they correlated to fluctuations in salinity.

Previous research on the effects of season and temperature on nitrification rates include a study done by Starry *et al*. (2005). They found seasonal variation, with summer having the highest rates of nitrification (0.95 µg N cm^{-3} d^{-1}) and winter the lowest (0.19 µg N cm^{-3} d^{-1}), followed by spring (0.29 µg N cm^{-3} d^{-1}). For their study stream (forested headwater stream with total area 8085 m^2), they calculated the following seasonal NO_3^- loads from nitrification (g N d^{-1}): autumn 206, winter 77, spring 113, and summer 384. Overall, rates were positively correlated to temperature and DO. Therefore, thermal limitation may exist in colder seasons and/or climates. In Chesapeake Bay, the ammonia-oxidizer communities were affected seasonally, with diversity increasing between spring and summer and decreasing between fall and winter, for which temperature was suspected to be the driving factor (Fortunato *et al*., 2009). Seasonal fluctuations in carbon sources (allochthonous input in the fall, such as leaves and wood) drive particulate organic matter (POM) which then drives dissolved organic matter (OM) concentrations. So temporally, season can account for more of an effect other than the change of temperature and timing of fertilizer application.

According to the International Fertilizer Industry Association (2011), higher temperatures increase the relative proportion of NH_3 to NH_4^+, while decreasing the solubility of NH_3. The solubility of NH_3 and its high affinity for water can raise the pH of stream water, which results in a more favorable environment for nitrification (Bansal, 1976). More acidic environments can slow nitrification rates because NH_3 gets protonated to NH_4^+, reducing the actual substrate concentration for ammonia oxidation (Kirchman, 2012). Strauss *et al*. (2002) found that pH and NH_4^+ availability affected sediment nitrification rates more than 11 other variables: nitrification increased with NH_4^+ availability and decreased with lower pH. In addition, the ratio of NH_3/NH_4^+ to NO_3^- affects nitrification.

This ratio is dictated by a number of factors, including influx of NH_3/NH_4^+, and the differential mobility of NH_3 versus NO_3^-. Because of its negative charge, NO_3^- is a more mobile form of N than NH_4^+, which adsorbs more readily to negatively charged soil organic matter and clay colloids (Kowalchuk and Stephen, 2001; Starry *et al*., 2005). This mobility can result in a rapid loss of N from fertilizer leaching or runoff of the NO_3^- into groundwater or surface waters (WA State Dept. of Ecology, 2013). In 2007, Fierer *et al*. studied stream bacterial communities in a 3000ha watershed and identified three distinct communities residing at locations dictated by pH levels. The dominant taxa for each location were: acidobacteria at pH 4.4; alphaproteobacteria at pH 5.3; and betaproteobacteria at pH 6.2. pH was significantly correlated with dissolved organic carbon (DOC) and dissolved organic nitrogen (DON): pH below 4.5 showed higher DOC and total dissolved nitrogen (TDN). The majority of the N was organic; inorganic comprised 10-20%. However, they acknowledge that stream water pH can be altered by numerous biotic and abiotic factors, including the hydrology and geology of the watershed, and vegetation. A study on AOB communities in a Hong Kong estuary showed that their distributions were affected by the presence of mangroves, as well as pH levels (Li *et al*., 2011).

The presence of heavy metals also affects bacterial distribution and community compositions. In the Coeur d'Alene River in Idaho, a study done in 2011 by Rastogi *et al*. investigated the effect of metal contamination (As, Fe, Pb and Zn) on communities of sediment bacteria; specifically ammonia-oxidizers and methanogens. Their results showed that proteobacteria-lineages, such as *Pseudomonas, Ralstonia,* and *Acinetobacter* were abundant, which fit their prediction, since these microbes are typically found in heavy metal environments. In 2005, Fields *et al*. compared microbial communities among an uncontaminated groundwater site and three acid-uranium contaminated sites. They found higher microbial diversity in the uncontaminated site, with 79 unique taxa present compared to 19, 27 and 34 from the contaminated sites.

Physical properties of the stream channel, such as flow rate, turbidity, scouring, mixing, and other hydrodynamics, can be a source of disturbance and impact microbial activities

(Bansal, 1976). Marine AOB assemblages were driven by the changes in intensity of currents, waves and upwelling in a study done by Dang *et al*. (2010). Generally, nitrifiers are slow growers (Junier *et al*., 2010) and don't respond rapidly to changes in their environment. They must convert a substantial amount of NH_3 for growth since the energetic yield from ammonia oxidation is low (ΔG = -272 kJ mol $^{-1}$) (Kirchman, 2012). Because of their slow growth, they may not be able to recover from a disturbance rapidly enough to process acute N-loading, which may coincide with runoff during precipitation events (flashy streams and rivers).

Understanding how microbial communities respond to physical and chemical factors, as well as rates of nitrification can be affected can provide important information on the overall diversity of microbial communities in an agriculturally impacted landscape. Rates of aquatic nitrification are often measured in the lab with microcosm assays or sediment biofilm reactors (SBR). Concentrations of NH_4^+ (µg / L) in a microcosm reference assay can be compared to one blocked with nitrapyrin, which inhibits nitrification (Kemp and Dodds, 2002; Starry *et al*., 2005). With SBRs, concentrations are also compared; however, hydrodynamic mechanisms are also included and can be set to mimic a range of hydrologic conditions (Butturini *et al*., 2000). In addition to system rates, microbial conversion rates have also been measured for *Nitrosomonas* (1-30 million µg N day^{-1} g dry cells^{-1}) and *Nitrobacter* (5-70 million µg N day^{-1} g dry cells^{-1}) (Dept. of Environmental Sciences, U of Virginia, 2015). In my study I used molecular methods to measure the relative abundances of nitrifying bacteria in order to obtain information about the possible nitrifying activity.

Microbial Metabolism

Prokaryotes reside in every ecosystem on earth's surface, from the polar regions to hydrothermal vents. Although the majority occupy neutral conditions, many are extremophiles, pushing the upper and lower limits of: temperature (psychrophiles and hyperthermophiles), pH (alkalophiles and acidophiles), salinity (halophiles) and pressure (piezotolerant and hyperpiezophiles). Temperature tolerance ranges from <15°C to >

110°C, with most residing between 15 - 40 °C (Kirchman, 2012); pH tolerance ranges from 0.7 (Baker-Austin and Dopson, 2007) to 11 (Ulukanli and Digrak, 2002), with the majority residing between 5 and 8; salinity tolerance ranges from 1- >15% NaCl, with the average halophile thriving at 6-15% (Kirchman, 2012); and pressure tolerance ranges from 1- >80 MPa (Kirchman, 2012). In addition to these environmental parameters, microbial distribution is controlled by physiological constraints and they are organized and characterized in large part on how they obtain carbon (for cellular growth) and energy (to fuel metabolism). Those that use organic C (commonly glucose) are referred to as heterotrophs and those that use inorganic carbon sources, such as CO_2, are autotrophs. For energy derivation, there are four distinct classifications: phototrophic microbes undergo oxygenic photosynthesis; chemotrophs use inorganic and organic compounds; chemolithotrophs use inorganic salts; and chemoheterotrophs use organic compounds. Energy derivation via reduction-oxidation reactions (redox) in microbes follows the same basic principle found in eukaryotes. During these catabolic reactions, electrons are transferred from donor molecules (organic or inorganic) to acceptor molecules (terminal electron acceptors), and a release of energy occurs during the transfer that is used immediately or stored in the cell for future chemical or physical work. Bacteria have the added advantage of using multiple electron transport chains (branched, modular and inducible), and the capability to use them simultaneously. The most common electron donors are organic molecules, which are required by animals, fungi, unicellular eukaryotes, and plants. Lithotrophic microbes, however, use inorganic electron donors such as hydrogen, ammonia, nitrite, carbon monoxide, sulfur, sulfide, and ferrous iron. In an aerobic environment, the primary electron acceptor is oxygen. Anaerobic environments exhibit a broader range of possibilities, including nitrite, nitrate, carbon dioxide, sulfate, and ferric iron (Yamanaka, 2008).

Examples of some common microbial redox strategies include: ammonia and nitrite oxidizers that use NH_3 and NO_2^-, respectively, as their electron donors, O_2 as their electron acceptor and CO_2 to supply the carbon for building cellular components; and denitrifiers that derive energy from oxidizing ferrous iron (Fe_2^-) and use NO_3^- as their electron acceptor. Sulfate reducing bacteria exhibit a wide range of electron donor compounds, including H_2, acetate (CH_3CO^{-2}), amino acids and sugars (Kirchman, 2012);

and sulfate acts as the terminal electron acceptor. Methanogens are obligate anaerobes that obtain electrons from hydrogen gas (H_2) and use CO_2 as their electron acceptor. This variety in physiological niches helps explain the ubiquity of microbes.

The O_2 Issue

Although many microbes require molecular oxygen (O_2), it is highly reactive and a significant factor that affects their distribution and proliferation. Toxic by-products of O_2 transformation in a cell include hydrogen peroxide (H_2O_2) and superoxide (O_2^-), which, combined with iron (Fe), create the highly reactive hydroxyl radical (OH^-). As single-celled organisms, they are spatially limited, and most do not have internal structures to sequester and isolate O_2 conversion processes to avoid damaging the cell. Many aerobes mitigate the toxic effects of O_2 exposure with detoxifying enzymes such as catalase, which rapidly breaks down H_2O_2, and superoxide dismutase, which breaks down O_2^- - preferably prior to OH^- formation, which can kill the cell. There is a wide range of microbial response to O_2 and microbes are classified based on their requirement for, or tolerance of it. Obligate aerobes are those that require O_2 as their terminal electron acceptor; facultative anaerobes prefer O_2 but can grow in its absence using fermentation; microaerophilic microbes thrive in environments with low concentrations of O_2; and obligate anaerobes are irreversibly damaged in the presence of O_2.

All of the aforementioned factors for microbial metabolism drive their biogeographical patterns of abundance and community structures. Generally they are very diverse with highly specific requirements, and yet are able to reside in the same micro-ecosystem as long as some overlap exists in their physical and chemical tolerance. Visualized as a Venn diagram, the area of overlap created by the circles would drive the community structure. Because overlap must exist, proximity is critical. The N-cycle, for example, contains constituents that are: aerobic (N-fixers and nitrifiers) and anaerobic (N-fixers and denitrifiers); light tolerant (N-fixers) and light intolerant (nitrifiers and denitrifiers); and some with varying demands for energy-deriving substrates. Therefore, a complete conversion of N through the nitrogen cycle requires oxic / anoxic interfaces (such as sediment) so that the associated microbes are close enough to each other to obtain the

chemical by-products that they need for their metabolism, while avoiding toxicity or desiccation. Another example of microbial communities reliant on spatial and physiological overlap is a microbial mat. Mats are aggregates of microbes that form over time, and as the layers accumulate, the physiological requirements of the constituents must be met through diffusional exchange with their "neighbors". Diverse microbial groups coincide in this manner, mutually exchanging chemicals required for their growth and proliferation. This overlap in environmental requirements provides a challenge when culturing a community of microbes, as some are more fastidious than others; providing all of the elements necessary for their growth is extremely problematic and often impossible. Therefore, while many studies on aquatic microbes have analyzed sediment samples by culturing them in the lab, this excludes those microbes that are not easily cultured (Findlay and Sinsabaugh, 1999; Halda-Alija and Johnston, 1999). Current molecular techniques, by contrast, provide a rapid and accurate analysis of microbial communities by analyzing the DNA / RNA composition regardless of their ability to be cultured in the lab. This is possible because a system-wide extraction of genetic information occurs, including all of the microbes present in the sediment samples. DNA analysis provides an efficient and accurate way to phylogenetically characterize microbial communities. Two polymerase chain reaction (PCR) techniques commonly used in microbial research to analyze community profiles are terminal restriction fragment length polymorphism (T-RFLP) and quantitative polymerase chain reaction (qPCR) (Huse *et al*., 2008; Kirk *et al*., 2004; Nocker *et al*., 2007; Wang and Qian, 2009; Zak *et al*., 2006). T-RFLP conducted on the small ribosomal subunit *16S rRNA* (~1500 bp) is specifically useful for comparing differences among community compositions. This technology involves the use of restriction enzymes - typically four-base cutters - that cut at specific recognition sites along a hyper-variable region in the DNA sequence. Each terminal restriction fragment (T-RF) that is generated corresponds to a unique taxon in the sample. qPCR performed on specific functional genes, such as the ammonia monooxygenase gene (*AMO*), measures gene abundance in a sample, which quantifies functionally similar microbes. Of the three genes that encode the subunits of AMO (*amoA, amoB and amoC*), *amoA* (491 bp) is the most common target for amplification and the one used in this study.

The objective of my research was to relate microbial communities to patterns of land use and water quality. The tributary streams of my study area, the Latah Creek Watershed (LCW) in eastern Washington, have varying degrees of agriculture in their drainages, and samples from these stream sediments captured microbial communities at different spatial gradients of land use along the watershed. I used molecular methods to assess overall microbial diversity and the relative abundance of ammonia oxidizing bacteria (AOB). Characterizing the microbial communities enhances our understanding of spatial and temporal variation within the watershed and adds to our growing knowledge of small regional aquatic ecosystems.

My research aimed to answer: *To what extent does agriculture in a drainage affect sediment microbial community compositions and the abundance of nitrifying bacteria, and is there temporal variation?* I addressed three main predictions: 1) I would find higher species diversity in sample sites with less agriculture in their drainages; 2) I would find a higher abundance of nitrifying bacteria in drainages with higher percentages of agriculture; and 3) communities in streams with less agriculture in their watersheds may be more similar to each other than those from streams in high agriculture drainages.

Methods and Materials

Study Area

Latah (aka Hangman) Creek begins at the base of the Rocky Mountains near Sanders, Idaho, flows northwest into Washington State near the town of Tekoa, and continues until it feeds into the Spokane River (Map 1). It is part of the USGS Pacific Northwest Water Resource, Region 17, Hydrologic Unit Code (HUC) #17, subbasin # 17010306. The watershed encompasses approximately 2.8 km^2, the majority of which is dominated by dry-land farming of wheat, peas, barley and lentils (1,116 km^2), followed by forested land (484 km^2) and urban/residential (51 km^2). Major tributaries of the 97 km main channel are Upper Latah, Lower Latah, Marshall, Rock, and California Creeks. There are two USGS monitoring stations on the main channel: #12424000 in Spokane County near the Spokane River confluence; and #12422990 in Whitman County at the state line near Tekoa. Average discharge for Latah Creek is 6.54 cu m/s, with an average maximum of 566 cu m/s (winter and spring) and an average minimum of 0.28 cu ft/s (summer) (WA State Dept. of Ecology, 2012). The USGS characterizes current flow conditions as "flashy" due to anthropogenic modifications to the landscape, such as an increase in agriculture, impervious cover and timber harvest, as well as the removal of riparian and wetland areas. In addition, many reaches of Latah Creek and its tributaries are below state water quality standards for fecal coliform, turbidity, and temperature and considered impaired based on the pH and dissolved oxygen levels (WA State Dept. of Ecology, 2012; Spokane County Conservation District, 2005; WRIA 56 Watershed Implementation Team, 2008). Affected tributaries in this study are: Rattler Run (turbidity and temperature), Rock Creek (DO, temperature and turbidity), Cove Creek (DO), California Creek (temperature) and Marshall Creek (temperature). There are ten wastewater treatment plants in the watershed, six of which discharge into surface water, including Rattler Run and Rock Creek (WA State Dept. of Ecology, 2012).

The watershed traverses through Benewah County in northwestern Idaho, and Whitman and Spokane Counties in eastern Washington. This region is known as the Palouse and

resides over the middle Colombia Basin. It is characterized by rolling hills of deep loess which were distributed during the Pleistocene as windblown deposits from glacial outwash to the west and south of the region. Loess is a composite of fine-grained (20-50 micrometers) clay, silt and sand mixed with calcium carbonate. These deposits in the Palouse generally range from 5 - 130 cm deep and provide a highly fertile substrate for agricultural farming. Beneath the blanket of loess are bedrock areas of basalt, granite and gneiss. Historically, native flora on the Palouse was dominated by perennial grasses, forbs and shrubs such as bluebunch wheatgrass (*Pseudorigneria spicatum*), Idaho fescue (*Festuca idahoensis*), arrowleaf balsamroot (*Balsamorhiza sagittata*), common snowberry (*Symphoricarpos albus*), and wild rose (*Rosa spp.*), often with an overstory of ponderosa pines (*Pinus ponderosa*) (USGS, 1998-2003). Riparian species included hawthorn (*Crataegus spp.*), willow (*Salix spp.*), aspen and cottonwood (*Populus spp.*), alders (*Alnus spp.*), serviceberry (*Amelanchier alnifolia*) and chokecherry (*Prunus virginiana*) (WA State Dept. of Ecology, 2013). However, less than 1% of the native prairie and riparian communities remain and the Palouse is now considered one of the most endangered ecosystems in the United States (Noss *et al.*, 1995). The decline in the native landscape began in the mid-19th century when agriculture moved into the region and intensified with improvements in farming equipment and fertilizer production. Agriculture now occupies 90% of the Palouse (Hogan and Fund, 2014) (Appendix, Table 24), with soft winter wheat (*Triticum aestivum* L.) as the predominant crop (USDA, 2012). Soil acidification and erosion currently plague the region (Hall *et al.*, 1999; Koenig *et al.*, 2011; Schroeder and Pumphrey, 2013). In addition to ammonia based fertilizer (predominantly ammonium sulfate) (Appendix, Table 25), applications of chemicals to control insects, weeds, grass, brush and nematodes, and to control diseases is standard (Appendix, Table 25).

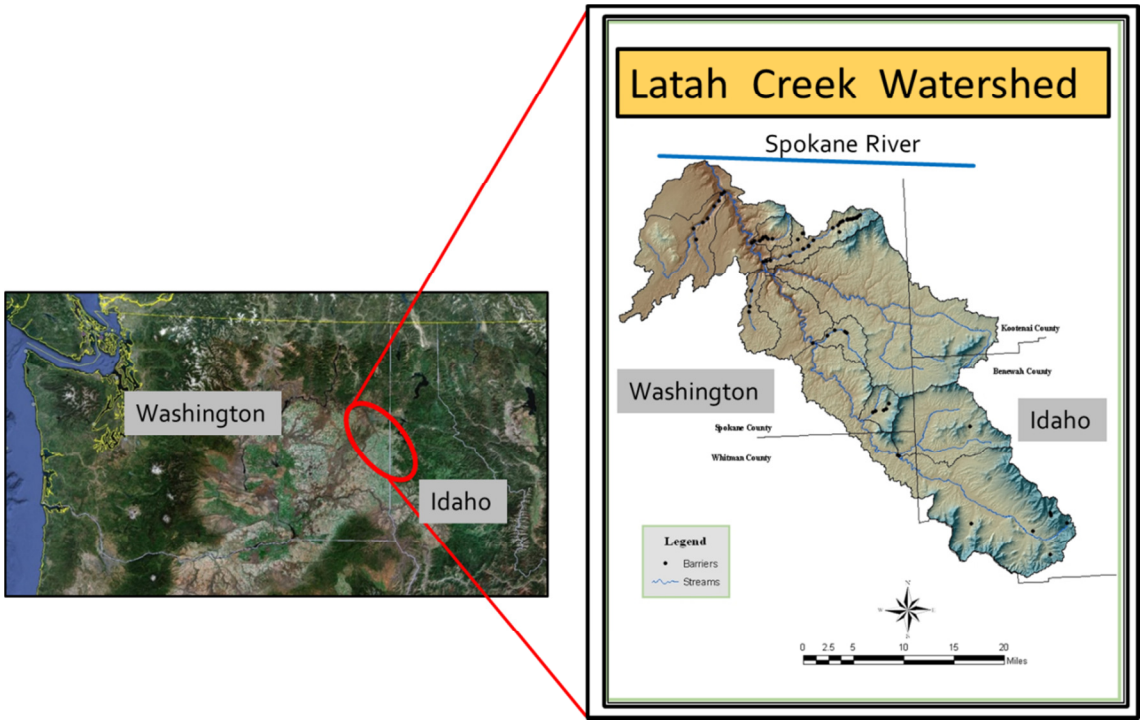

Map 1. Latah Creek Watershed. Modified from WA State Dept. of Ecology.

Sediment and Water Sample Collection Protocol

Sediment samples were collected in June and October 2012 from ten tributary locations within the watershed (Map 2). These sites began at the forested headwaters near Sanders, Idaho and terminated at Marshall Creek near the Spokane River confluence, and reside in varying percentages of agriculture (Figures 3-5). The tributaries in this study, and their associated HUC12 numbers, include: the headwaters (#170103060101), Cove Creek (#170103060201), Upper Rock Creek (#170103060205), North Fork Rock Creek (#170103060204), Rattler Run Creek (#170103060202), California Creek (#170103060302) and Marshall Creek (#170103060305). I used Geographic Information System (ArcGIS) software to estimate the percentage of agriculture for each of the locations (Tables 1and 2).

At each of the ten sampling locations, six individual sediment samples were taken within a fifty foot reach (from 6 inches to within 15 feet of each other, depending on the stream

bed characteristics), and above and below riffles when possible to capture any variation created by flow differences. The samples were collected as close to the edge of the bank as possible, as studies have shown that nitrifiers reside in this typically quiescent area of the stream versus the center of the channel (Altmann *et al*., 2003). Care was taken to begin the sampling downstream and progress upstream so as not to disturb the existing stratification of the sediment, as Altmann *et al*. (2003) found that nitrifiers predominantly reside in the uppermost layers of the sediment. Each sample was collected by inverting a 60 x 15 mm sterile petri dish into undisturbed sediment and sliding a sterile metal spatula under the open end of the dish and lifting it out of the stream (Figure 6). This technique maintained the stratification of the sediment layers and kept the sediment from washing out of the dish upon removal from the stream. A new spatula was used for each location and was sterilized with 95% EtOh between individual sample collections. Once removed from the stream, the petri dishes were capped, placed into sterile Whirl-Pak bags, and stored in a cooler with ice for transport to the lab. Once in the lab they were stored at -80°C.

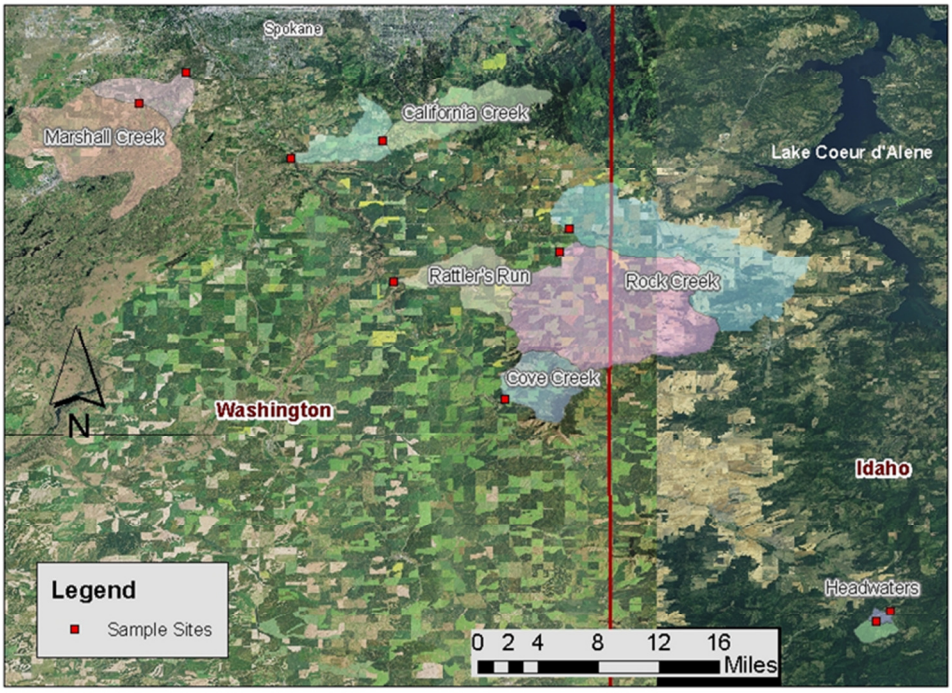

Map 2. Latah Creek tributaries and associated drainages sampled in this study. Map created with ArcGIS software.

Figure 3. Forested headwaters, site #1, 0% agriculture.

Figure 4. California Creek, site #8, 44% agriculture.

Figure 5. Rattler Run Creek, site #6, 96% agriculture.

Figure 6. Sediment samples collected in 60 x 15 mm petri dishes.

Two water samples were taken at each of the ten site locations for June and October. For all samples, 150mL Nalgene bottles were acid washed in 10% HCl overnight, rinsed three times with distilled water in the lab and rinsed two times in the field with stream water. Water was collected with a syringe immersed approximately 6" beneath the surface and filtered with Whatman GF/F glass microfiber filters. Water samples were stored in a cooler on ice for transport to the lab and then stored at 4 °C. NO_2^-, NO_3^-, NH_4^+, dissolved inorganic nitrogen (DIN) and soluble reactive phosphorus (SRP) were measured in duplicate for each filtered sample on an Alpkem 3 Flow Analyzer as per manufacturer's protocol (Tables 1 and 2).

During each site visit, water temperature, pH, conductivity ($\mu S/cm^c$) and dissolved oxygen (DO mg/L)) were measured *in situ* with a YSI 556 Multi-Probe (Tables 1 and 2). Flow measurements were taken during fall sampling with a Flo-Mate, Model 2000 (Marsh-McBirney). The stream width was measured wet-bank to wet-bank and divided into 10 equal distances. At each of these points the depth was measured and the flow was recorded at 0.4 of the depth. These 10 values were averaged to obtain a mean flow (m/s) for each sample location (Table 2).

Molecular Techniques

DNA Extraction

I devised a novel method to remove a stratified core from the sediment by using a brass cork-borer tool that was machined to yield a 1/8” inside diameter, and fashioned with a steel rod. The boring tool was pressed onto the frozen sediment and hammered gently down into the disc with a rubber mallet until it reached the bottom of the petri dish. Insertion of the steel rod created a vacuum in the tool, resulting in solid core removal (Figure 7). This method captured the nitrifying microbes on the bottom layer of the petri dish (i.e., the top of the *in situ* sediment layer) and maintained stratification of the sample core. One core was collected from each petri dish, for a total of 120 cores: one from each of the six samples taken at ten locations over two seasons. I extracted sediment and pore-water genomic DNA with PowerSoil DNA Isolation Kits (Mo Bio Laboratories, Carlsbad, CA). DNA was analyzed with 0.8% agarose gel electrophoresis against a 1Kb ladder (New England BioLabs, Inc., Ipswich, MA) and quantified with standard methods at 260nm on a Nanodrop 2000 (Thermo Scientific). Purity was determined with the 260/280 nm absorbance ratio.

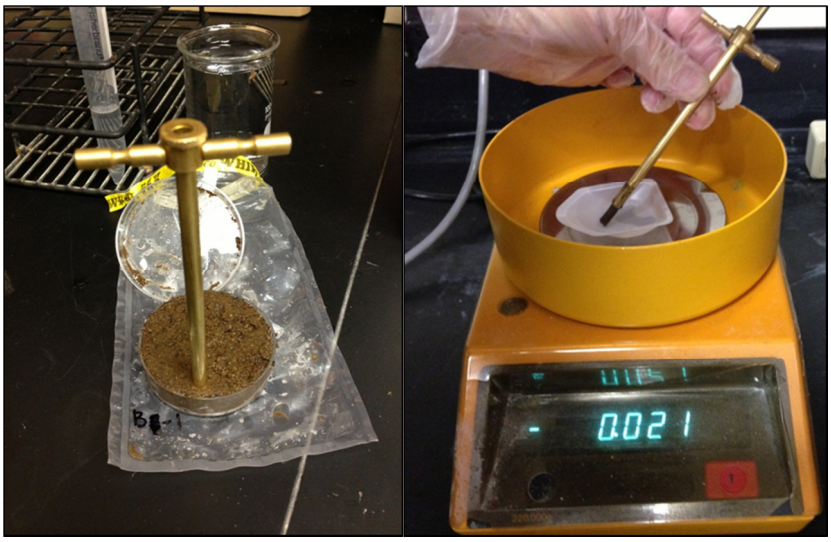

Figure 7. Cork-boring tool used to remove a solid core of sediment for DNA extraction.

T-RFLP

I conducted PCR on a BioRad MyCycler Thermal Cycler with a fluorescently labeled *16S rRNA* primer set. The fluorescent tag on the 5' end of the forward sequence was 6-FAM (6-carboxyfluorescein) - 8F - AGA GTT TGA TCC TGG CTC AG -3'(Integrated DNA Technologies, Coralville, IA); the reverse unlabeled oligonucleotide sequence was: 1492R – 5'-TAC GGT TAC CTT GTT ACG ACT T-3' (New England BioLabs, Inc. Ipswich, MA). 50 ng of template DNA was amplified in a final volume of 50 µl: 5 µL 10X *Taq* buffer (New England BioLabs, Inc., Ipswich, MA); 1 µl dNTP mix (New England BioLabs, Inc. Ipswich, MA) at a concentration of 10mM; 5µl of each primer at a concentration of 5µM; 0.25µL of 5000 U/mL *Taq* DNA polymerase (New England BioLabs, Inc. Ipswich, MA); and brought to final volume with Molecular Biology Grade Water (MBGW) (Mo Bio Laboratories, Carlsbad, CA). PCR protocol was as follows: initial denaturation at 95ºC for 30s; 30 amplification cycles of denaturation (30s at 95ºC); annealing (45s at 55ºC); elongation (90s at 68ºC); and final extension (5min. at 68ºC). PCR products were confirmed (pre and post cleanup) with 0.8% agarose gel electrophoresis against a 1kb ladder (New England BioLabs, Inc., Ipswich, MA) stained with ethidium bromide (EtBr) and photographed under UV (Appendix, Figure 33). Products were cleaned with UltraClean PCR Clean-Up Kits (Mo Bio Laboratories, Carlsbad, CA). Positive control was *Escherichia coli* (Dr. Prakash Bhuta, Eastern Washington University, Cheney, WA). DNA concentration was quantified with a Nanodrop 2000 (Thermo Scientific) prior to and following PCR clean-up. Restriction digests of the PCR products were conducted separately (in duplicate) with two 4-base cutters, HaeIII [GG/CC] and HhaI [GCG/C] (New England BioLabs, Inc. Ipswich, MA), at 37ºC for 6 hours in 30 µl (final volume) mixtures. For HaeIII: 1 µg of purified PCR product; 3 µl of 10X Buffer 4 (New England BioLabs, Inc. Ipswich, MA), 1 µl of the enzyme (20,000 U/mL), and MBGW. For HhaI: 1 µg of purified PCR product, 3 µl of 10X Buffer 4 (New England BioLabs, Inc. Ipswich, MA), 1 µl of the enzyme (10,000 U/ mL), 3 µl of 10X Bovine Serum Albumin (New England BioLabs, Inc. Ipswich, MA), and MBGW. Digests were heat inactivated as per manufacturer instructions: HaeIII (80ºC for 20 min), HhaI (65ºC for 20 min). Fragments were processed by Idaho State University, Molecular Research Core Facility (Pocatello, ID) on an Applied Biosystems

3130XL DNA sequencer with ROX 1000 size standard (BioVentures, Murfreesboro, TN).

Genemapper v3.2 software (Applied Biosystems) was used to analyze the 480 electrophoretic profiles and associated data files for each sample (Figure 24 and Appendix, Figures 38-77 for the first replicate run). Local Southern Method was used and manual peak calling with heavy smoothing was made for peaks with a minimum height of 50 RFU above background fluorescence (Clement *et al*., 1998). Raw data was then separated by season and enzyme, and fragment lengths were rounded to the nearest integer. Fragments < 30 bp were treated as background noise and discarded since they include the length of the forward primer (20 bp), and therefore represent only a 10 bp species specific sequence. Fragments >825 bp were discarded to avoid unrestricted fragments, since a recognition site should have been detected within the primer-less species specific 805 bp sequence (Blackwood and Buyer, 2007; Braker *et al*., 2001). Total peak area was calculated for each replicate run and individual peak areas that made up < 1% of the total area were discarded (Blackwood and Buyer, 2007; Yu *et al*., 2005). Total area was recalculated and fragment averages (length and peak area) were calculated along with standard deviation. Terminal restriction fragments (T-RF's) 1 bp apart were considered to be separate taxa. For troubleshooting guidelines regarding T-RFLP on the *16S rRNA* see Appendix.

qPCR

qPCR on the *amoA* gene was conducted using primers *amoA-1F* (5'- GGG GTT TCT ACT GGT GGT-3'') and degenerative *amoA-2R* (5'- CCC CTC KGS AAA GCC TTC TTC -3') (Integrated DNA Technologies, Inc., Skokie, IL) (Park *et al*., 2008) on a Bio-Rad MiniOpticon using *CFX* Manager v3.1 software. Triplicates of each sample were run, along with a standard, *Nitrosomonas europaea*, supplied by Dr. Daniel Arp, Oregon State University. The negative control was *Escherichia coli*, supplied by Dr. Prakash Bhuta, Eastern Washington University, Cheney, WA. 20 µl reactions were run as follows: 10 µl iQ SYBR Green Supermix (Bio-Rad Laboratories, Inc. Richmond,

CA), 5 µl MBGW, 2 µl of each primer at a concentration of 5µM, and 1 µl template DNA. Template DNA was diluted 10 fold to reduce the concentration. Protocol was as follows: initial denaturation at 94ºC for 5 min; 40 amplification cycles of denaturation (30s at 94ºC), annealing (45s at 53ºC), elongation (60s at 72ºC) and plate read. A melt curve was conducted at the end of each qPCR run from 55ºC - 99ºC with an increase of 0.05ºC every 10s. Success was confirmed by the presence of a single melting peak and 1.0% agarose gel electrophoresis against a 100 bp ladder (New England BioLabs, Inc., Ipswich, MA), stained with EtBr and photographed under UV (Appendix, Figure 34). For troubleshooting guidelines regarding qPCR on the *amoA* see Appendix.

Data Analysis

Relationships between physical, chemical, and response variables within the watershed were assessed with General Linear Models and JMP 6.0 statistical software. The significance level for all analyses was $\alpha \leq 0.05$. The physical variables included watershed area (WA), % agriculture per sample site, season, and *in situ* water temperature (°C) (Tables 1 and 2). Chemical variables included concentrations of NH_4^+ (ppm), pH, conductivity (µS /cm^c), dissolved inorganic nitrogen (DIN), dissolved oxygen (DO mg/L), nitrogen-to-phosphorus ratio (N:P), and soluble reactive phosphorus (SRP, ppm) (Tables 1 and 2). Response variables included: # of taxa and % taxa dominance (from the T-RFLP data); and Cq values (from the qPCR data). % taxa dominance was calculated by averaging the peak areas per site and season. The fragments with the top three highest averages per site and season were included in the General Linear Model. For each analysis, all physical and chemical variables were included in the model, followed by a step-wise elimination process to determine the best final model for each analysis based on how well the model explained the data. Variables with little or no contribution to the model were removed, with the exception of season and % agriculture, which were left in for all analyses since they are key independent variables.

Results

Physical and Chemical

Physical (WA, % agriculture, season, and water temperature), chemical (NH_4^+, pH, conductivity, DIN, DO, N:P, and SRP), and response (# taxa, % taxa dominance and Cq values) variables were assessed with General Linear Models. Across all sites; pH was higher in spring than fall ($P = 0.019$) (Table 3, Figures 8 and 9), SRP concentrations were higher in fall than spring ($P = 0.018$) (Table 4, Figures 10 and 11), and temperatures were warmer during spring than fall ($P = 0.004$) (Table 5, Figures 12 and 13). There was a marginally significant effect of season on levels of NH_4^+ ($P = 0.065$) (Table 6, Figure 14). Conductivity increased with % agriculture ($P = 0.007$) and was higher in fall compared with spring ($P = 0.056$) (Table 7, Figures 15 and 16). The two-way interaction between % agriculture and WA had a significant effect on N:P ($P = 0.044$) (Table 8). No factors had a significant effect on DO or DIN (Tables 9 and 10).

Site	Coordinates	WA (km^2)	% Ag	DO (mg/L)	Temp °C	Cond. µS/cm^c	pH	SRP (ppm)	NH_4^+ (ppm)	NO_3^- (ppm)	DIN (ppm)
1	Headwaters N 47° 03.946' W 116° 47.148'	5.2	0	10.8	9.3	0.066	7.3	0.033	0.004	0.015	0.020
2	Headwaters N 47° 04.692' W 116° 46.274'	7.3	1	10.5	11.9	0.078	7.7	0.026	0.007	0.007	0.015
3	Cove Creek N 47° 16.893' W 117° 08.293'	30.6	27	10.3	12.5	0.351	7.7	0.028	0.022	3.954	3.987
4	S Fork Rock Crk N 47° 23.599' W 117° 14.902'	34.6	87	11.0	15.9	0.293	8.0	0.017	0.018	1.755	1.785
5	N Fork Rock Crk N 47° 25.239' W 117° 05.337'	116.2	77	7.6	18.9	0.299	7.2	0.024	0.025	0.524	0.553
6	Rattler Run Crk N 47° 31.442' W 117° 15.375'	149.1	96	10.0	16.4	0.433	8.1	0.083	0.119	4.752	4.881
7	California Crk N 47° 26.651' W 117° 04.683'	38.9	24	10.3	11.6	0.158	7.7	0.039	0.014	0.343	0.360
8	California Crk N 47° 30.767' W 117° 20.777'	24.8	44	10.8	14.1	0.234	8.1	0.029	0.013	1.202	1.221
9	Marshall Crk N 47° 35.737' W 117° 26.813'	90.7	39	11.0	14.0	0.299	8.1	0.019	0.018	1.214	1.238
10	Marshall Crk N 47° 33.903' W 117° 29.606'	22.6	35	14.8	18.4	0.292	8.2	0.013	0.024	1.053	1.084

Table 1. Spring site data. WA = watershed area, % Ag = % agriculture, DO = dissolved oxygen, Cond. = conductivity, SRP = soluble reactive phosphorus and DIN = dissolved inorganic nitrogen. Flow was not measured during spring sample collection.

Site	Coordinates	WA (km^2)	% Ag	DO (mg/L)	Temp °C	Cond. µS/cm^c	pH	SRP (ppm)	NH_4^+ (ppm)	NO_3^- (ppm)	DIN (ppm)	Flow (m/s)
1	Headwaters N 47° 03.946' W 116° 47.148'	5.2	0	13.7	8.7	0.090	7.1	0.094	0.019	0.002	0.025	0.012
2	Headwaters N 47° 04.692' W 116° 46.274'	7.3	1	10.3	10.9	0.132	6.9	0.065	0.006	0.000	0.009	0.009
3	Cove Creek N 47° 16.893' W 117° 08.293'	30.6	27	13.1	10.1	0.402	7.6	0.185	0.034	4.185	4.228	0.009
4	S Fork Rock Crk N 47° 23.599' W 117° 14.902'	34.6	87	9.7	10.3	0.364	6.1	0.028	0.002	1.704	1.716	0.076
5	N Fork Rock Crk N 47° 25.239' W 117° 05.337'	116.2	77	8.4	12.3	0.473	6.6	0.051	0.020	0.005	0.028	0.046
6	Rattler Run Crk N 47° 31.442' W 117° 15.375'	149.1	96	12.3	5.2	0.535	7.5	0.021	0.016	3.193	3.211	0.024
7	California Crk N 47° 26.651' W 117° 04.683'	38.9	24	10.1	7.7	0.230	7.5	0.047	0.001	2.141	2.145	0.003
8	California Crk N 47° 30.767' W 117° 20.777'	24.8	44	11.6	6.6	0.354	7.8	0.032	0.005	2.113	2.122	0.003
9	Marshall Crk N 47° 35.737' W 117° 26.813'	90.7	39	13.3	8.5	0.303	7.7	0.047	0.004	1.309	1.318	0.113
10	Marshall Crk N 47° 33.903' W 117° 29.606'	22.6	35	13.9	10.7	0.299	7.5	0.358	0.029	1.548	1.583	0.040

Table 2. Fall site data. WA = watershed area, % Ag = % agriculture, DO = dissolved oxygen, Cond. = conductivity, SRP = soluble reactive phosphorus and DIN = dissolved inorganic nitrogen.

Source	SS	F	P
WA	0.108	0.484	0.497
% Agriculture	0.141	0.632	0.438
Season	1.513	6.777	**0.019**

Table 3. Results of General Linear Model relating pH to watershed area (WA), % agriculture in watershed, and season. There was a significant effect of season ($P = 0.019$). No other factors were significant.

Source	SS	F	P
WA	0.001	0.011	0.920
% Agriculture	0.057	0.636	0.441
Season	0.665	7.472	**0.018**
WA x % agriculture	0.044	0.490	0.497
WA x season	0.004	0.040	0.845
% Agriculture x season	0.045	0.511	0.488
WA x % agriculture x season	0.105	1.177	0.299

Table 4. Results of General Linear Model relating SRP (ppm, log transformed) to watershed area (WA), % agriculture in watershed, season, and 2-way and 3-way interactions between independent variables. There was a significant effect of season ($P = 0.018$). No other factors were significant.

Source	SS	F	P
WA	0.032	0.005	0.944
% Agriculture	8.156	1.306	0.275
Season	76.44	12.24	**0.004**
WA x % agriculture	2.848	0.456	0.512
WA x season	0.680	0.109	0.747
% Agriculture x season	7.925	1.269	0.282
WA x % agriculture x season	0.001	0.000	0.990

Table 5. Results of General Linear Model relating temperature (°C) to watershed area (WA), % agriculture in watershed, season, and 2-way and 3-way interactions between independent variables. There was a significant effect of season ($P = 0.004$). No other factors were significant.

Source	SS	F	P
WA	0.010	0.054	0.820
% Agriculture	0.007	0.038	0.850
Season	0.744	4.116	**0.065**
WA x % agriculture	0.044	0.242	0.632
WA x season	0.067	0.369	0.556
% Agriculture x season	0.031	0.173	0.685
WA x % agriculture x season	0.441	2.440	0.144

Table 6. Results of General Linear Model relating NH_4^+ (ppm, log transformed) to watershed area (WA), % agriculture in watershed, season sampled, and 2-way and 3-way interactions between independent variables. Season was marginally significant ($P = 0.065$). No other factors were significant.

Source	SS	F	P
WA	0.010	1.776	0.203
% Agriculture	0.053	9.892	**0.007**
Season	0.023	4.280	**0.056**
% Agriculture x season	0.004	0.741	0.403

Table 7. Results of General Linear Model relating conductivity ($\mu S/cm^c$) to watershed area (WA), % agriculture in watershed, season, and 2-way interaction between % agriculture and season. There was a significant effect of % agriculture ($P = 0.007$), and a marginally significant effect of season ($P = 0.056$). No other factors were significant.

Source	SS	F	P
WA	0.410	0.708	0.413
% Agriculture	1.858	3.205	0.094
Season	0.786	1.356	0.262
WA x % agriculture	2.792	4.817	**0.044**

Table 8. Results of General Linear Model relating N:P (log transformed) to watershed area (WA), % agriculture in watershed, season, and 2-way interaction between independent variables. There was a significant effect with the interaction between WA and % agriculture ($P = 0.044$). No other factors were significant.

Source	SS	F	P
WA	47.23	0.112	0.743
% Agriculture	3.49	0.008	0.929
Season	77.42	0.184	0.675
WA x % agriculture	46.48	0.111	0.745
WA x season	131.93	0.314	0.586
% agriculture x season	435.67	1.037	0.329
WA x % agriculture x season	11.02	0.026	0.874

Table 9. Results of General Linear Model relating DO (mg/L) to watershed area (WA), % agriculture in watershed, season, and 2-way and 3-way interactions between independent variables. No factors were significant.

Source	SS	F	P
WA	0.372	0.507	0.490
% Agriculture	1.266	1.726	0.213
Season	0.003	0.004	0.950
WA x % agriculture	2.137	2.915	0.114
WA x season	0.020	0.028	0.870
% Agriculture x season	0.016	0.021	0.887
WA x % agriculture x season	0.033	0.045	0.835

Table 10. Results of General Linear Model relating dissolved inorganic nitrogen (DIN) (ppm, log transformed) to watershed area, % agriculture in watershed, season, and 2-way and 3-way interactions between independent variables. No factors were significant.

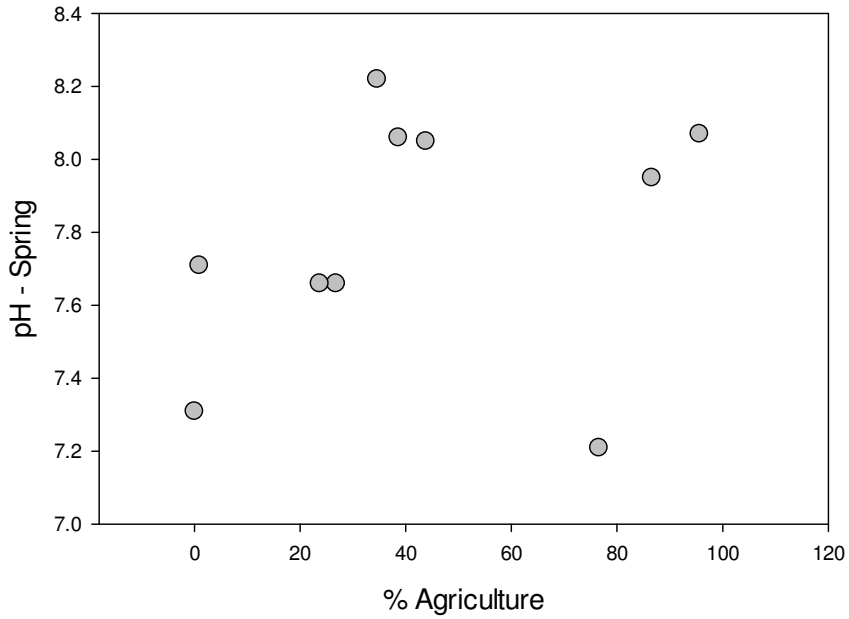

Figure 8. Scatter plot showing results of General Linear Model on spring pH. Season had a significant effect ($P = 0.019$).

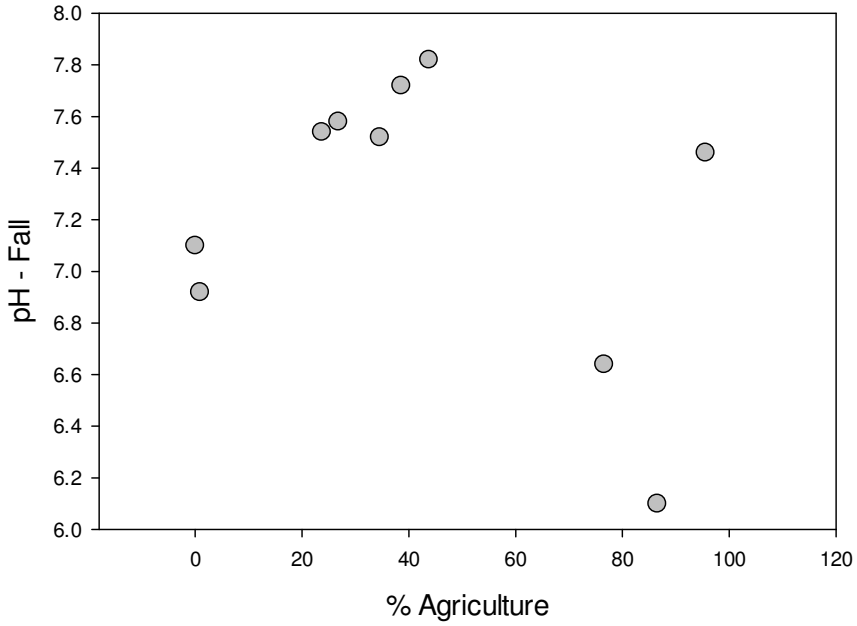

Figure 9. Scatter plot showing results of General Linear Model on fall pH. Season had a significant effect ($P = 0.019$).

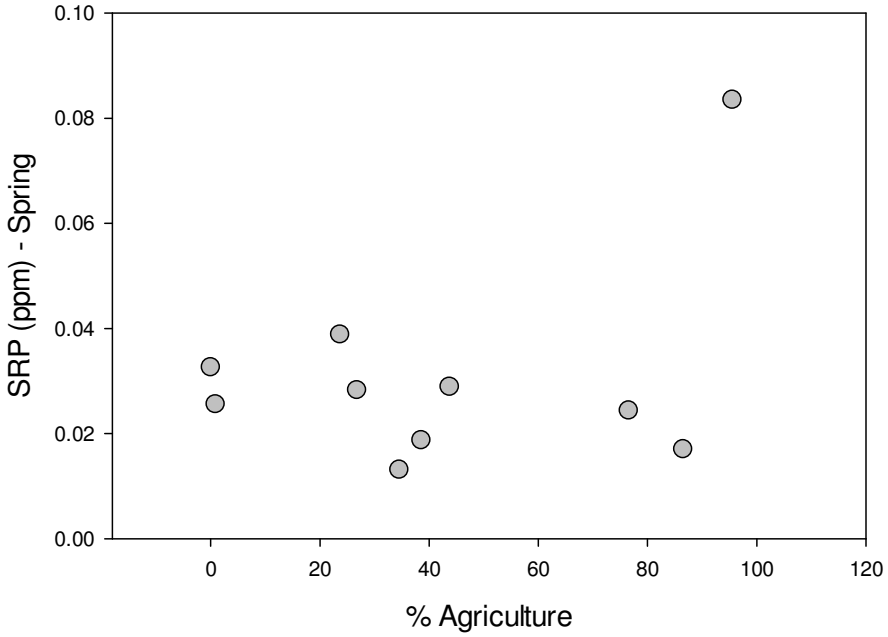

Figure 10. Scatter plot showing results of General Linear Model on spring soluble reactive phosphorus (SRP). Season had a significant effect ($P = 0.018$).

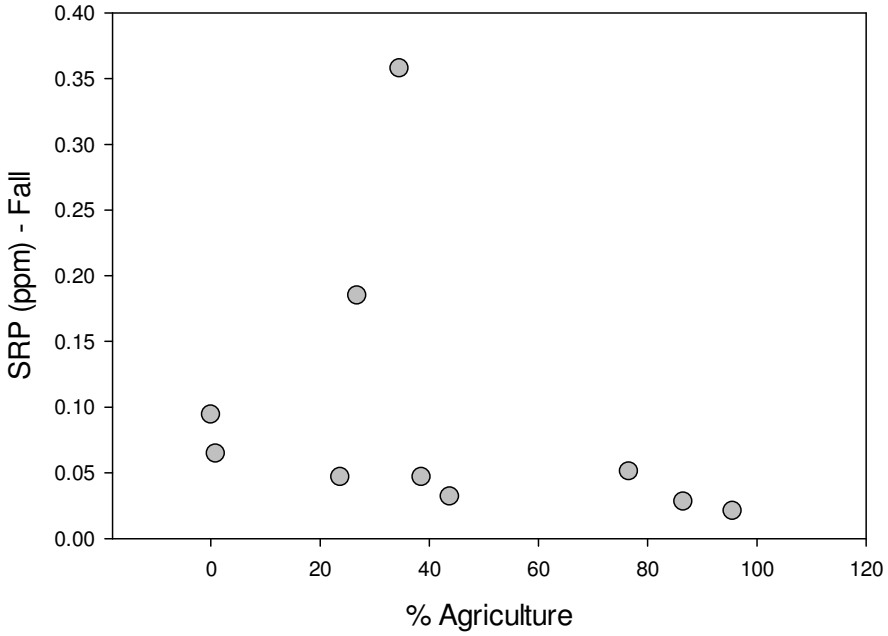

Figure 11. Scatter plot showing results of General Linear Model on fall soluble reactive phosphorus (SRP). Season had a significant effect ($P = 0.018$).

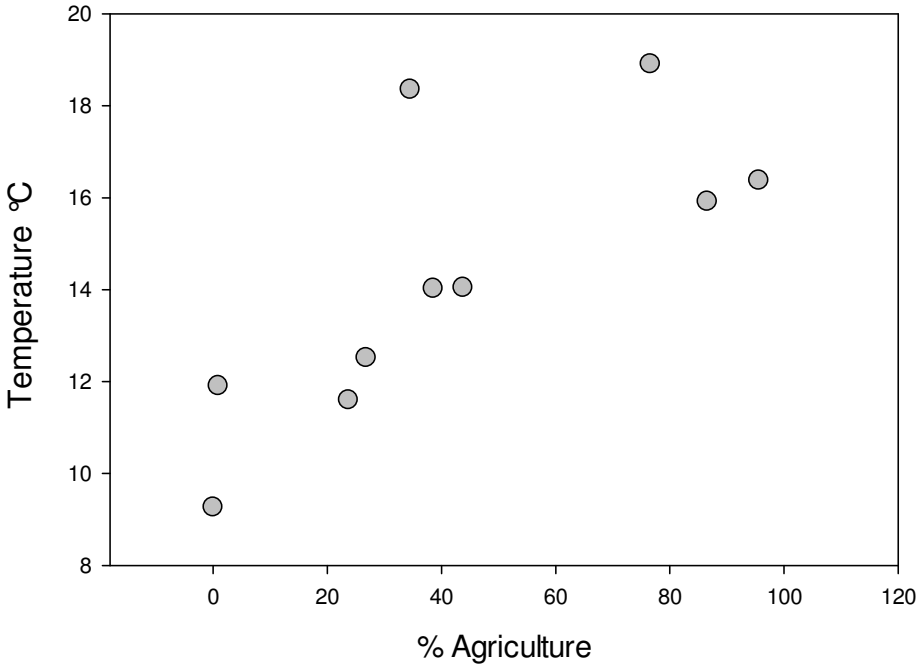

Figure 12. Scatter plot showing results of General Linear Model on spring temperature (°C). Season had a significant effect ($P = 0.004$).

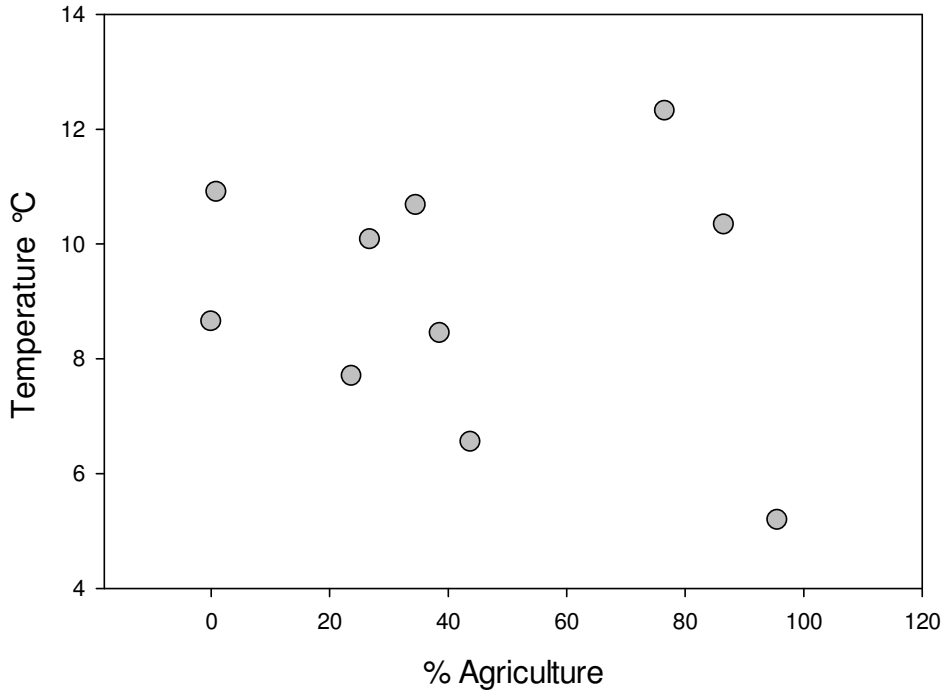

Figure 13. Scatter plot showing results of General Linear Model on fall temperature (°C). Season had a significant effect ($P = 0.004$).

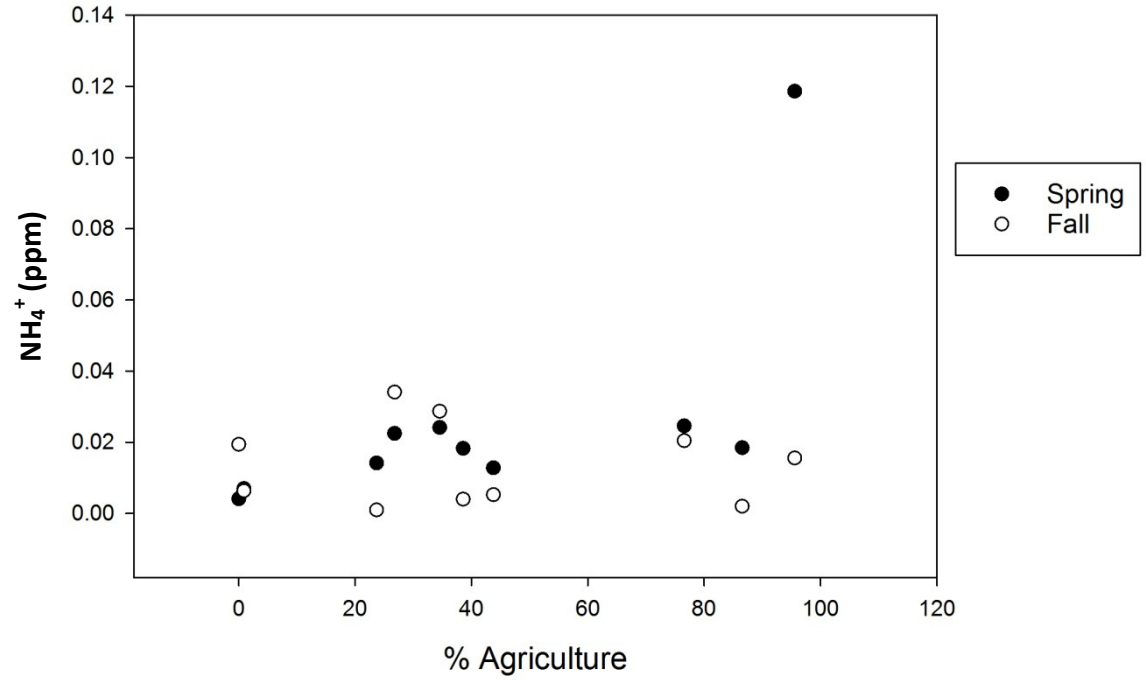

Figure 14. Scatter plot showing results of General Linear Model on NH_4^+. Season had a marginal effect ($P = 0.065$).

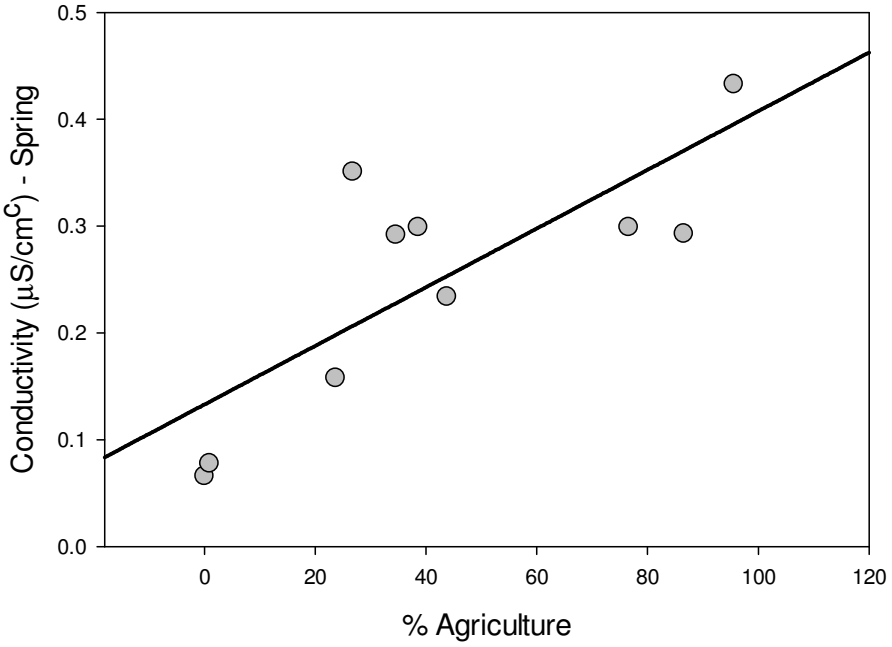

Figure 15. Scatter plot showing results of General Linear Model on spring conductivity. % agriculture had a significant effect ($P = 0.007$). Season was marginally significant ($P = 0.056$).

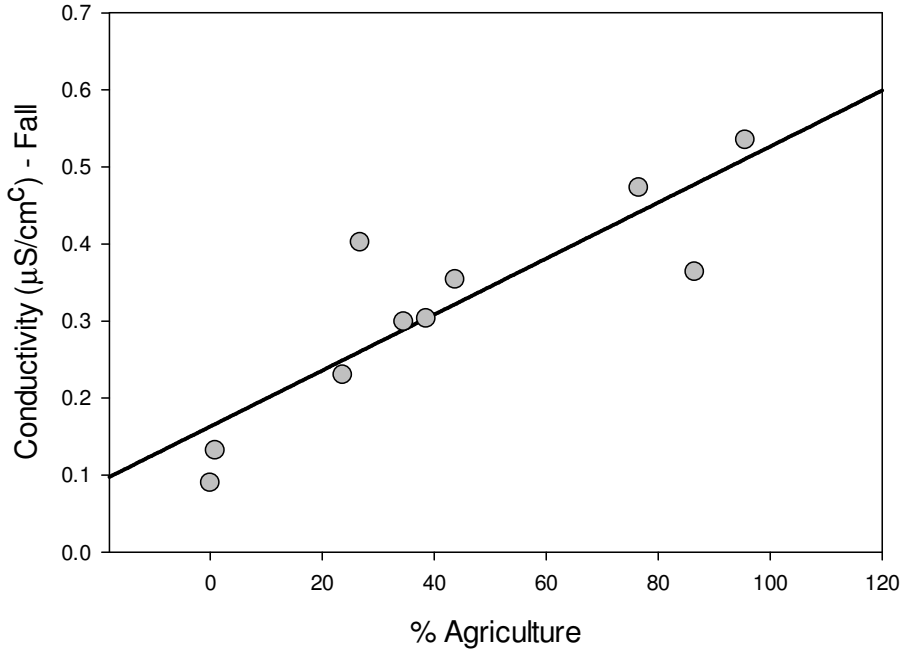

Figure 16. Scatter plot showing results of General Linear Model on fall conductivity. % agriculture had a significant effect ($P = 0.007$). Season was marginally significant ($P = 0.056$).

Molecular Data

T-RFLP

No physical or chemical factors had a significant effect on the # of taxa detected with the HaeIII restriction enzyme (Table 11). However, % taxa dominance for HaeIII T-RF's decreased with watershed area, so relative abundance of bacterial taxa identified with this enzyme was more even at sites with a larger watershed area ($P = 0.052$) (Table 12, Figures 17 and 18). There were more taxa detected with the HhaI enzyme in spring than in fall ($P = 0.032$) (Table 13, Figures 19 and 20), and higher % dominance (lower evenness) in fall compared to spring ($P = 0.007$) (Table 14, Figure 22 and 23).

Source	SS	F	P
WA	3.457	0.777	0.390
% Agriculture	4.639	1.059	0.318
Season	4.675	0.283	0.601
Conductivity	23.030	1.485	0.239
pH	0.170	0.010	0.921
DIN (log transformed)	10.969	0.678	0.421
SRP (log transformed)	7.827	0.479	0.498
NH_3	46.697	3.289	0.086

Table 11. Results of General Linear Model relating # of taxa detected with the HaeIII restriction enzyme to watershed area (WA), % agriculture in the watershed, season and water data. No factors were significant.

Source	**SS**	**F**	**P**
WA	1054.160	4.348	**0.052**

Table 12. Results of General Linear Model relating % taxa dominance detected with the HaeIII restriction enzyme to watershed area (WA). There was a significant effect of WA ($P = 0.052$).

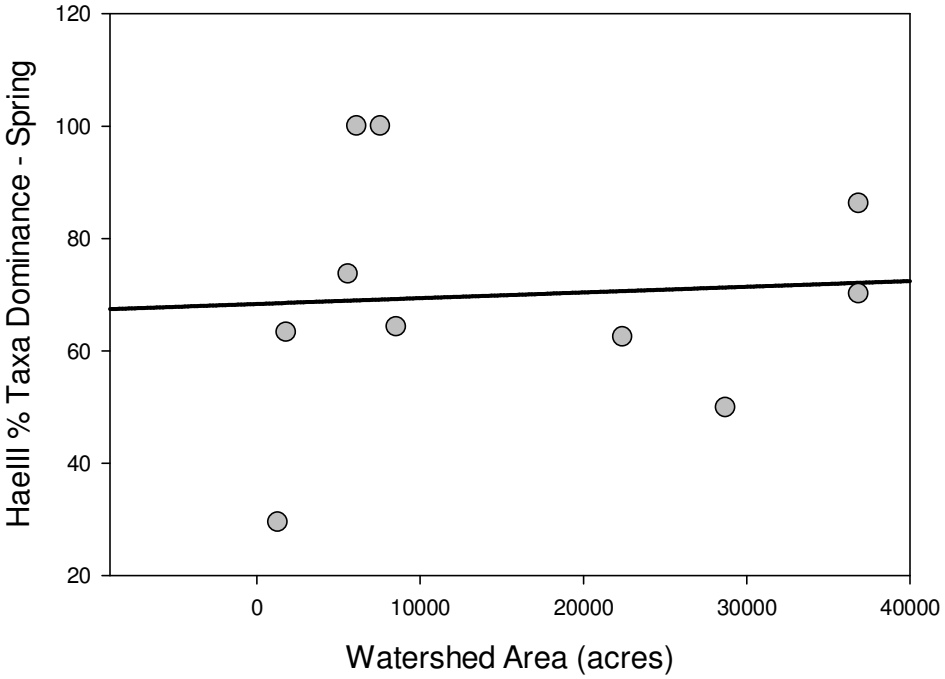

Figure 17. Scatter plot showing results of General Linear Model relating spring % taxa dominance detected with the HaeIII restriction enzyme to watershed area (acres). There was a significant effect of WA ($P = 0.052$).

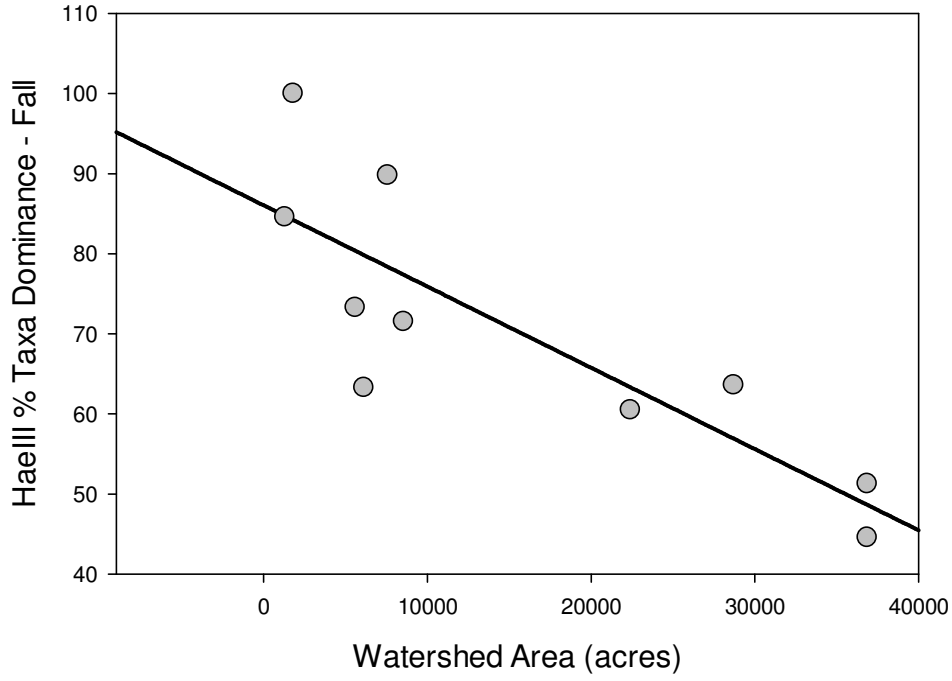

Figure 18. Scatter plot showing results of General Linear Model on fall % taxa dominance detected with the HaeIII restriction enzyme. There was a significant effect of WA ($P = 0.052$).

Source	SS	F	P
WA	6.707	0.212	0.652
% Agriculture	12.252	0.387	0.544
Season	178.560	5.643	**0.032**
WA x % agriculture	62.494	1.975	0.182
WA x season	44.943	1.420	0.253

Table 13. Results of General Linear Model relating # of taxa detected with the HhaI restriction enzyme to watershed area (WA), % agriculture in watershed, season, and 2-way interactions. There was a significant effect of season ($P = 0.032$). No other factors were significant.

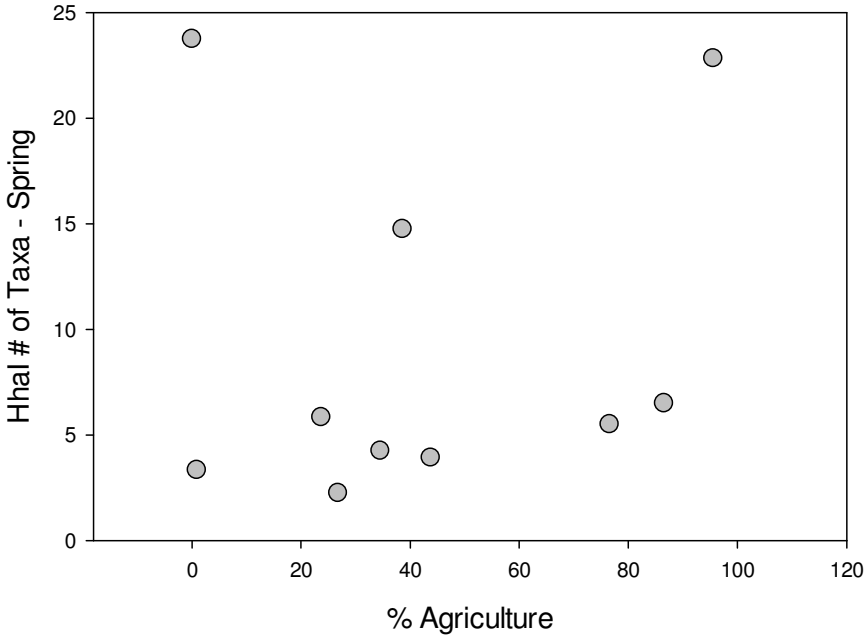

Figure 19. Scatter plot showing results of General Linear Model on spring # of taxa detected with the HhaI restriction enzyme. There was a significant effect of season ($P = 0.032$).

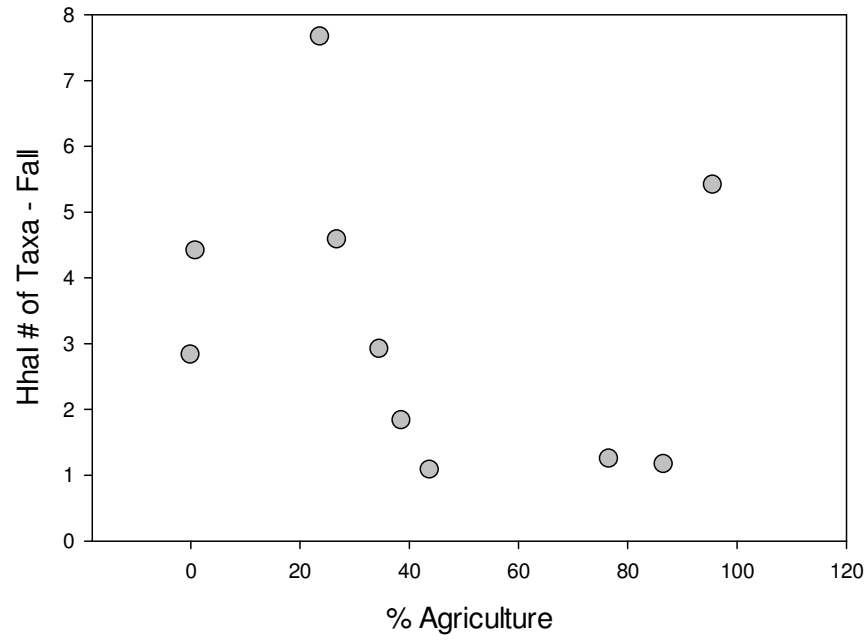

Figure 20. Scatter plot showing results of General Linear Model on fall # of taxa detected with the HhaI restriction enzyme. There was a significant effect of season ($P = 0.032$).

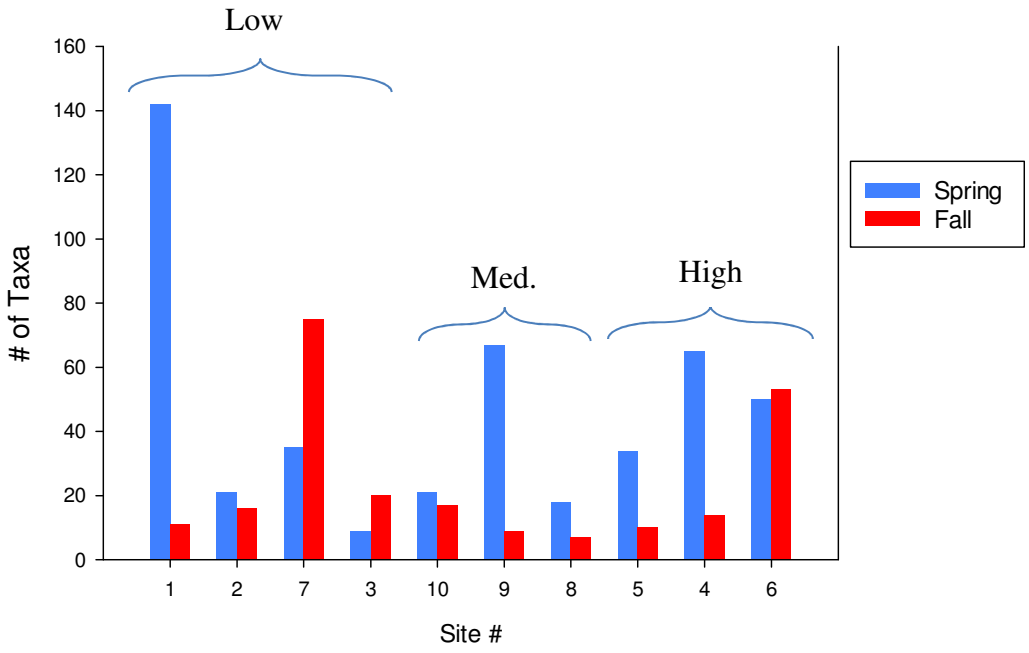

Figure 21. # of taxa detected with both restriction enzymes (data combined), and grouped by % agriculture in their drainages (low: 0-33%, med.: 34-68%, high: 69-100%).

Source	SS	F	P
WA	75.070	0.311	0.586
% Agriculture	621.050	2.570	0.130
Season	2402.430	9.943	**0.007**
WA x % agriculture	983.960	4.072	0.062

Table 14. Results of the General Linear Model relating % taxa dominance detected with the HhaI restriction enzyme to watershed area (WA), % agriculture in watershed, season, and the 2-way interactions of WA and % agriculture. There was a significant effect of season ($P = 0.007$). No other factors were significant.

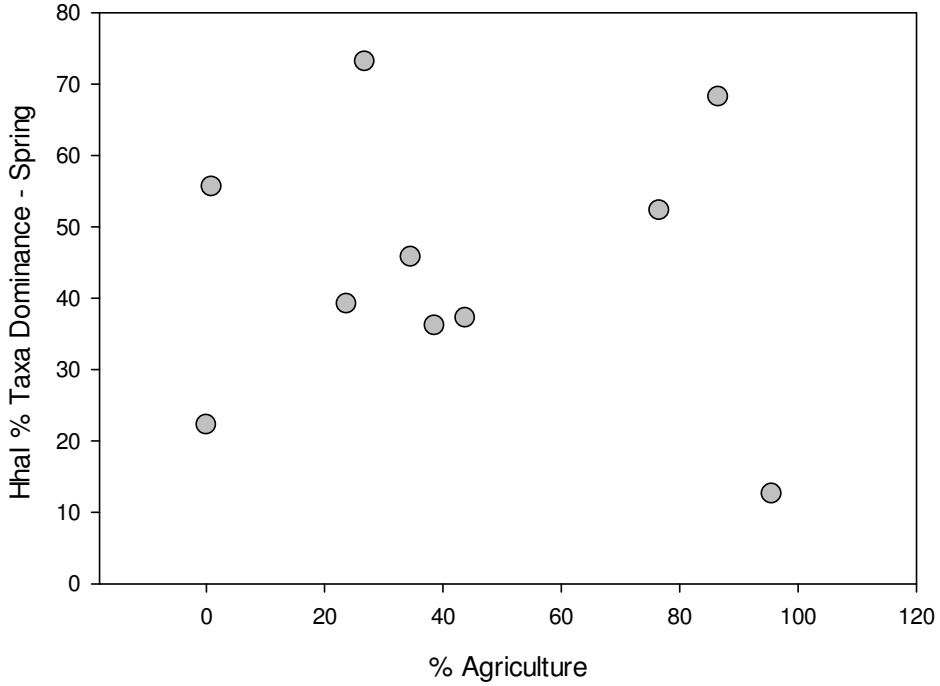

Figure 22. Scatter plot showing results of General Linear Model on spring % taxa dominance detected with the HhaI restriction enzyme. There was a significant effect of season ($P = 0.007$).

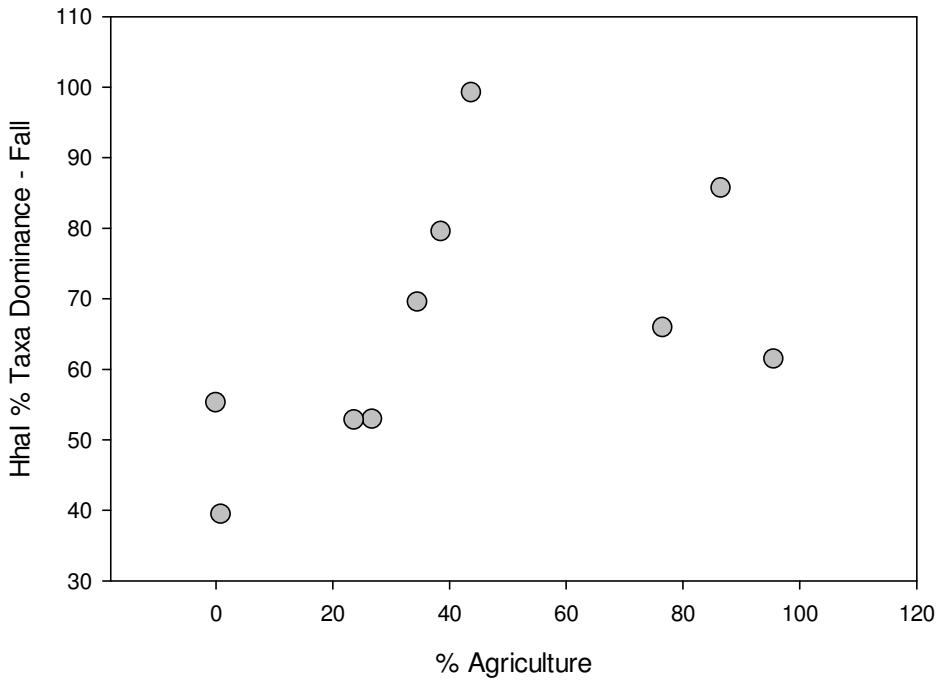

Figure 23. Scatter plot showing results of General Linear Model on fall # of taxa detected with the HhaI restriction enzyme. There was a significant effect of season ($P = 0.007$).

HhaI digested samples produced the greatest numbers of T-RFs. HhaI cleavage of amplified *16S rRNA* products yielded a total of 125 different T-RFs in spring (73 found in spring only) and 68 in fall (16 found in fall only); both seasons combined yielded 52 shared T-RFs (found in both) (Table 15). For spring, the three most abundant fragment lengths for all sites combined were 67bp, 97bp and 57bp; for fall they were: 56bp, 67bp and 55bp (Table 16). HaeIII cleavage of amplified *16S rRNA* fragments yielded a total of 106 different T-RFs in spring and 64 in fall; both seasons combined yielded 41 shared T-RFs (Table 17). For spring, the top three most abundant fragment lengths for all sites combined were 32bp, 67bp and 217bp; for fall they were: 31bp, 380bp and 67bp (Table 18).

T-RFs unique to spring		T-RFs unique to fall	T-RFs found in both	
31	228	34	35	97
36	229	85	37	175
40	231	178	38	201
43	232	331	39	202
44	233	341	41	203
49	235	361	55	204
50	236	376	56	205
53	278	391	57	206
54	295	414	61	208
58	309	423	62	210
59	334	522	63	227
60	337	563	67	230
66	338	569	68	277
69	343	644	73	293
75	344	812	77	294
83	359	844	78	342
94	364		79	358
96	368		84	363
98	369		86	365
99	370		87	366
105	372		88	367
106	373		89	378
116	374		90	390
117	402		91	568
142	403		92	570
146	412		93	571
154	472			
185	476			
186	510			
197	514			
200	520			
207	527			
209	562			
211	566			
215	567			
218	755			
226				

Table 15. HhaI fragments (bp) for spring and fall.

Spring T-RFs	Freq.	Spring T-RFs	Freq.	Fall T-RFs	Freq.	Fall T-RFs	Freq.
67	58	142	5	56	58	568	2
97	47	204	5	67	54	569	2
57	44	514	5	55	21	570	2
90	43	49	4	91	16	644	2
55	41	58	4	90	14	812	2
56	41	73	4	97	14		
205	39	99	4	294	13		
39	33	206	4	37	12		
77	32	236	4	86	10		
84	32	295	4	205	9		
92	31	368	4	84	8		
31	30	520	4	201	8		
201	30	35	3	210	8		
86	25	78	3	57	7		
66	24	106	3	92	7		
61	22	207	3	293	7		
88	22	209	3	35	6		
91	21	278	3	89	6		
211	20	366	3	365	6		
342	20	373	3	38	5		
365	19	378	3	202	5		
38	17	403	3	378	5		
363	17	567	3	68	4		
227	16	568	3	178	4		
68	14	41	2	203	4		
94	13	43	2	227	4		
203	13	44	2	341	4		
343	13	50	2	342	4		
89	12	54	2	61	3		
367	12	98	2	63	3		
372	12	116	2	77	3		
208	11	146	2	88	3		
63	10	154	2	363	3		
93	10	175	2	34	2		
40	9	197	2	39	2		
62	9	200	2	41	2		
231	9	226	2	62	2		
105	7	228	2	73	2		
202	7	235	2	79	2		
210	7	293	2	85	2		
36	6	294	2	87	2		
75	6	334	2	175	2		
215	6	338	2	204	2		
218	6	344	2	206	2		
230	6	359	2	208	2		
277	6	369	2	230	2		
364	6	370	2	277	2		
374	6	562	2	361	2		
412	6	571	2	563	2		

Table 16. HhaI fragments (bp) and their frequencies for spring and fall. See Appendix for single occurrence fragments (Table 26).

T-RFs unique to spring		T-RFs unique to fall	T-RFs found in both	
36	212	71	31	215
40	214	93	32	216
41	220	100	33	217
42	221	131	35	218
44	226	198	38	219
49	227	209	39	222
54	229	233	55	235
58	230	248	56	249
59	231	250	62	251
66	234	261	63	257
68	237	307	64	292
69	239	313	67	329
72	240	315	192	379
77	243	321	193	380
79	244	325	195	381
96	245	328	196	399
97	246	398	199	401
98	254	406	200	403
116	255	454	202	404
128	258	613	206	611
138	259	693	213	
172	260	700		
173	262			
186	265			
187	266			
190	267			
194	270			
197	297			
201	320			
203	377			
204	427			
210	783			

Table 17. HaeIII fragments (bp) for spring and fall.

Spring T-RFs	Freq.	Spring T-RFs	Freq.	Fall T-RFs	Freq.	Fall T-RFs	Freq.
32	52	216	3	31	61	39	2
67	23	243	3	380	25	64	2
217	12	255	3	67	22	93	2
39	11	265	3	32	10	100	2
193	11	35	2	37	8	131	2
222	11	41	2	206	8	192	2
58	10	42	2	213	8	209	2
66	10	44	2	38	7	218	2
329	9	49	2	35	6	233	2
38	8	54	2	193	6	235	2
196	8	59	2	215	6	248	2
212	8	72	2	329	5	249	2
230	8	77	2	63	4	250	2
266	8	79	2	196	4	251	2
380	8	98	2	199	4	257	2
33	7	190	2	202	4	261	2
40	7	194	2	216	4	307	2
257	7	197	2	217	4	313	2
63	6	199	2	222	4	315	2
381	6	204	2	381	4	398	2
62	5	210	2	613	4	399	2
262	5	214	2	62	3	401	2
64	4	218	2	195	3	406	2
138	4	227	2	33	2		
192	4	229	2				
202	4	231	2				
206	4	237	2				
213	4	244	2				
215	4	245	2				
219	4	246	2				
235	4	251	2				
259	4	254	2				
297	4	260	2				
377	4	292	2				
403	4	320	2				
31	3	399	2				
36	3	401	2				
186	3	404	2				
200	3	611	2				

Table 18. HaeIII fragments (bp) and their frequencies for spring and fall. See Appendix for single occurrence fragments (Table 27).

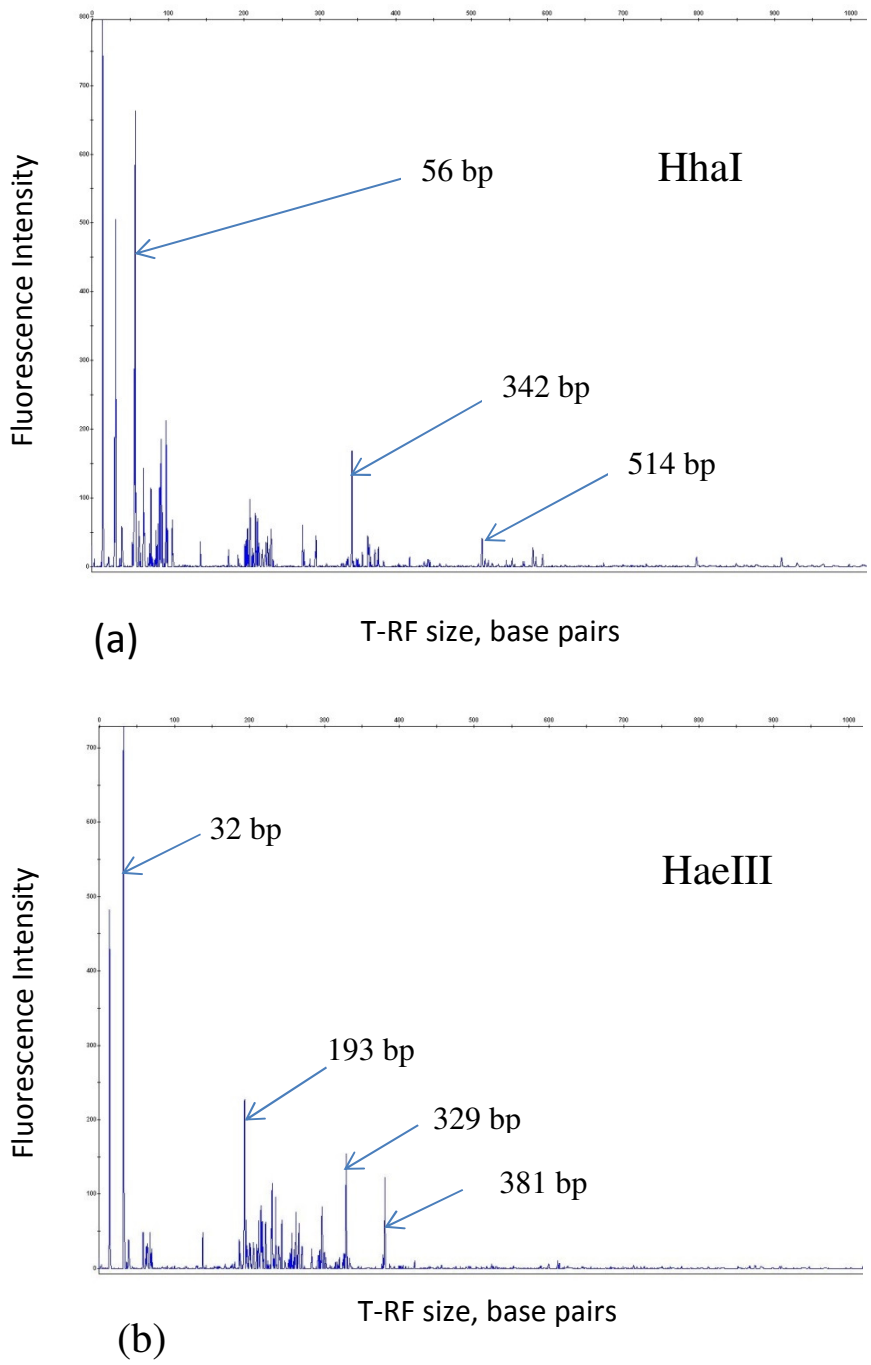

Figure 24. T-RF electropherograms for sample B1.5 cut with a) HhaI and b) HaeIII. Select peaks are labeled with their associated fragment length as a reference. See Appendix, Figures 38-77, for electropherograms from the first replicate run for both restriction enzymes.

A one-way analysis of variance (Levene test) was conducted to compare within-site variation in # of taxa (per sample) among sites. For spring: HaeIII # taxa, sites #1 and #4 showed the highest variation ($P < 0.0001$) (Table 19, Figure 26); and HhaI # taxa, sites #4 and #5 showed the highest variation ($P < 0.007$) (Table 20, Figure 25). For fall: sites #6 and #7 showed the highest variation for both HaeIII (Table 19, Figure 28) and HhaI (Table 20, Figure 27) ($P < 0.001$). The lowest variation for fall HaeIII # taxa were sites #2 and #5 (Table 19, Figure 28), and for HhaI # taxa it was sites #4 and #8 (Table 20, Figure 27).

Site	Std. Dev	Mean absolute difference to mean	Mean absolute difference to median
B1*	**10.590**	9.083	9.083
B2	1.732	1.333	1.333
B3**	**0.492**	0.417	0.417
B4*	**10.998**	7.444	5.333
B5	1.497	1.222	0.917
B6	1.472	1.056	0.833
B7	1.602	1.278	1.667
B8**	**0.492**	0.417	0.417
B9	2.769	2.333	2.333
B10	2.010	1.361	0.917
C1	0.801	0.611	0.583
C2**	**0.408**	0.278	0.167
C3	0.801	0.611	0.583
C4	1.049	0.833	0.833
C5**	**0.683**	0.444	0.333
C6*	**5.794**	4.944	4.000
C7*	**10.080**	7.778	6.583
C8	1.000	0.833	0.667
C9	1.215	0.833	0.750
C10	1.183	0.833	0.833

Table 19. One-way analysis of HaeIII # of taxa by site for spring (B1-B10, Levene test, ($P < 0.001$) and fall (C1 – C10, Levene test, $P < 0.001$). * = sites with highest variation, ** = sites with lowest variation.

Site	Std. Dev	Mean absolute difference to mean	Mean absolute difference to median
B1	8.067	5.750	5.750
B2**	**1.966**	1.667	1.667
B3**	**1.943**	1.250	1.083
B4*	**12.380**	8.333	6.000
B5*	**11.210**	8.000	5.000
B6	2.338	1.833	1.833
B7	3.642	2.500	2.500
B8	3.040	2.083	2.083
B9	9.294	7.500	6.750
B10	2.300	1.917	1.917
C1	0.816	0.667	0.667
C2	3.024	2.417	2.417
C3	3.513	2.306	1.917
C4**	**0.516**	0.389	0.333
C5	1.255	1.083	1.083
C6*	**7.826**	6.722	5.250
C7*	**8.010**	5.722	4.833
C8**	**0.204**	0.139	0.083
C9	0.816	0.556	0.500
C10	1.855	1.583	1.583

Table 20. One-way analysis of HhaI # of taxa by site for spring (B1-B10, Levene test, $P < 0.007$) and fall (C1-C10, Levene test, $P < 0.001$). * = sites with highest variation, ** = sites with lowest variation.

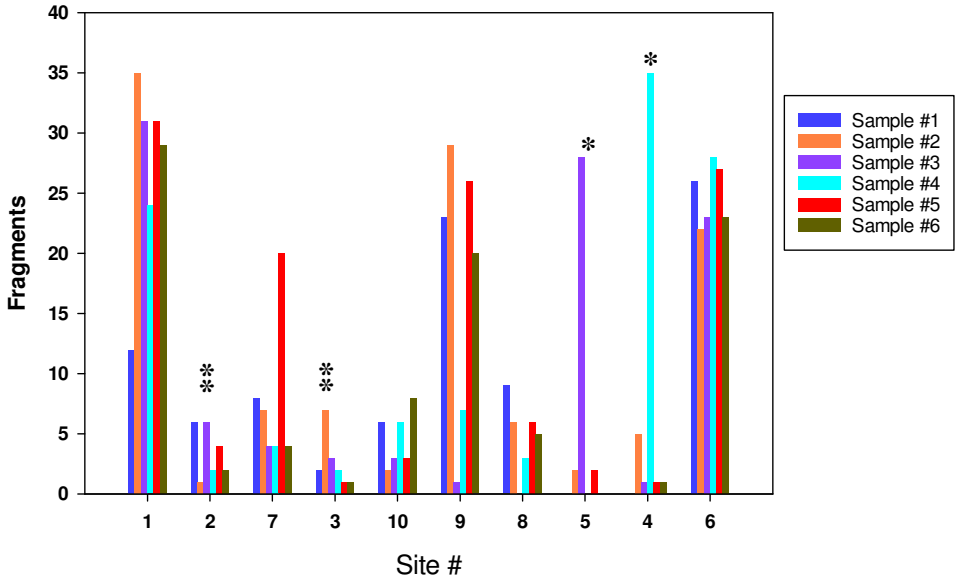

Figure 25. Spring HhaI fragments for all 10 sites, 6 samples per site. * = highest variation, ** = lowest variation. Levene test ($P < 0.001$).

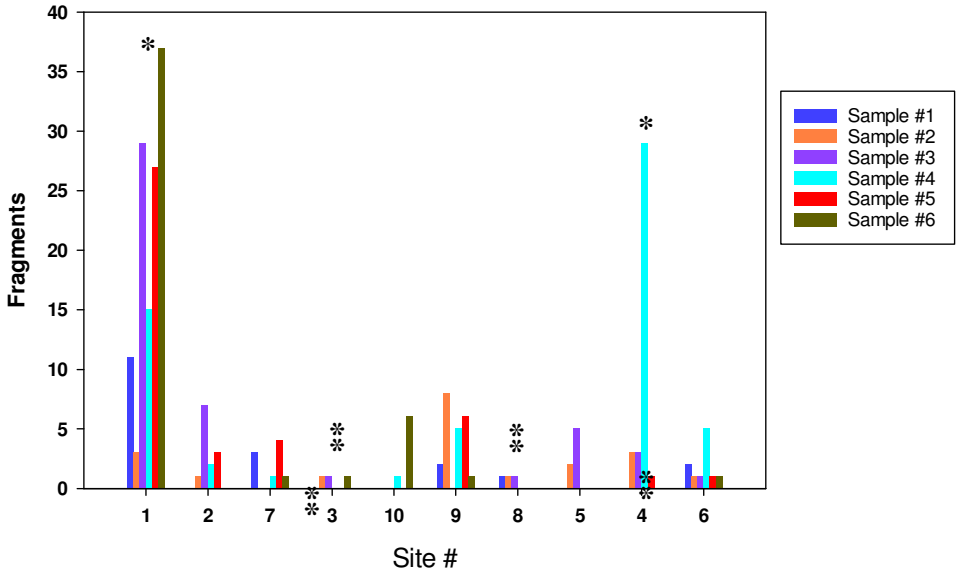

Figure 26. Spring HaeIII fragments for all 10 sites, 6 samples per site. * = highest variation, ** = lowest variation. Levene test ($P < 0.001$).

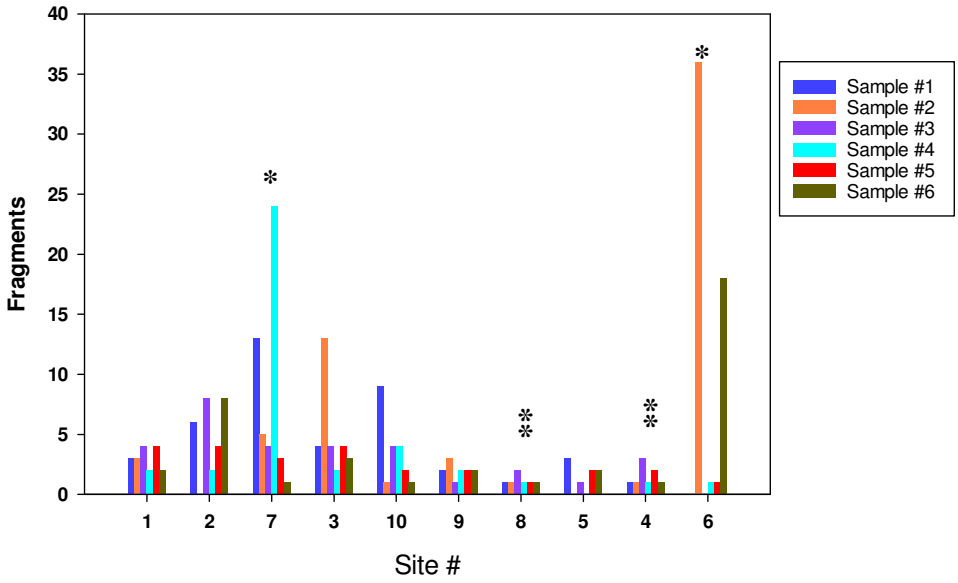

Figure 27. Fall HhaI fragments for all 10 sites, 6 samples per site. * = highest variation, ** = lowest variation. Levene test ($P < 0.001$).

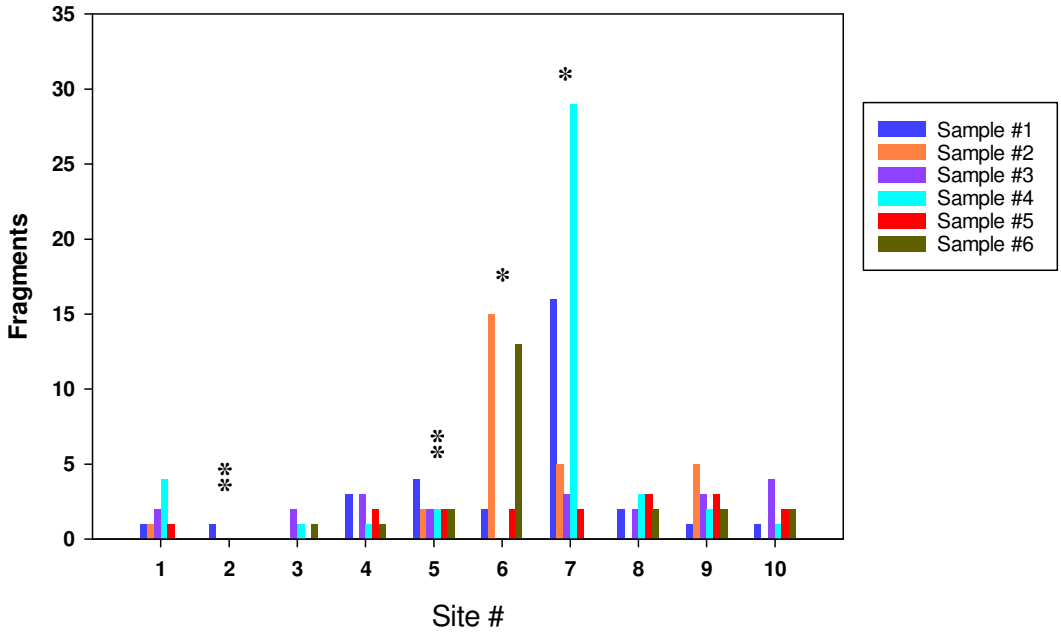

Figure 28. Fall HaeIII fragments for all 10 sites, 6 samples per site. * = highest variation, ** = lowest variation. Levene test ($P < 0.001$).

qPCR

All 120 samples were run in triplicate and the Cq (quantification cycle /cycle threshold) values were averaged to obtain an average Cq per sample. Averages were also calculated for each site and season by averaging the 6 sample Cq values per site. (Tables 21 and 22). See Appendix for quantitative curves, Figures 35, 36 and 37.

Cq Avg	% Ag	Site
24.67	96	6
24.87	35	10
25.00	87	4
25.89	77	5
26.03	44	8
26.37	27	3
26.90	39	9
27.59	0	1
27.83	24	7
28.63	1	2

Table 21. Cq threshold averages for *amoA* per site for spring, listed in ascending order. Lower Cq values correspond to a higher abundance of nitrifying bacteria.

Cq Avg	% Ag	Site
24.58	87	4
24.77	96	6
25.10	35	10
25.41	77	5
25.68	0	1
25.78	27	3
26.58	44	8
26.68	1	2
26.92	39	9
27.74	24	7

Table 22. Cq threshold averages for *amoA* per site for fall, listed in ascending order. Lower Cq values correspond to a higher abundance of nitrifying bacteria.

Relationships between physical and chemical variables and cycles to threshold (Cq) were assessed with General Linear Models and JMP 6.0 statistical software. The significance level for all analyses was $\alpha \leq 0.05$. The General Linear Model was run with % agriculture in the watershed, season, dissolved inorganic nitrogen (DIN) and 2-way interactions between % agriculture and season, % agriculture and DIN, season and DIN, and a 3-way interaction with season, DIN and % agriculture. Cq declined significantly with increasing % agriculture ($P = 0.007$) (Table 23, Figures 29-32), which indicates an exponential increase in nitrifier abundance with % agriculture. No other factors were significant.

Source	SS	F	P
% Agriculture	9.050	10.60	**0.007**
Season	0.387	0.454	0.513
DIN	0.284	0.332	0.575
% Agriculture x season	0.269	0.315	0.590
% Agriculture x DIN	0.022	0.025	0.876
Season x DIN	0.493	0.577	0.462
Season x DIN x % agriculture	0.705	0.826	0.381

Table 23. Results of General Linear Model relating *amoA* abundance (qPCR Cq values) to % agriculture in the watershed, season, dissolved inorganic nitrogen (DIN), and 2-way and 3-way interactions between independent variables. There was a significant effect of % agriculture ($P = 0.007$). No other factors were significant.

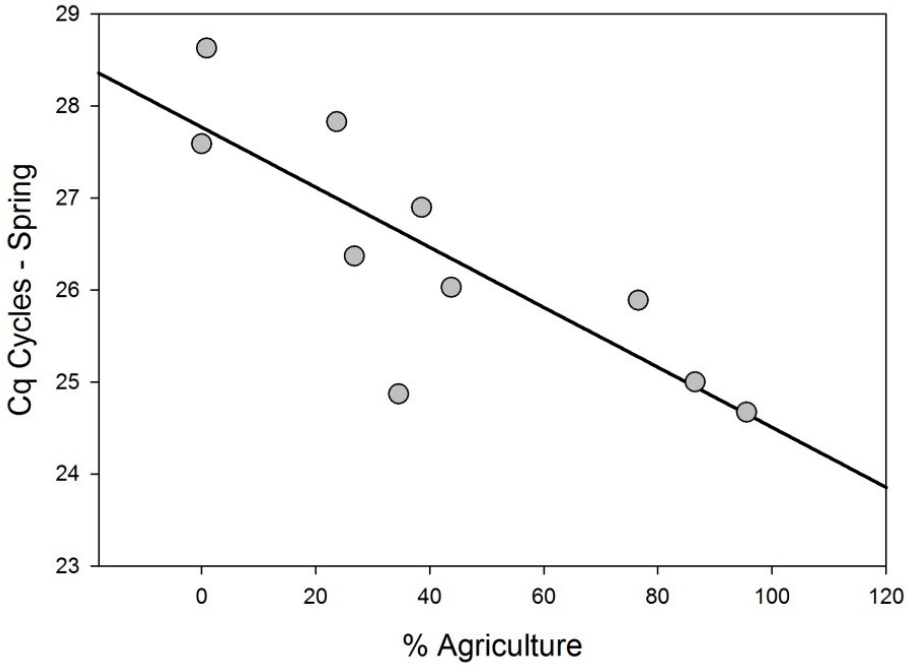

Figure 29. Scatter plot showing results of General Linear Model on spring abundance of *amoA* (lower Cq indicates a higher abundance of *amoA*). There was a significant effect of % agriculture ($P = 0.007$).

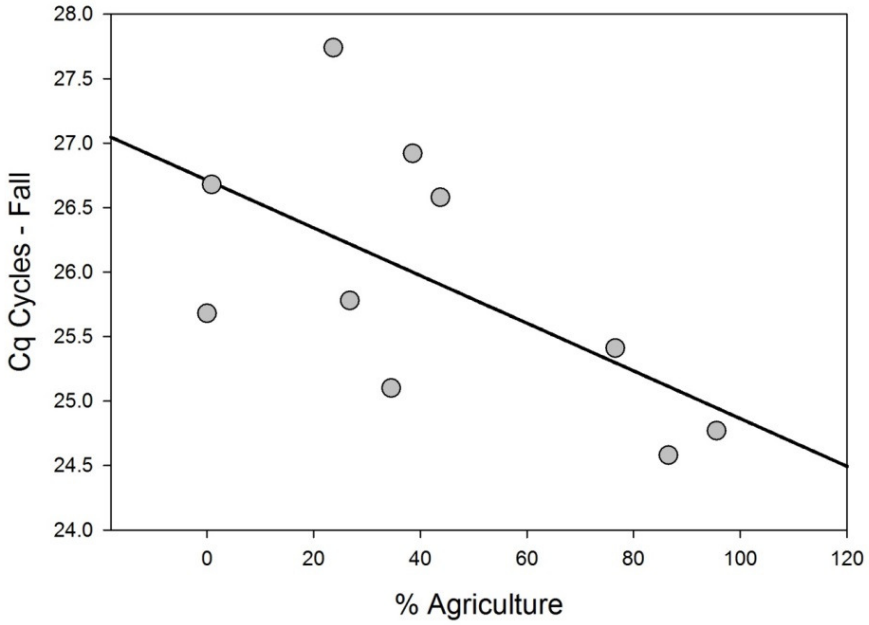

Figure 30. Scatter plot showing results of General Linear Model on fall abundance of *amoA* (lower Cq indicates a higher abundance of *amoA*). There was a significant effect of % agriculture ($P = 0.007$).

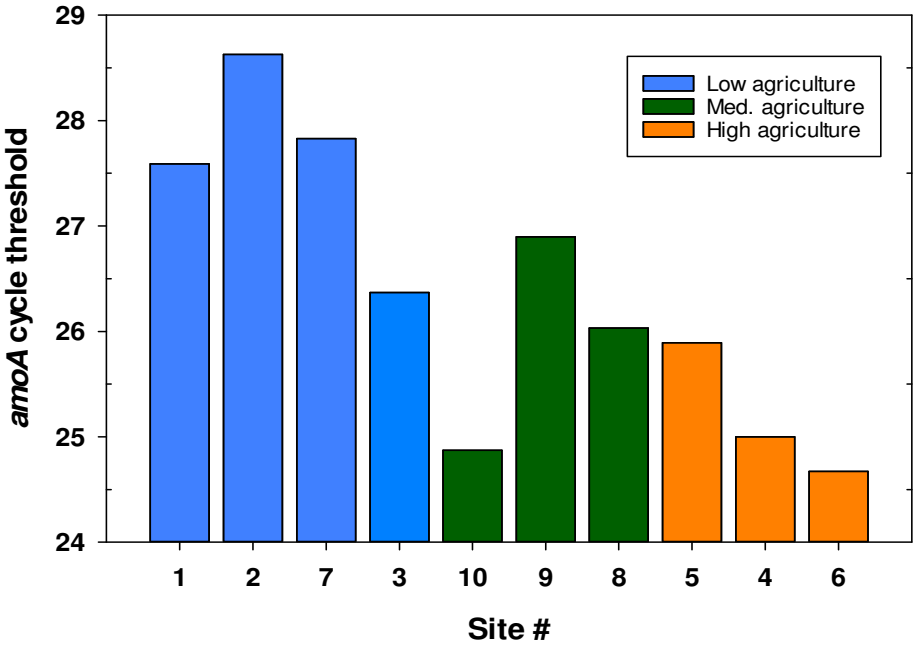

Figure 31. Cq (cycle thresholds) for spring samples, separated by % agriculture in the drainages (low: 0-33%, med.: 34-68%, high: 69-100%). There was a significant effect of % agriculture ($P = 0.007$).

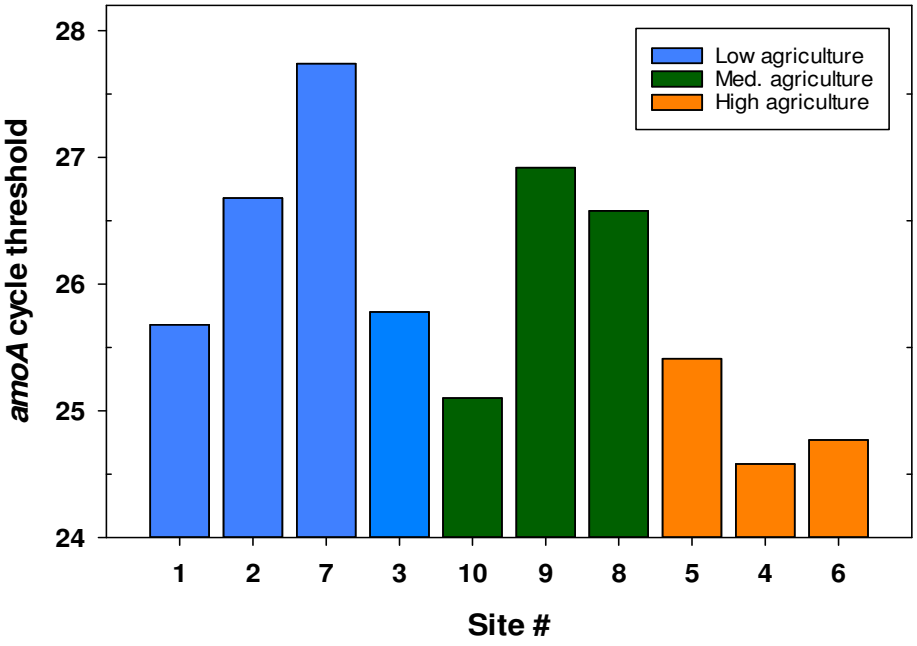

Figure 32. Cq cycle thresholds for fall samples, separated by % agriculture in the drainages (low: 0-33%, med.: 34-68%, high: 69-100%). There was a significant effect of % agriculture ($P = 0.007$).

Discussion

Aquatic systems undergo constant dynamic change and no single factor has been identified as having sole control over microbial distribution or abundance (Kemp and Dodds, 2002). Knowledge regarding microbial biogeographic patterns, from millimeters to 1,000's of kilometers, is lacking (Fierer *et al*., 2007), as well as information regarding their response time to changes in physical and chemical properties of their environment. The complex interaction of environmental parameters makes it challenging to identify key factors that truly affect microbial communities in the system.

My research does, however, show a strong relationship across the Latah Creek Watershed between increased % agriculture and increased nitrifier abundance; stronger than any other factor. Nitrifiers ultimately control the conversion of ammonia to nitrate, and they are slow growers, so the presence of a high abundance of nitrifiers could indicate that they are responding to chronic ammonia influx versus pulses of influx, which are transient. Therefore, it is not unusual that the NH_4^+ levels were not high at the sites where there was a higher concentration of nitrifying bacteria, since the *in situ* measurements represent snapshots in time, as opposed to long-term conditions. In addition, during the spring, increased heterotrophic uptake of NH_4^+ can affect levels; the majority of sample sites were inundated with invasive reed canary grass (*Phalaris arundinacea*), which reached six feet tall by the fall sampling period. It is possible that biotic uptake by reed canary grass in the spring had a significant impact on reducing the concentration levels of NH_4^+.

Nitrate has the highest mobility of the N compounds, so an increase in the production of nitrate, combined with its high mobility, can result in nitrate being transported out of the ecosystem before heterotrophic uptake or reduction to N_2 by denitrifiers. Combined with the anthropogenic production of ammonia, this downstream movement of high concentrations of nitrate represents a fundamental shift in the nitrogen cycle.

Although % agriculture in the drainage did not have a significant effect on diversity based on the T-RF data, other physical variables did show significant interactions. Season had a significant effect on species richness: in spring the # of taxa increased with % agriculture, and in the fall it decreased. The # of taxa was higher overall for all spring samples versus fall samples, which could be a result of temperature alone, or some combination of temperature, pH and conductivity (which were all affected by season). Watershed area significantly impacted species evenness: in the spring there was a lower % taxa dominance with increased watershed area, whereas fall showed a clear negative correlation. Ultimately, spring had a higher number of species and a more even distribution of these species as compared to fall. With sequence data, the distribution of functional groups (e.g., nitrifiers and denitrifiers) could be identified, since the fragment analysis alone does not identify genus or species. Consequently, only comparative diversity measures can be made in this study versus absolute measures. The majority of the taxa - for richness and evenness - could, in fact, be nitrifiers responding to % agriculture in the drainage.

Since samples were not pooled, a unique opportunity existed to assess variation within each sample site, and to address temporal and spatial distribution. Overall, spring showed more variation than fall sites for both restriction enzymes, and encompassed the three sites with the highest variation. Fall showed less variation and encompassed the two sites with the lowest variation. The data clearly show high diversity throughout the watershed, both temporally and spatially, for # of taxa even though samples were taken from within 6" to 15' of one another. It begs the question of what factor, or factors, causes this variation; is it distance, substrate, physical and chemical parameters, or something else?

Several physical and chemical variables were significantly affected by season; these included pH, SRP, temperature, NH_4^+, and conductivity. These correlations may help explain landscape-scale conditions that could have impacted the microbial biogeographic patterns. pH was higher in the spring than in the fall, which could have been a result of calcium carbonate, a known component of Palouse loess, entering the streams due to runoff from spring snow melt and/or precipitation. *N. europaea* prefers a pH range of 6.0

– 9.0 (Kirchman, 2012), which fell within site measurements for both seasons. SRP was slightly higher in the fall compared to the spring. This could have been a result of summer evaporation of the water column, which resulted in a higher concentration of SRP. As would be expected, water temperatures were higher overall for spring compared to fall. Season was marginally significant on NH_4^+ and conductivity; with higher levels in spring for both variables. As with SRP, higher concentrations of NH_4^+in the spring may be reflective of summer evaporation. Conductivity is a measure of the ability of water to pass an electrical current through it, which is dictated by the concentration of ions in the water column. Sodium and nitrate ions result from the breakdown of sodium nitrate ($NaNO_3$), a common component of commercial fertilizer. It is a known aquatic pollutant regulated by the Clean Water Act (USDA, 1995) that can enter streams via runoff from precipitation events, such as those that occur during the spring. Since % agriculture had a significant effect on conductivity (both seasons showed positive correlations) it does seem likely that conductivity was affected by ions from fertilizer.

Although pH measurements fell within normal ranges for this watershed at the time of sampling, in agricultural landscapes it can be affected by terrestrial soil pH. The application of N-based fertilizer can negatively impact the dynamics of nutrient uptake and retention; during the oxidation of ammonia by nitrifying microbes, hydrogen protons are released into the soil which lowers the pH.

$$NH_3 + 1.5O_2 \text{ ---> } NO_2^- + H^+ (+H_2O)$$

Chemical equation for the oxidation of ammonia.

One consequence of lowered pH is the release of free aluminum in the soil and most crops grown in the Palouse are sensitive to both acidic soils and/or aluminum and thus crop production suffers (Shroeder and Pumphrey, 2013). This phenomenon occurs at lower than, or equal to, 5.5 pH - above 6 is preferable. Testing done in Whitman County showed that pH was lower at the surface than at depth, and that it is a trend that continues (USDA, 2012). At a pH of 5.5 and lower, root growth for most plants becomes limited and negatively affects their ability to take up water and nutrients. When wheat germinates

it sends out shallow lateral seminal roots prior to the nodal root development. Nodal roots are thicker and stronger and extend horizontally from the stem; some even remain at surface level. A minority of the mature seminal roots grows to 6.6 feet long, but most of the root base occupies the top more acidic 12" of soil (Kirby, 1993). Nutrients not taken up, such as N, P, K, Ca, Mg, S and Mo, are then able to be washed or blown away, possibly into local aquatic systems. Forested areas that have been converted to cropland are at a higher risk for acidification due to the initially low soil pH typical of the forest floor. Researchers are experimenting with aluminum tolerant plants (such as oats & winter triticale), as well as augmenting the soil with the addition of lime, as they have done for decades. This, however, is not a long-term solution, as changes in agricultural practices are necessary to stop the acidifying trend (e.g. timing and strength of fertilizer applications, better record keeping to calculate post-crop nitrogen addition, and crop rotation).

The biogeographic distribution of macro-organisms is largely driven by regulatory factors in their landscape, and it is plausible to expect micro-organisms to respond in the same manner. Although this research cannot say with absolute certainty that agriculture alone dictated the nitrifier abundance, we do know that ammonia levels can drive their abundance and distribution (Cebron, 2003; Wakelin *et al*., 2008; Wang *et al*., 2010). More robust multi-variate analyses are needed to resolve the microbial community patterns seen in my data; ultimately, the wide variation in the data strengthens the argument that we have much to learn about the factors that affect the distribution of environmental microbes. This study showed that the *in situ* capture of sediment microbes paired with molecular analysis is an effective method to measure environmental factors and their possible effect on microbial distribution and abundance, and more specifically that agriculture can impact the abundance of sediment nitrifying bacteria.

Conclusion

In addition to their key roles in global decomposition and nutrient cycling, microbes serve as a direct food source for unicellular eukaryotes and their metabolic conversions of substrates create diverse chemical compounds that help to drive biogeochemical processes and trophic systems in their environment (Findlay and Sinsabaugh, 1999; Horner-Devine *et al*., 2004; Paerl and Pinckney, 1996; Wakelin *et al*., 2008). Understanding factors that influence microbial distribution and abundance is important, and my results identify physical, chemical and spatial factors in Latah Creek Watershed that appear to affect sediment microbial diversity and nitrifier abundance. This knowledge contributes to the understanding of microbial activities in small regional watersheds, especially those that are impacted by agriculture.

Future research could include: characterization of sediment grain size, which has been shown to affect nitrification (Butturini *et al*., 2000); metals analysis of the sediment; a greater number of seasons; C:N ratio analysis (organic C); incorporation of width and type of riparian areas; use of a different enzyme in lieu of HaeIII (e.g. MspI) since the combination of restriction enzyme and primers are extremely influential; and sequencing the fragments.

Literature Cited

Abell, G. C. J., Banks, J., Ross, D. J., Keane, J. P., Robert, S. S., Revill, A. T., and Volkman, J. K. (2011) Effects of estuarine sediment hypoxia on nitrogen fluxes and ammonia oxidizer gene transcription. *Microb Ecol* **75**: 111-122.

Alexander, R. B., Boyer, E. W., Smith, R. A., Schwarz, G. E., and Moore, R. B. (2007) The role of headwater streams in downstream water quality. *J of Amer Water Res Assoc* **43** (1).

Altmann, D., Stief, P., Amann, R., de Beer, D., and Schramm, A. (2003) In situ distribution and activity of nitrifying bacteria in freshwater sediment. *Environ Microbiol* **5**: 798-803.

Baker-Austin, C., and Dopson, M. (2007) Life in acid: pH homeostasis in acidophiles. *TRENDS in Microbiol* **15**: 165-171.

Bansal, M.K. (1976) Nitrification in natural streams. *Journal: Water Pollution Control Federation*. **48**: 2380-2393.

Bernhardt, E.S., Hall, R.O., and Likens, G.E. (2002) Whole-system estimates of nitrification and nitrate uptake in streams of Hubbard Brook experimental forest. *Ecosystems* **5**: 419-430.

Bernot, M. J., and Dodds. W. K. (2005) Nitrogen retention, removal and saturation in lotic ecosystems. *Ecosystems* **8**: 442-453.

Blackwood, C. B., and Buyer, J. S. (2007) Evaluating the physical capture method of terminal restriction fragment length polymorphism for comparison of soil microbial communities. *Soil Biology & Biochemistry* **39**: 590-599.

Braker, G., Ayala-Del-Rio, H. L., Devol, A. H., Fesefeldt, and Tiedje, J. M. (2001) Community structure of denitrifiers, *Bacteria*, and *Archaea* along redox gradients in Pacific Northwest marine sediments by terminal restriction fragment polymorphism analysis of amplified nitrite reductase (*nirS*) and 16S rRNA genes. *Appl Environ Microbiol* **67**: 1893-1901.

Butturini, A., Battin, T.J., and Sabater, F. (2000) Nitrification in stream sediment

biofilms: the role of ammonium concentration and DOC quality. *Water Res* **34**: 629-639.

Cebron, A., Berthe, T., and Garnier, J. (2003) Nitrification and nitrifying bacteria in the lower Seine River and estuary (France). *Appl Environ Microbiol* **69**: 7091-7100.

Clement, B. G., Kehl, L. E., DeBord, K. L., and Kitts, C.L. (1998) Terminal restriction fragment patterns (TRFPs), a rapid, PCR-based method for the comparison of complex bacterial communities. *J Microbiol Methods* **31**: 135-142.

Craig, J. P., and Weil, R.R. (1993) Nitrate leaching to a shallow Mid-Atlantic coastal plain aquifer as influenced by conventional no-till and low-input sustainable grain production systems. Water Science & Technology **28**: 691-700.

Dang, H., Li, J., Chen, R., Wang, L., Guo, L., Zhang, Z., and Klotz, M. G. (2010) Diversity, abundance, and spatial distribution of sediment ammonia-oxidizing betaproteobacteria in response to environmental gradients and coastal eutrophication in Jiaozhou Bay, China. *Appl Environ Microbiol* **76**: 4691-4702.

Department of Environmental Sciences, University of Virginia. Retrieved from www.evsc.Virginia.edu, 2015.

Fields, M., Yan, T., Rhee, S., Carroll, S., Jardine, P., Watson, D., Criddle, C., and Zhou, J. (2005) Impacts on microbial communities and cultivable isolates from groundwater contaminated with high levels of nitric acid-uranium waste. *Microb Ecol* **53**: 417-428.

Fierer, N., Morse, J.L., Berthrong, S. T., Bernhardt, E.S., and Jackson, R.B. (2007) Environmental controls on the landscape-scale biogeography of stream bacterial communities. *Ecology* **88**: 2162-2173.

Findlay, S., and Sinsabaugh, R. (1999) Unravelling the sources and bioavailability of dissolved organic matter in lotic aquatic ecosystems. *Marine Freshwater Res* **50**: 781-790.

Food and Agriculture Organization of the United Nations - Statistics Division (2013) Retrieved from http://faostat.fao.org, 2015.

Fortunato, C. S., Carlini, D. B., Ewers, E., and Bushaw-Newton, K. L. (2009) Nitrifier

and denitrifier molecular operational taxonomic unit compositions from sites of a freshwater estuary of Chesapeake Bay. *Can J Microbiol* **55**: 333-346.

Francis, C., Roberts, K., Beman, J., Santoro, A., and Oakley, B. (2005) Ubiquity and diversity of ammonia-oxidizing archaea in water columns and sediments of the ocean. *Proc Natl Acad Sci USA* **102**: 14683-14688.

Galloway, J. N., Schlesinger, W. H., Levy II, H., Michaels, A., and Schnoor, J. L. (1995) Nitrogen fixation: atmospheric enhancement-environmental response. *Global Biogeochem Cycles* **9**: 235-252.

Halda-Alija, L., and Johnston, T. (1999) Diversity of culturable heterotrophic aerobic bacteria in pristine stream bed sediments. *Can J Microbiol* **45**: 879-884.

Hall, M., Young, D.L., and Walker, D.J. (1999) Agriculture in the Palouse. University of Idaho, College of Agriculture, Cooperative Extension System *Bul* 794.

Hofman, T., and Lees, H. (1953) The biochemistry of the nitrifying organisms (IV) The respiration and intermediary metabolism of *Nitrosomonas*. *J Biochem* **54**: 579-583

Hogan, C. and Fund, W. (2014) Palouse grasslands. Retrieved from http://www.eoearth.org/view/article/155127, 2015.

Horner-Devine, M., Carney, K., and Bohannan, B. (2004) An ecological perspective on bacterial biodiversity. *Proc Royal Soc London Series B-Biol Sci* **271**: 113-122.

Huse, S. M., Dethlefsen, L., Huber, J. A.,Welch, D. M., Relman, D. A., and Sogin, M. L. (2008) Exploring microbial diversity and taxonomy using SSU rRNA hypervariable tag sequencing. *Plos Gen* **4**: e1000255.

International Fertilizer Industry Association. (2011) Retrieved from www.fertilizer.org, 2015.

Junier, P., Molina, V., Dorador, C., Hadas, O., Kim, O., Junier, T., Witzel, K., and Imhoff, J.F. (2010) Phylogenetic and functional marker genes to study ammonia-oxidizing microorganisms (AMO) in the environment. *Appl Microbiol Biotechnol* **85**: 425-440.

Kemp, M. J., and Dodds, W. K. (2002) The influence of ammonium, nitrate, and

dissolved oxygen concentrations on uptake, nitrification, and denitrification rates associated with prairie stream substrata. *Limnol and Ocean* **47**: 1380-1393.

Kemp, M. J., and Dodds, W. K. (2002b) Comparisons of nitrification and denitrification in prairie and agriculturally influenced streams. *Ecological Applications.* **12**: 998-1009.

Kirby, E.J.M. (1993) Effect of sowing depth on seedling emergence, growth and development in barley and wheat. *Field Crops Res* **39**: 101-111.

Kirchman, D. L. (2012) Processes in Microbial Ecology. Oxford University Press, Inc., New York.

Kirk J., Beaudette, L., Hart, M., Moutoglis, P., Khironomos, J., Lee, H., and Trevors J. (2004) Methods of studying soil microbial diversity. *J Microbiol Methods* **58**: 169-188.

Koenig, R., Schroeder, K., Carter, A., Pumphrey, M., Paulitz, T., Campbell, K., and Huggins, D. (2011) Soil acidity and aluminum toxicity in the Palouse region of the Pacific Northwest. Retrieved from http://pubs.wsu.edu, 2014.

Kowalchuk, G., and Stephen, J. (2001) Ammonia-oxidizing bacteria: a model for molecular microbial ecology. *Annual Rev Microbiol* **55**: 485-529.

Li M., Cao, H., Hong, Y. and Gu, J. (2011) Spatial distribution and abundances of ammonia-oxidizing archaea (AOA) and ammonia-oxidizing bacteria (AOB) in mangrove sediments. *Appl Microbiol and Biotech* **89**: 1243-1254.

McCaig, A., Phillips, C., Stephen, J., Kowalchuk, G., Harvey, S., Herbert, R., Embley, T., and Prosser, J. (1999) Nitrogen cycling and community structure of proteobacterial beta-subgroup ammonia-oxidizing bacteria within polluted marine fish farm sediments. *Appl Environ Microbiol* **65**: 213-220.

McCrackin, M. L., Harrison, J. A., and Compton, J. E. (2013) A comparison of NEWS and SPARROW models to understand sources of nitrogen delivered to US coastal areas. *Biogeochem* **114**: 281-297.

Nocker, A., Burr, M., and Camper, A.K. (2007) Genotypic microbial community profiling: a critical technical review. *Micro Ecol* **54**: 276-289.

Norton, J. M., Alzerreca, J.J., Suwa, Y., and Klotz, M. G. (2002) Diversity of ammonia monooxygenase operon in autotrophic ammonia oxidizing bacteria. *Arch Microbiol* **177**: 139-149.

Noss, R. F., LaRoe III, E.T., and Scott, J. M. (1995) Endangered ecosystems of the United States: a preliminary assessment of loss and degradation. Biological Report 28, U. S. Department of the Interior, National Biological Service, Washington, D. C., USA.

Paerl, H., and Pinckney, J. (1996) A mini-review of microbial consortia: Their roles in aquatic production and biogeochemical cycling. *Micro Ecol* **31**: 225-247.

Park, S., Park, B., and Rhee, S. (2008) Comparative analysis of archaeal 16S rRNA and amoA genes to estimate the abundance and diversity of ammonia-oxidizing archaea in marine sediments. *Extremophiles* **12**: 605-615.

Petersen, D. G., Blazewicz, S. J., Firestone, M., Herman, D. J., Turetsky, M., and Waldrop, M. (2012) Abundance of microbial genes associated with nitrogen cycling as indices of biogeochemical process rates across a vegetation gradient in Alaska. *Environ Microbiol*. **14**: 993-1008.

Qiu, S., Chen, G., and Zhou, Y. (2010) Abundance and diversity of ammonia-oxidizing bacteria in relation to ammonium in a chinese shallow eutrophic urban lake. *Brazilian J Microbiol* **41**: 218-226.

Rastogi, G., Barua, S., Sani, R.K., and Peyton, B. M. (2011) Investigation of microbial populations in the extremely metal-contaminated Coeur d'Alene river sediments. *Microb Ecol* **62**: 1-13.

Robertson, G. P., and Vitousek, P. M. (2009) Nitrogen in agriculture: balancing the cost of an essential resource. *Annual Rev Environ and Resources* **34**: 97-125.

SantaLucia Jr., J. (1998) A unified view of polymer, dumbbell, and oligonucleotide DNA nearest-neighbor thermodynamics. *Proc. Natl. Acad. Sci. USA* **95**: 1460-1465.

Schroeder, K., and Pumphrey, M. (2013) It's all a matter of pH. Washington Grain Commission, *Wheat Life* **1**: 56-59.

Sinsabaugh, R., and Findlay, S. (1995) Microbial-production, enzyme-activity, and

carbon turnover in surface sediments of the Hudson River Estuary. *Microb Ecol* **30**: 127-141.

Spokane County Conservation District. (2005) Annual Report. Retrieved from www.sccd.org, 2012.

Starry, O. S., Valett, H. M. and M. E. Schreiber. (2005) Nitrification rates in a headwater stream: influences of seasonal variation in C and N supply. *J N Amer Benth Soc* **24**: 753-768.

Strauss, E. A., and Lamberti, G.A. (2000) Regulation of nitrification in aquatic sediments by organic carbon. *Limnol Oceanogr* **45**: 1854-1859.

Strauss, E. A., Mitchell, N. L., and Lamberti, G. A. (2002) Factors regulating nitrification in aquatic sediments: effects of organic carbon, nitrogen availability, and pH. *Can J Fish Aquat Sci.* **59**: 554-563.

Tesoriero, A. J., Liebscher, H., and Cox, S.E. (2000) Mechanism and rate of denitrification in an agricultural watershed: electron and mass balance along groundwater flow paths. *Water Resources Res* **36**: 1545-1559.

Ulukanli, Z., and Digrak, M. (2002) Alkaliphilic micro-organisms and habitats. *Turkish J Biol* **26**: 181-191.

USDA. (1995) Technical Advisory Panel Review for Sodium Nitrate, Retrieved from http://www.ams.usda.gov/AMSv1.0/getfile?dDocName=STELPRDC5085204, 2015.

USDA. (2012) United States Department of Agriculture. Retrieved from www.usda.gov, 2015.

USGS. (1998-2003) United States Geological Survey: Land use history of North America. Retrieved from http://landcover.usgs.gov/luhna/contents.php, 2015.

USGS. (2014) United States Geological Survey Retrieved from www.usgs.gov, 2014.

Venter, J., Remington, K., Heidelberg, J., Halpern, A., Rusch, D., Eisen, J., *et al*. (2004) Environmental genome shotgun sequencing of the Sargasso Sea. *Science* **304**: 66-74.

Vitousek, P., Aber, J., Howarth, R., Likens, G., Matson, P., Schindler, D., *et al*. (1997)

Human alteration of the global nitrogen cycle: Sources and consequences. *Ecol Appl* **7**: 737-750.

WA State Dept. of Ecology.(2012) Retrieved from www.ecy.wa.gov, 2014.

WA State Dept. of Ecology. (2013) Retrieved from www.ecy.wa.gov, 2015.

Wakelin, S. A., Colloff, M. J., and Kookana, R. S. (2008) Effect of wastewater treatment plant effluent on microbial function and community structure in the sediment of a freshwater stream with variable seasonal flow. *Appl Environ Microbiol* **74**: 2659-2668.

Wang, Y., and Qian, P. (2009) Conservative fragments in bacterial 16S rRNA genes and primer design for 16S ribosomal DNA amplicons in metagenomic studies. *Plos One* **4**: e7401.

Wang, S., Wang, Y., Feng, X., Zhai, L., and Zhu, G. (2011) Quantitative analyses of ammonia-oxidizing archaea and bacteria in the sediments of four nitrogen-rich wetlands in China. *Appl Microbiol Biotechnol*. **90**: 779–787

Wankel, S. D., Kendall, C., and Paytan, A. (2009) Using nitrate dual isotopic composition (delta(15)N and delta(18)O) as a tool for exploring sources and cycling of nitrate in an estuarine system: Elkhorn Slough, California. *J Geophysical Res-Biogeosci* **114**: G01011.

Wankel, S. D., Mosier, A. C., Hansel, C. M., Paytan, A., and Francis, C. A. (2011) Spatial variability in nitrification rates and ammonia-oxidizing microbial communities in the agriculturally impacted Elkhorn Slough Estuary, California. *Appl Environ Microbiol* **77**: 269-280.

Williams, M. R., Buda, A. R., Elliott, H. A., Singha, K., and Hamlett, J. (2015) Influence of riparian seepage zones on nitrate variability in two agricultural headwater streams. *J Amer Water Resources Assoc* **51**.

WRIA 56 Watershed Implementation Team. (2008) Detailed implementation plan: Hangman (Latah) Creek Watershed, Water Resource Inventory Area 56, **2-19-2008**.

Yamanaka, T. (2008) Chemolithoautotrophic bacteria. biochemistry and environmental biology. 1st edn. Japan. Springer.

Yu, C., Ahuja, R., Sayler, G., and Chu, K. (2005) Quantitative molecular assay for fingerprinting microbial communities of wastewater and estrogen-degrading consortia. *Environ Microbiol* **71**: 1433-1444.

Zak, D. R., Blackwood, C. B., and Waldrop, M. P. (2006) A molecular dawn for biogeochemistry. *Trends Ecol Evol* **21**: 288-295.

Zhang, Y., Ruan, X., den Camp, H. J. M. O., Smits, T. J. M., Jetten, M. S. M., and Schmid, M. C. (2007) Diversity and abundance of aerobic and anaerobic ammonium-oxidizing bacteria in freshwater sediments of the Xinyi River (China). *Environ Microbiol* **9**: 2375-2382.

Appendix

Crop Statistics and Chemical Data

County	Total Area (acres)		Harvested Cropland	Wheat	Barley	Beans	Forage
	Land	Water					
Benewah	501,760		63,174	31,802	2,542	NA	13,922
	497,280	4,672					
Whitman	1,393,920		659,460	441,417	83,709	65,037	58,922
	1,381,760	12,160					
Spokane	1,139,840		289,301	159,047	20,449	715	58,922
	1,128,960	10,880					

Table 24. Land and crop. Beans = dry, edible, excluding limas; forage = all hay, haylage, grass silage and greenchop. (NA = not available). Values based on 2012 US Census statistics and 2012 USDA, National Agricultural Statistics Service, Census of Agriculture data.

County	Fertilizer, Lime & Soil Conditioners (acres treated)	Acres treated to control:			
		Insects	Weeds, grass, brush	Nematodes	Diseases
Benewah	58,103	14,081	62,156	Unavailable	29,297
Whitman	560,571	178,809	766,795	18,693	319,057
Spokane	215,706	51,542	267,130	78,629	78,629

Table 25. Chemical application data for all counties. Values based on USDA 2012 data.

Troubleshooting Molecular Techniques

T-RFLP

Contamination, especially with the *16S rRNA*, since it is found in all prokaryotes, is of primary importance. Reaction formulas, reagent quality, and cycling protocols are also critical. Determining the melting temperature (Tm) of the DNA can be problematic, and there are several different methods. Tm is the temperature observed when 50% of a DNA sequence is single stranded and 50% is double stranded. The concentration, length and sequence of DNA, as well as the presence and concentration of ions in the reaction (e.g., K^+ and Mg^+) affect the Tm. The nearest neighbor method (SantaLucia 1998) is the National Center for Biotechnology Information (NCBI) default setting and the one used in this study. This method uses the enthalpy of 2 nucleotides (nt) as well as their adjacent nts to determine the most suitable Tm. This strategy is based on the energetically favorable interaction between two neighboring nt pairs, which decreases Tm. Some additional factors that affect PCR success include the state of the DNA (e.g., DNA is at risk of shearing during the bead-beating stage of the extraction process, possible degradation of the DNA from freezing / thawing cycles) and primer design.

Factors that affect the restriction accuracy in the T-RFLP process include the duration and temperature of the reaction and the choice of enzyme. “Star” activity describes cleavage of the DNA strand at similar, but not exact, nt target sequences, generating inaccurate fragment lengths. Suboptimal conditions that promote this are: enzyme concentration too high, salt concentration too low, and/or incubation time too long. Both HaeIII and HhaI can exhibit star activity. In the sequencer, anomalies in the T-RF’s can exist due to the ROX label traveling more slowly than the FAM label on the forward primer. Use of the 16S sRNA has some drawbacks as well. Bacteria can possess multiple copies of the gene, anywhere from 1 (*Pelagibacter ubique*) to 15 (*Clostridium paradoxum*), with an average of 4 (Kirchman, 2012), which can affect abundance measures. According to research done by Kowalchuck and Stephen (2001), the beta-subclass of AOB contain only one copy, so characterizing abundance of AOB based on a known 16S rRNA fragment may be useful. Additionally, the 16S rRNA gene can be very

similar among bacteria with diverse physiology, so the resultant fragments could be identical (Kirchman, 2012).

qPCR

qPCR can be affected by: fluorescence chemistry, proper annealing temperature, and uneven temperature on the heating block. iQ SYBR Green binds to all double-stranded DNA, so specificity must be checked with the melt curve function and / or gel electrophoresis, which were both done for this study. Annealing temperature is critical – the optimal temperature should produce products at the lowest C_q with no nonspecific amplification. In addition to the above, the *amoA* copy numbers can also vary among bacteria, from between two and three (Kowalchuck and Stephen, 2001; Norton *et al*., 2002), affecting quantitative values.

T-RFLP Single Fragment Lengths

Spring		Fall	
T-RFs	Freq.	T-RFs	Freq.
37	1	78	1
53	1	93	1
59	1	331	1
60	1	358	1
69	1	366	1
79	1	367	1
83	1	376	1
87	1	390	1
96	1	391	1
117	1	414	1
185	1	423	1
186	1	522	1
229	1	571	1
232	1	844	1
233	1		
309	1		
337	1		
358	1		
390	1		
402	1		
472	1		
476	1		
510	1		
527	1		
566	1		
570	1		
755	1		

Table 26. HhaI fragments (bp) that appeared only once for spring and fall.

Spring T-RFs	Freq.	Fall T-RFs	Freq.
37	1	55	1
55	1	56	1
56	1	71	1
68	1	198	1
69	1	200	1
96	1	219	1
97	1	292	1
116	1	321	1
128	1	325	1
172	1	328	1
173	1	379	1
187	1	403	1
195	1	404	1
201	1	454	1
203	1	611	1
220	1	693	1
221	1	700	1
226	1		
234	1		
239	1		
240	1		
249	1		
258	1		
267	1		
270	1		
379	1		
427	1		
783	1		

Table 27. HaeIII fragments (bp) that appeared only once for spring and fall.

Sub-watershed Maps

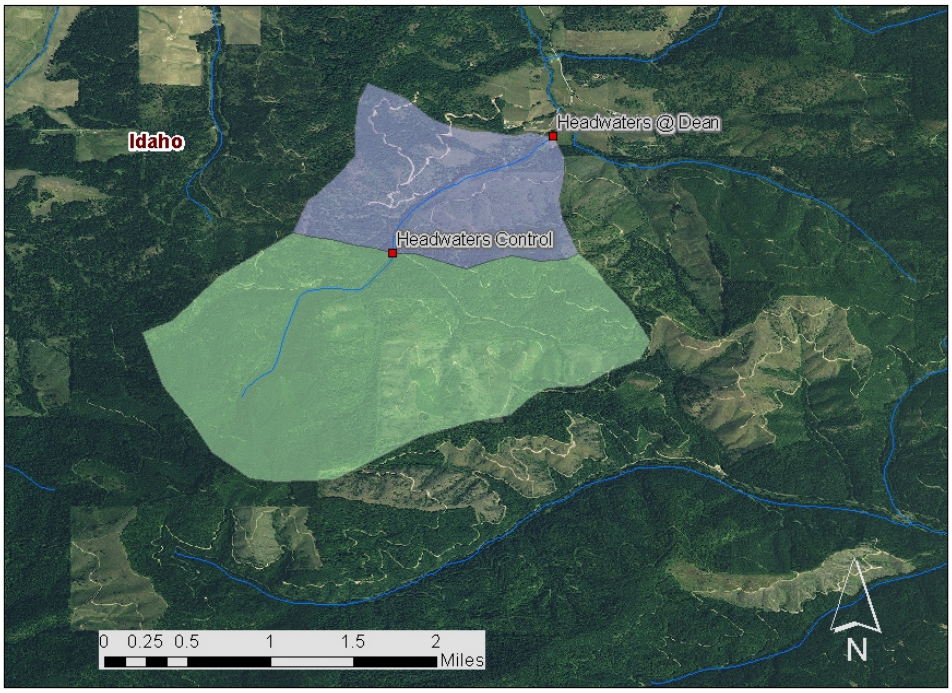

Map 3. Headwaters, site #1 and site #2.

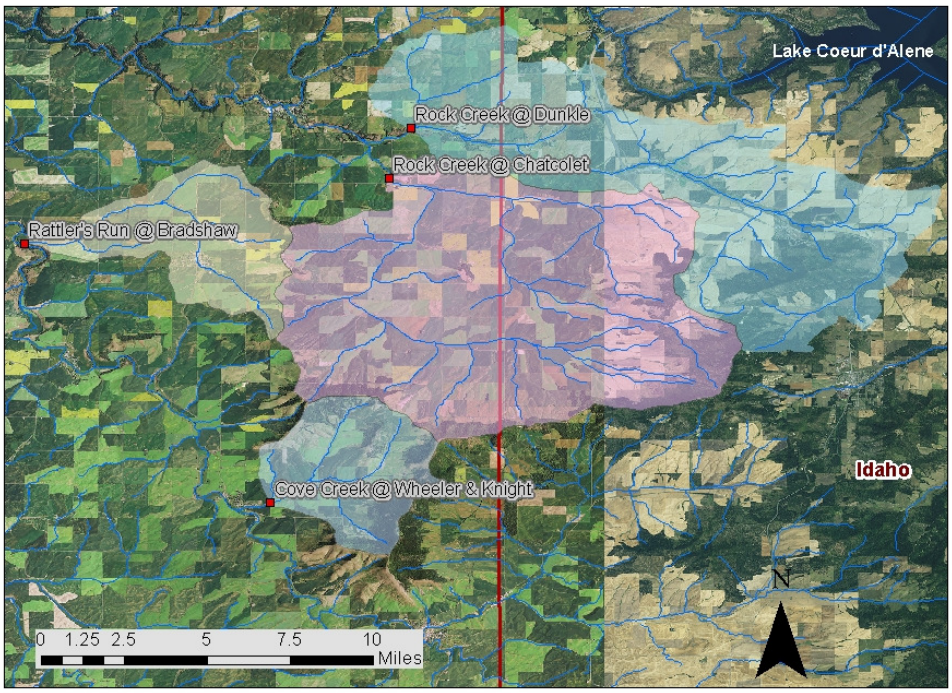

Map 4. Cove Creek (site #3), South Fork Rock Creek (site# 4), North Fork Rock Creek (site #5), and Rattler's Run Creek (site #6).

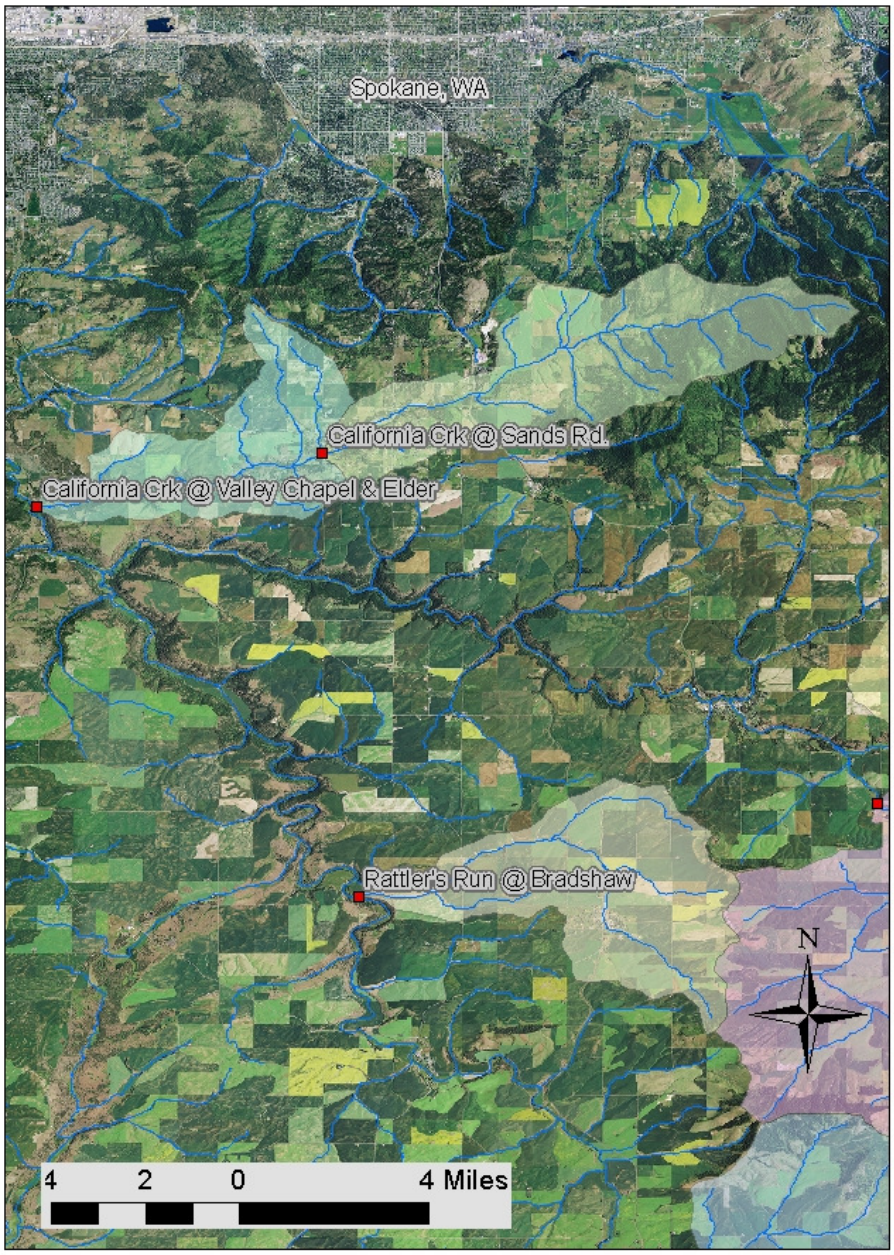

Map 5. Rattler's Run Creek (site #6), California Creek at Sands (site #7) and California Creek at Valley Chapel (site #8).

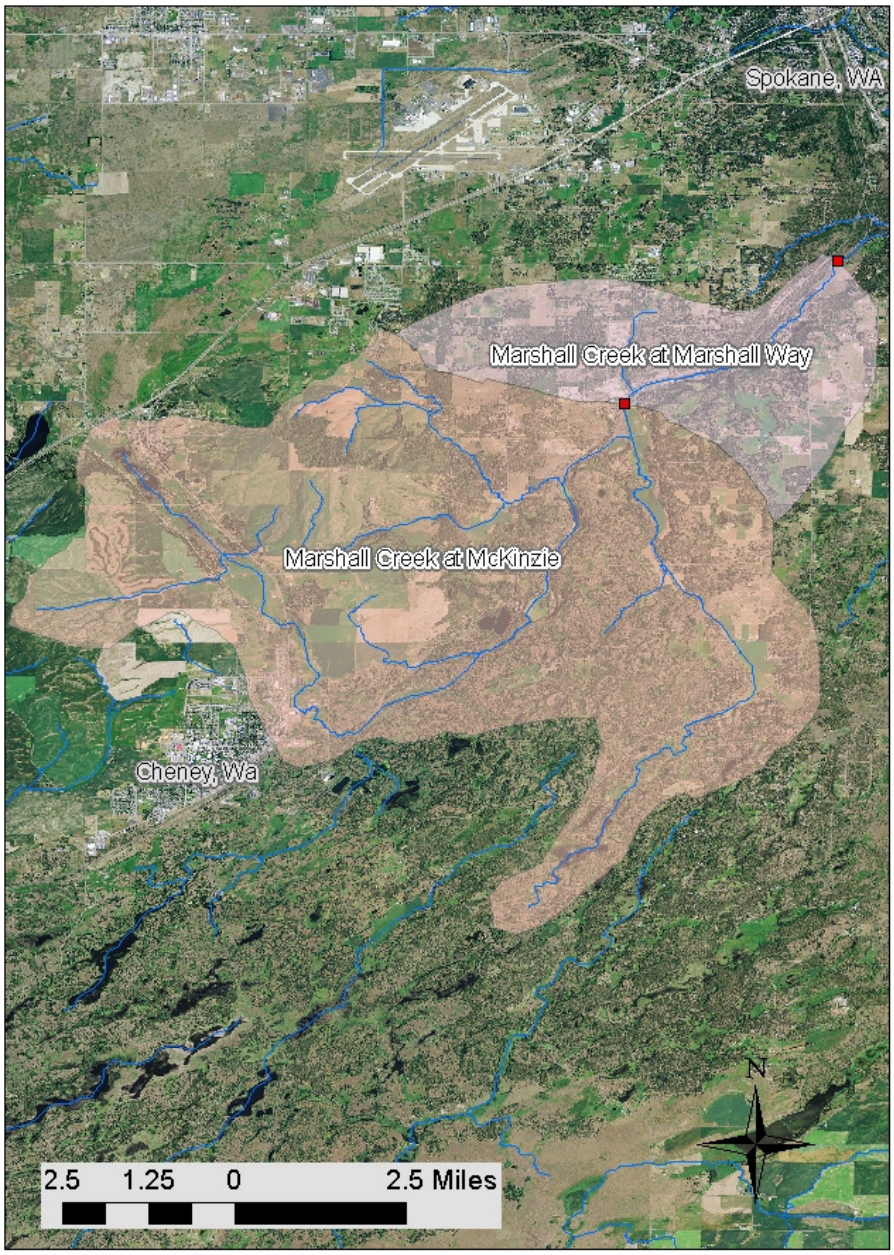

Map 6. Marshall Creek at McKinzie (site #9) and Marshall Creek at Marshall Way (site #10).

Agarose Gel Electrophoresis Photos

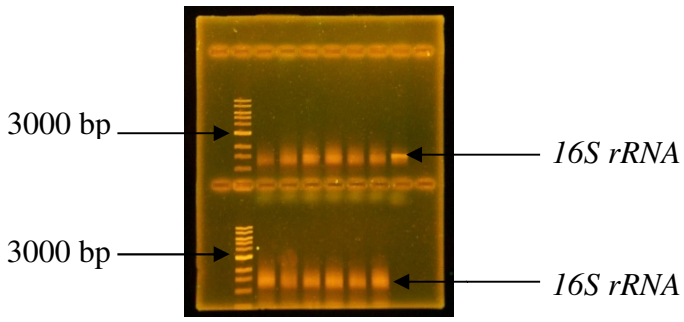

Figure 33. *16S rRNA* PCR products on a 0.8% agarose gel against a 1kb ladder, stained with EtBr and photographed under UV.

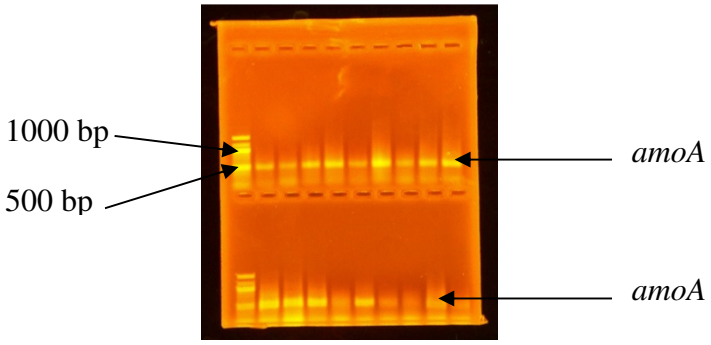

Figure 34. *amoA* qPCR products on a 1% agarose gel against a 100bp ladder, stained with EtBr and photographed under UV.

Graphs for qPCR and T-RFLP

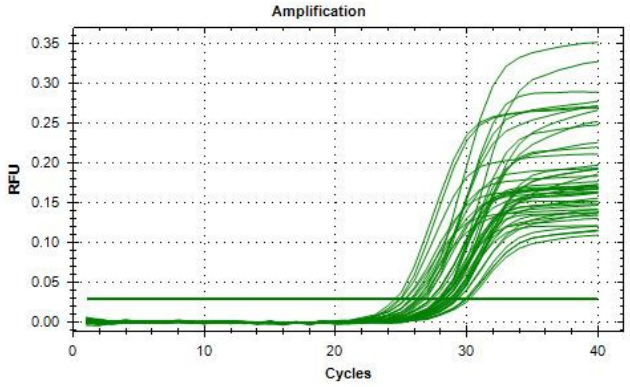

a)

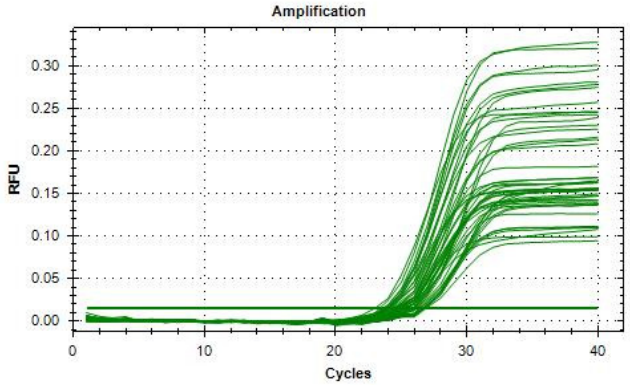

b)

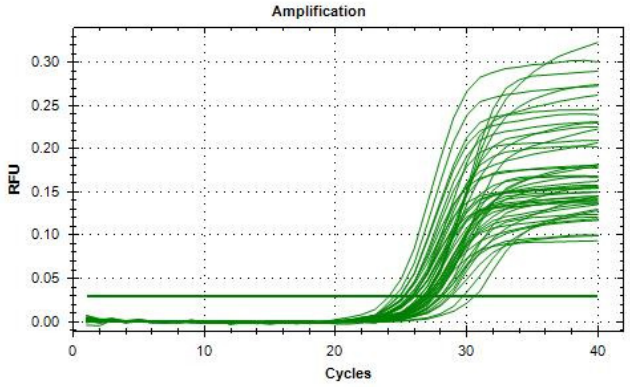

c)

Figure 35. qPCR on *amoA*. C_q (quantitative curves) for a) B1, B2, B3, b) B4, B5,B6, and c) B6, B7, B8, B9.

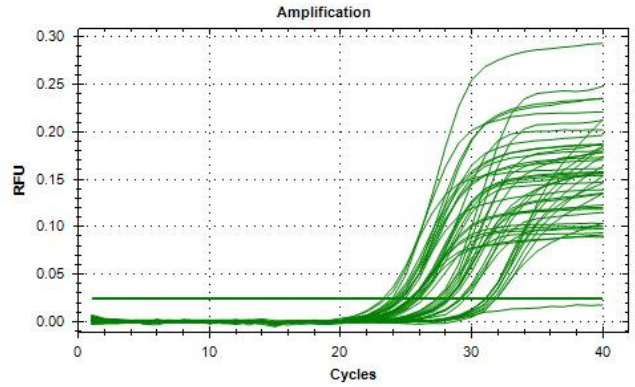

a)

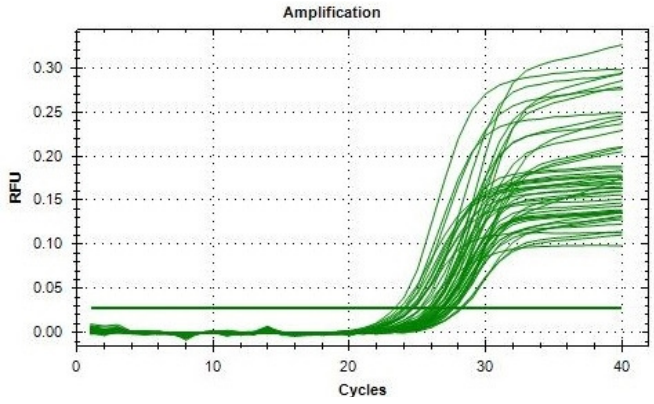

b)

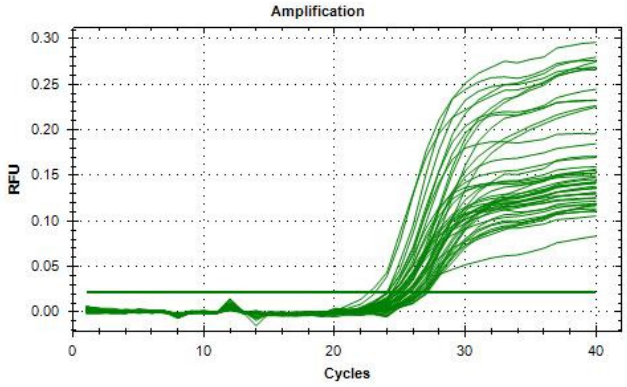

c)

Figure 36. qPCR on *amoA*. C_q (quantitative curves) for a) B9, B10, C1, b) C8, C9, C10, B1, and c) C3, C4.

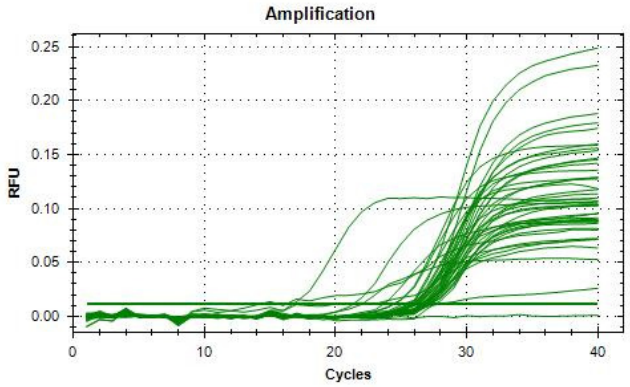

a)

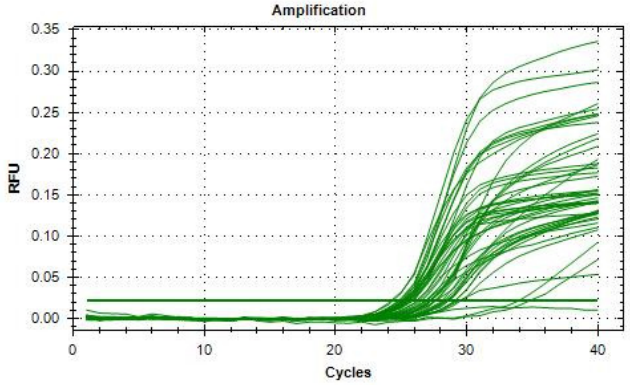

b)

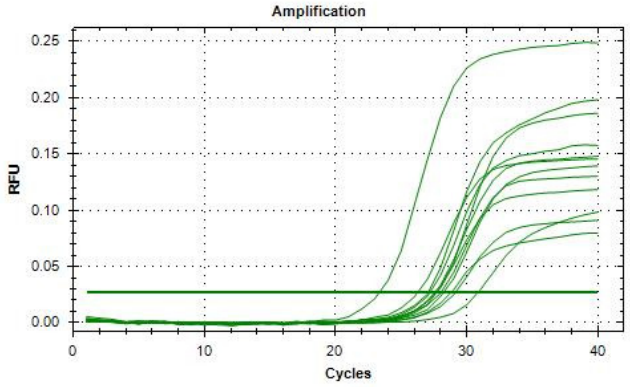

c)

Figure 37. qPCR on *amoA*. C_q quantitative curves for a) C1, C2, C6, b) C5, C7, C8, and c) C5, C6, C7, C8, B10.

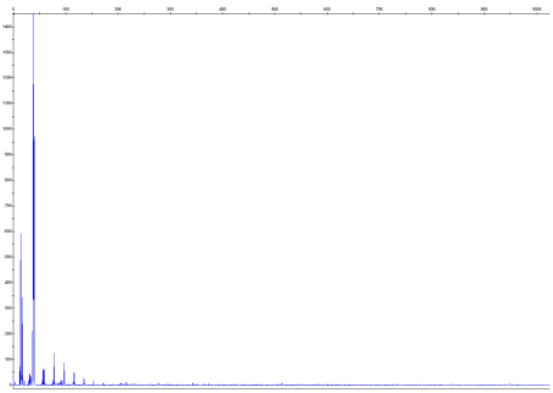

B1.1HhaI

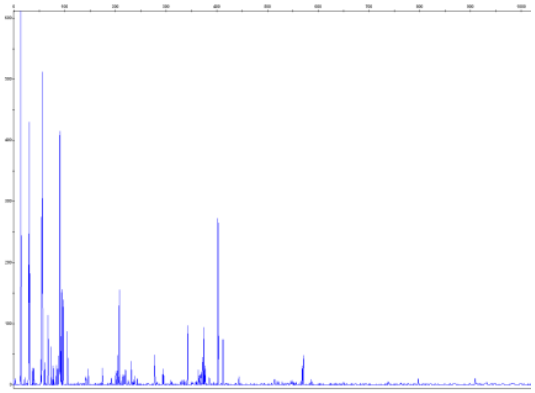

B1.4HhaI

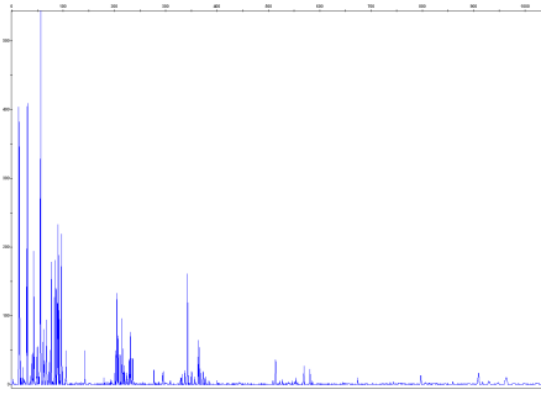

B1.2HhaI

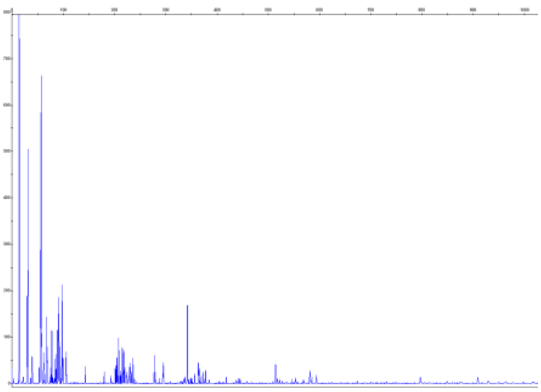

B1.5HhaI

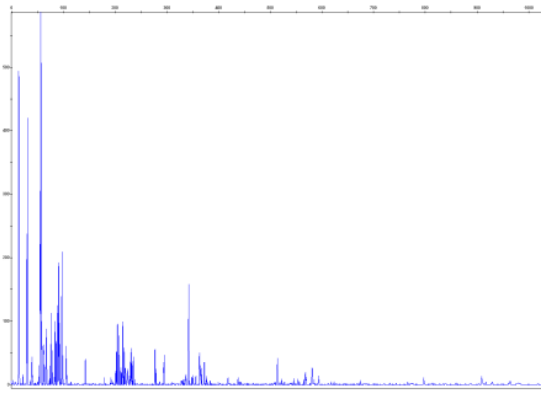

B1.3HhaI

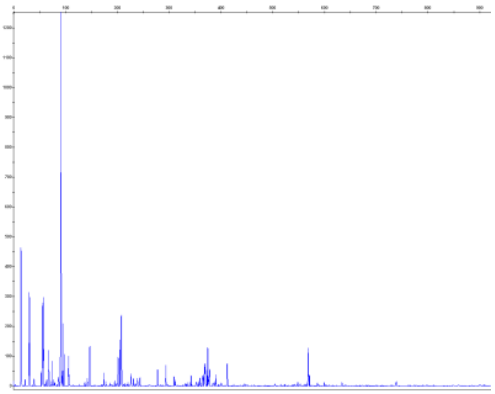

B1.6HhaI

Figure 38. HhaI T-RFLP electropherograms for Site #1, samples 1-6, spring

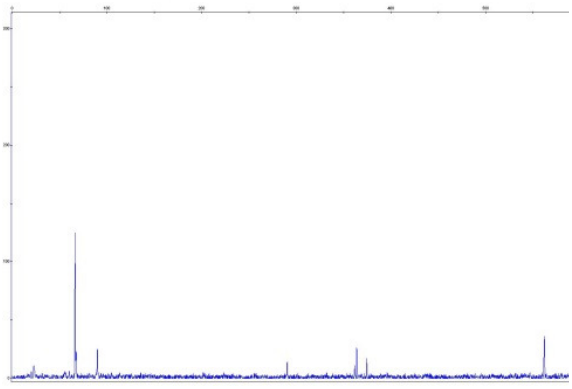

B2.1 HhaI

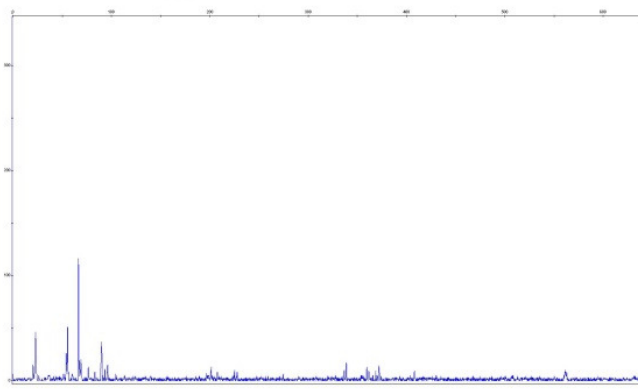

B2.4 HhaI

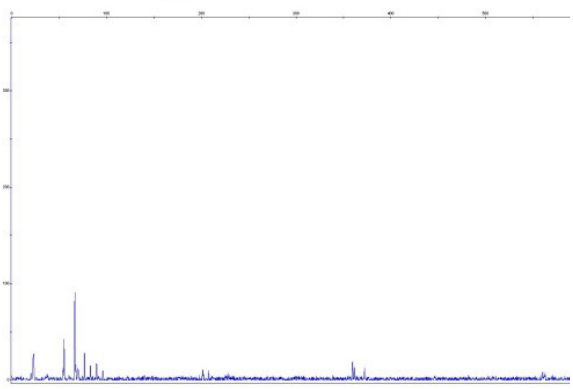

B2.2 HhaI

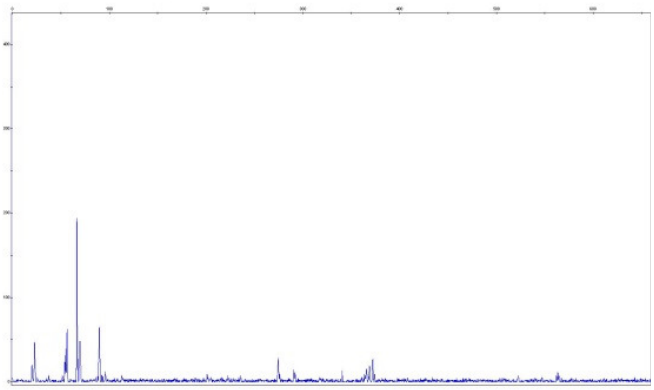

B2.5 HhaI

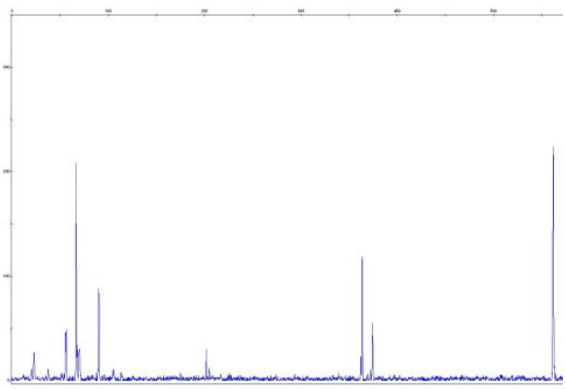

B2.3 HhaI

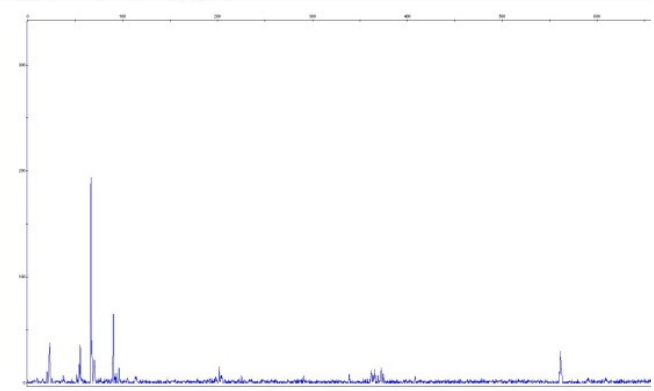

B2.6 HhaI

Figure 39. HhaI T-RFLP electropherograms for Site #2, samples 1-6, spring

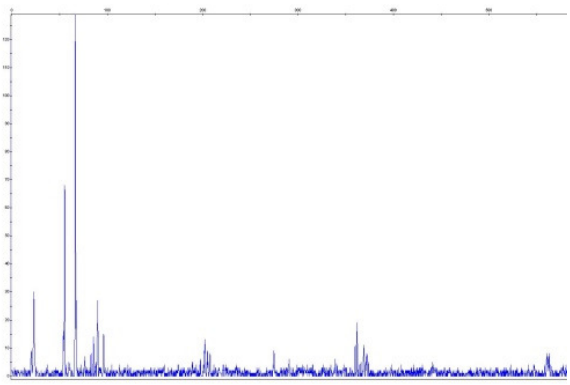

B3.1 HhaI

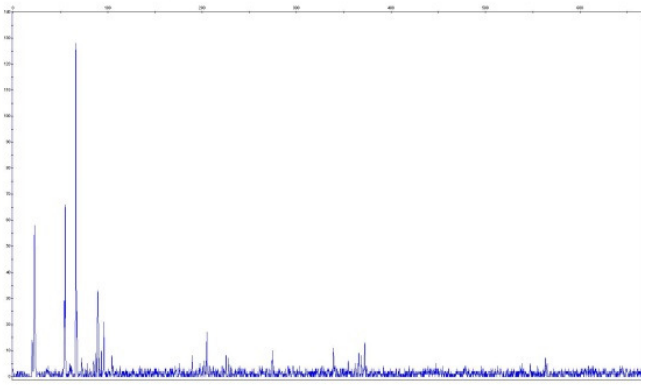

B3.4 HhaI

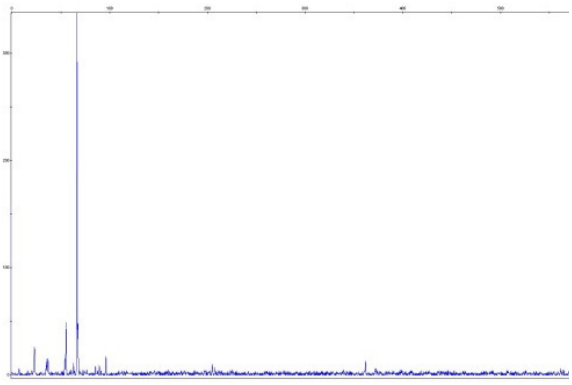

B3.2 HhaI

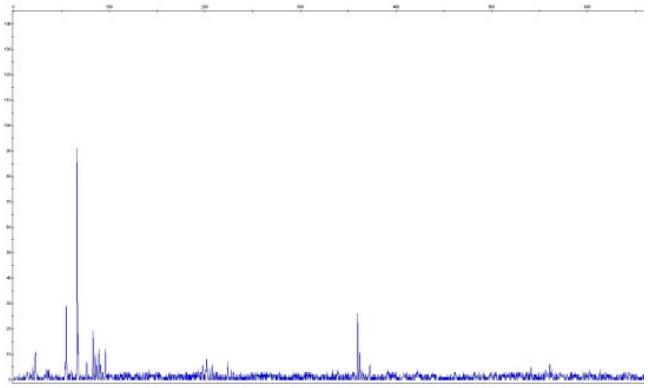

B3.5 HhaI

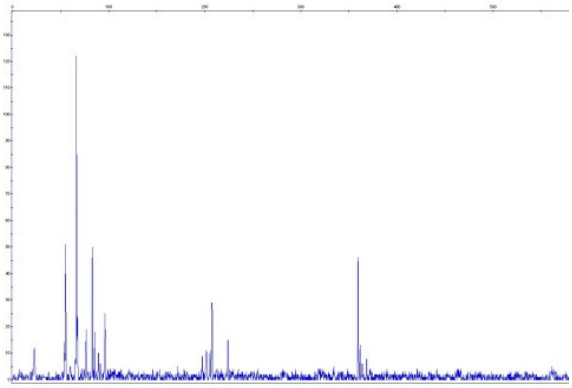

B3.3 HhaI

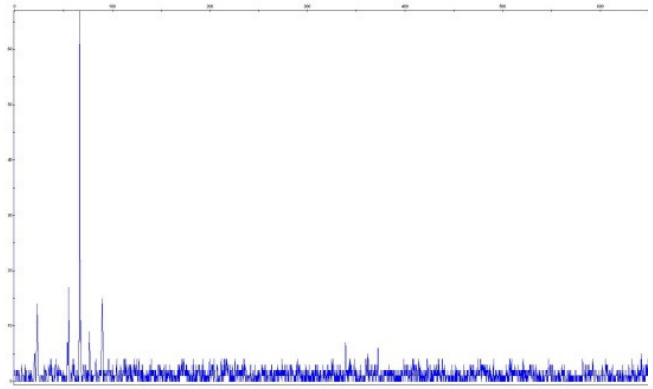

B3.6 HhaI

Figure 40. HhaI T-RFLP electropherograms for Site #3, samples 1-6, spring

B4.1HhaI

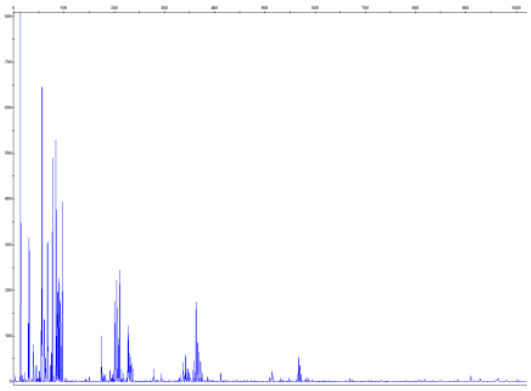

B4.4HhaI

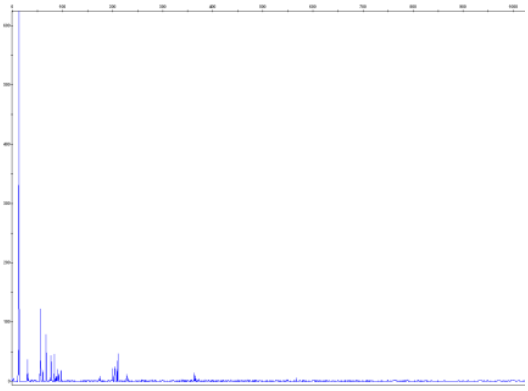

B4.2HhaI

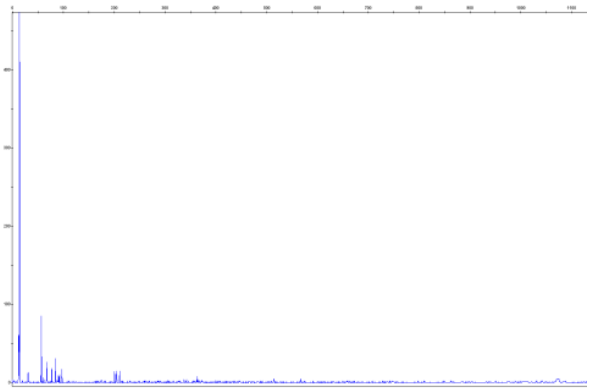

B4.5HhaI

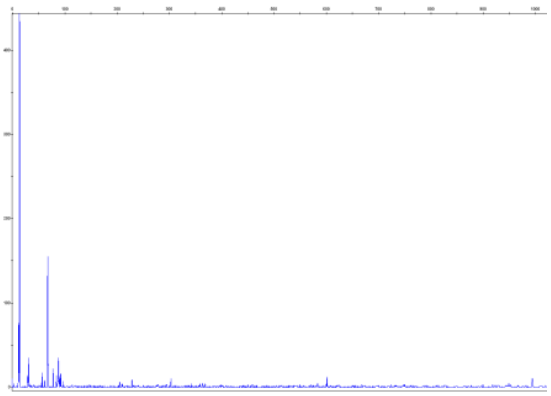

B4.3HhaI

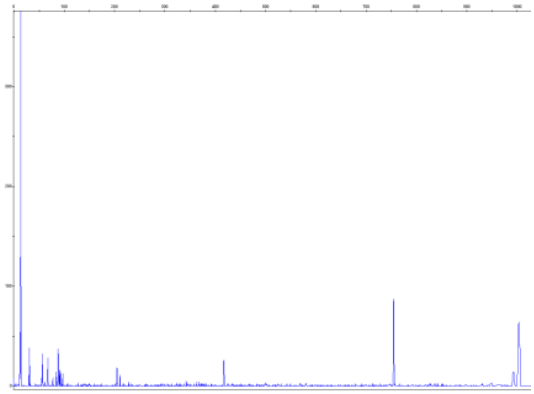

B4.6HhaI

Figure 41. HhaI T-RFLP electropherograms for Site #4, samples 1-6, spring

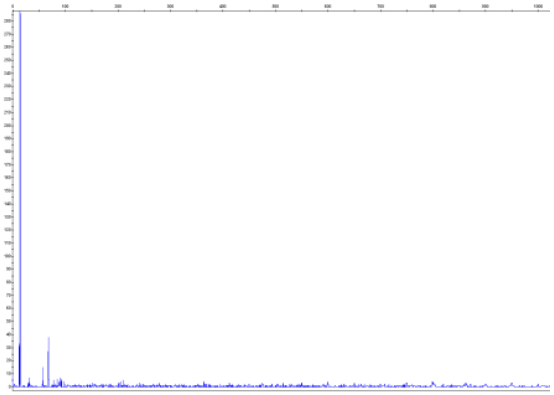

B5.1HhaI

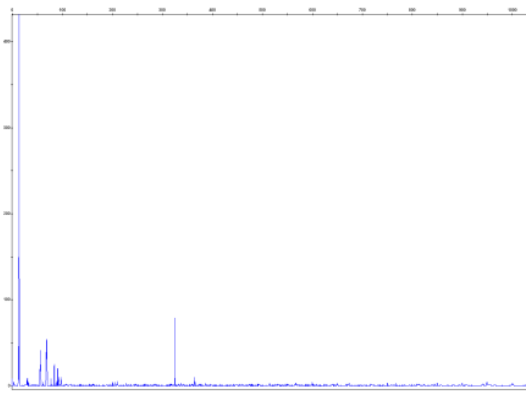

B5.4HhaI

B5.2HhaI

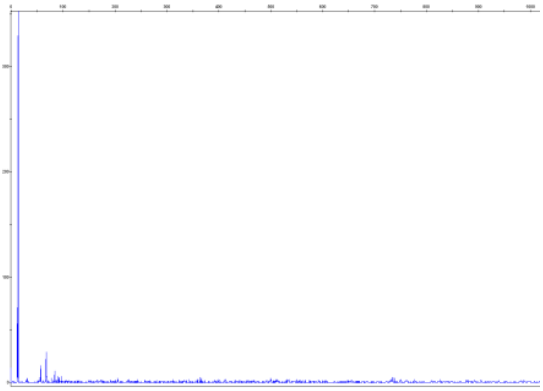

B5.5HhaI

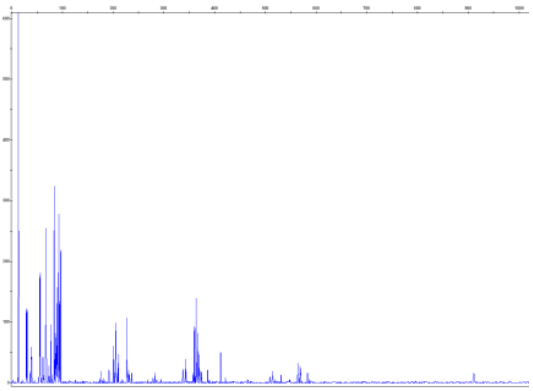

B5.3HhaI

B5.6HhaI

Figure 42. HhaI T-RFLP electropherograms for Site #5, samples 1-6, spring

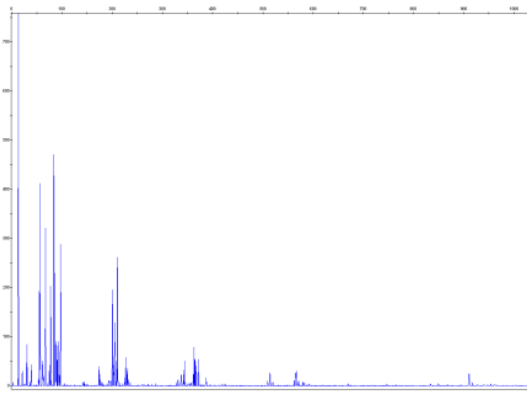

B6.1HhaI

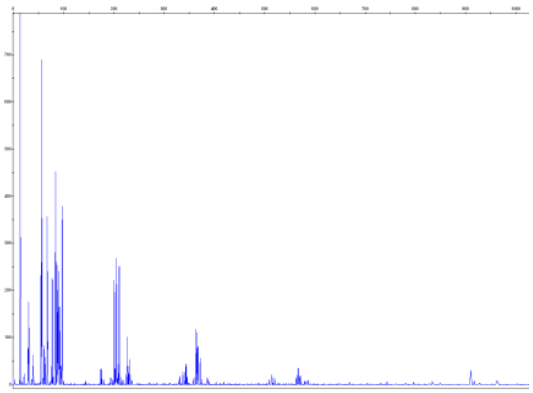

B6.4HhaI

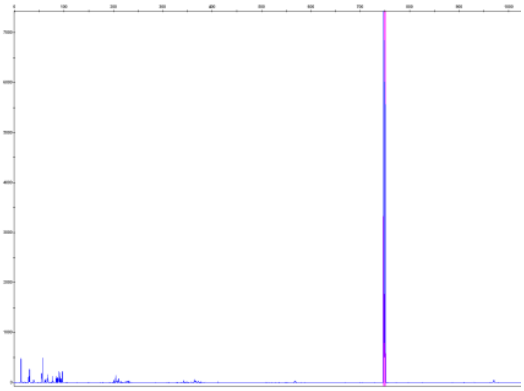

B6.2HhaI

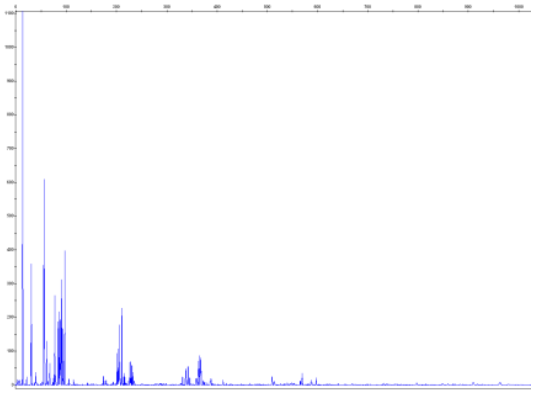

B6.5HhaI

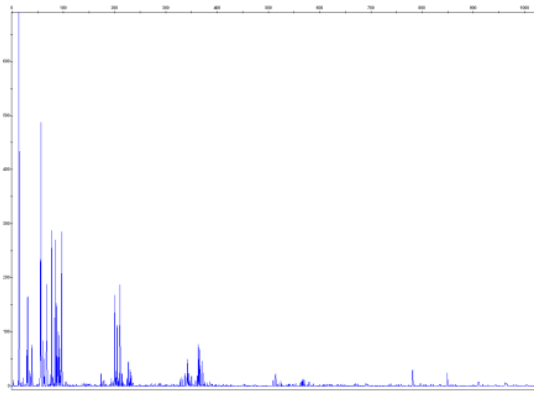

B6.3HhaI

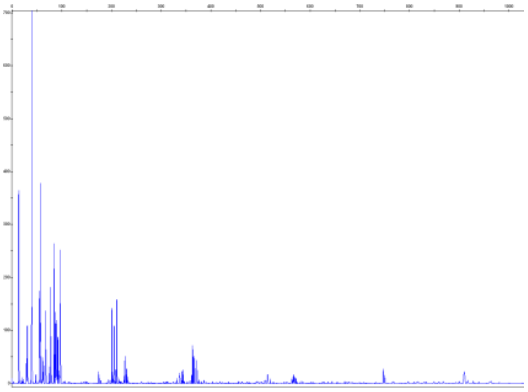

B6.6HhaI

Figure 43. HhaI T-RFLP electropherograms for Site #6, samples 1-6, spring

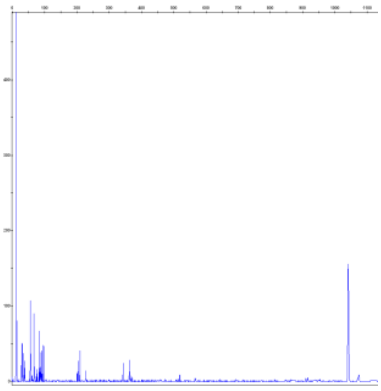

B7.1HhaI

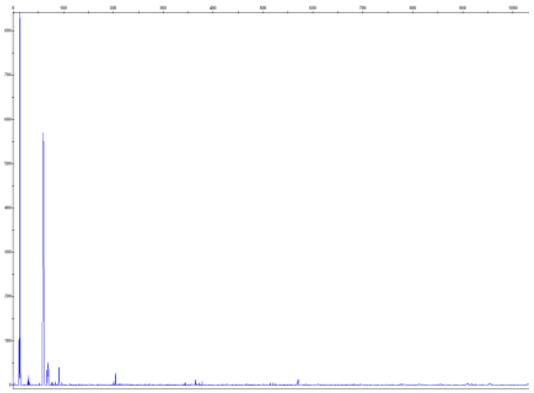

B7.4HhaI

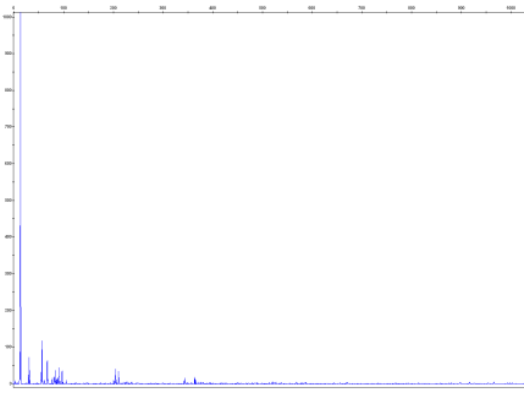

B7.2HhaI

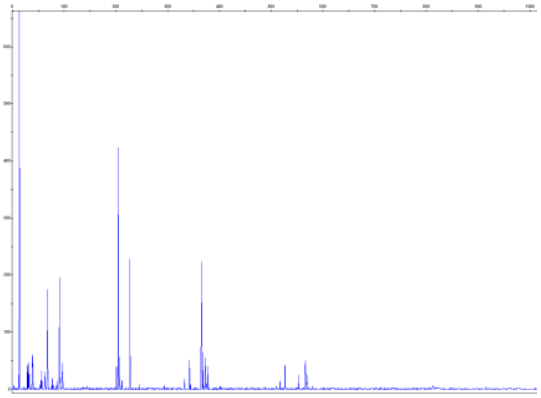

B7.5HhaI

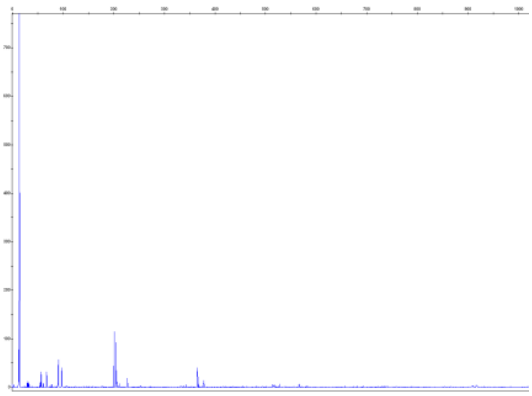

B7.3HhaI

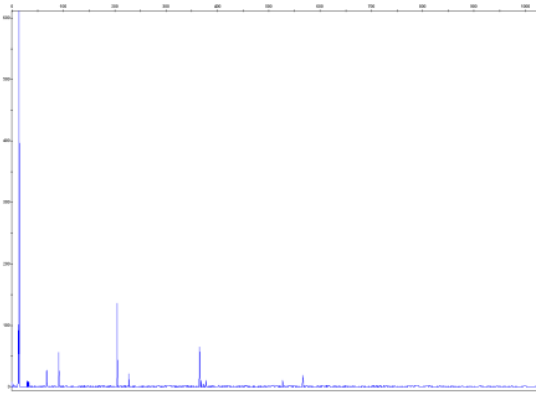

B7.6HhaI

Figure 44. HhaI T-RFLP electropherograms for Site #7, samples 1-6, spring

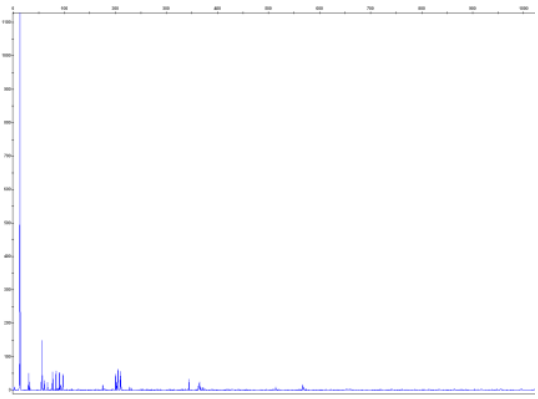

B8.1HhaI

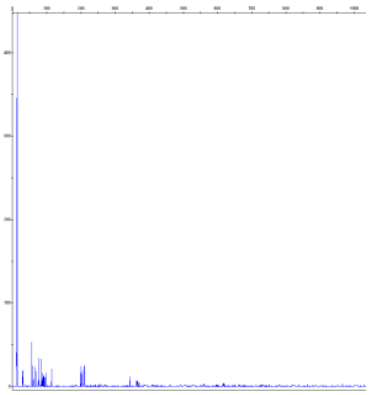

B8.4HhaI

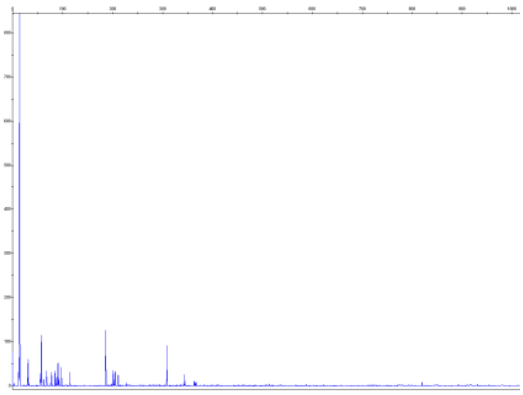

B8.2HhaI

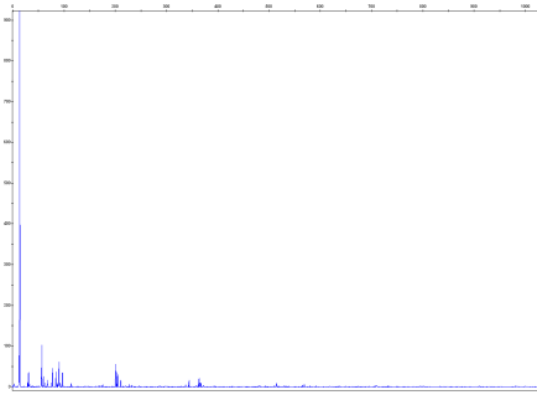

B8.5HhaI

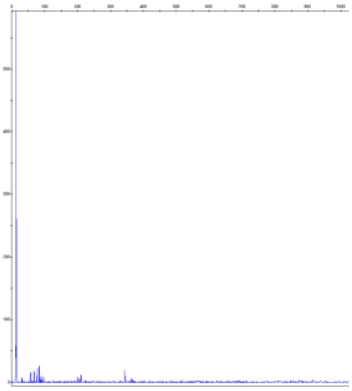

B8.3HhaI

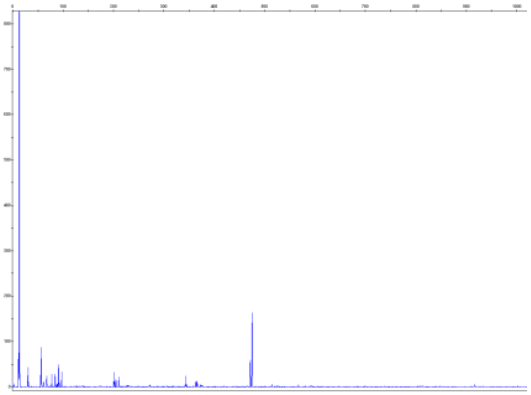

B8.6HhaI

Figure 45. HhaI T-RFLP electropherograms for Site #8, samples 1-6, spring

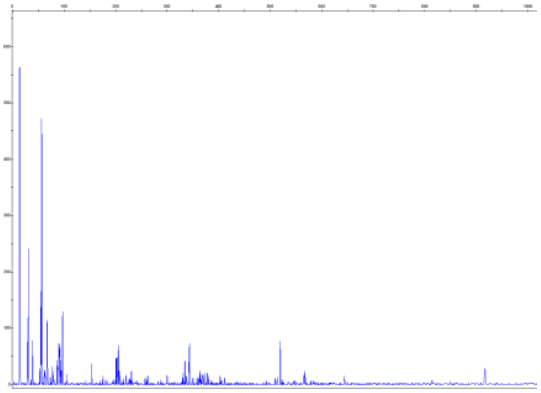

B9.1HhaI

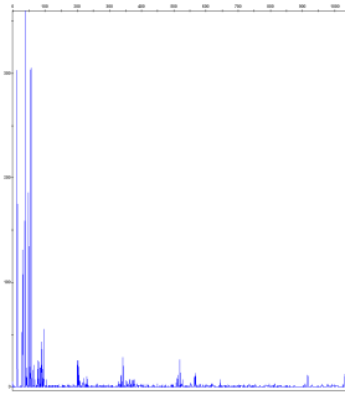

B9.4Hha

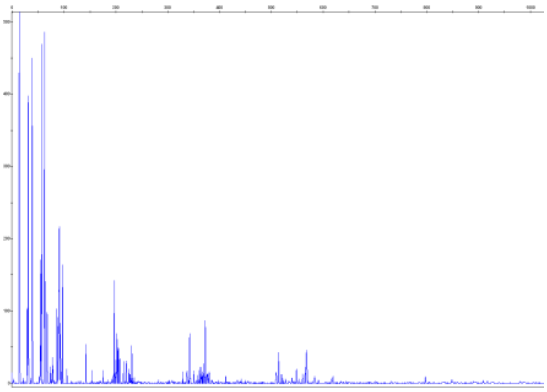

B9.2HhaI

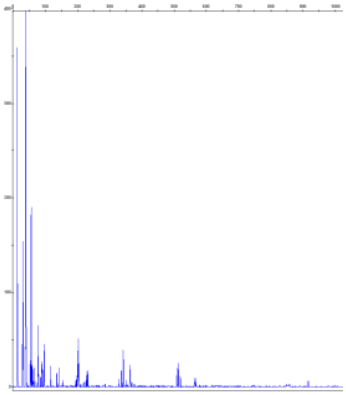

B9.5HhaI

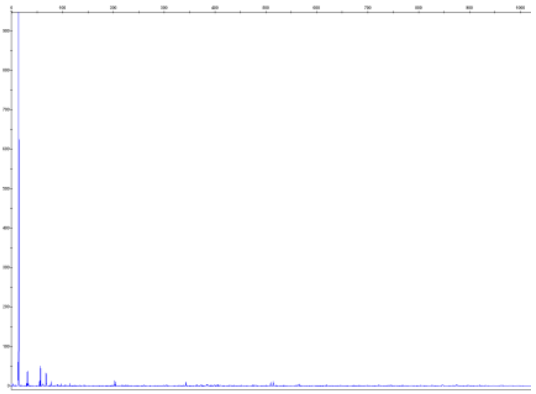

B9.3HhaI

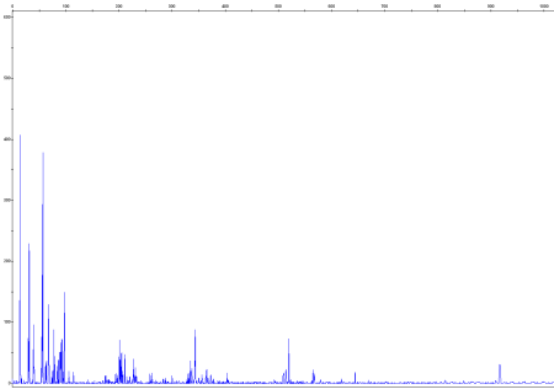

B9.6HhaI

Figure 46. HhaI T-RFLP electropherograms for Site #9, samples 1-6, spring

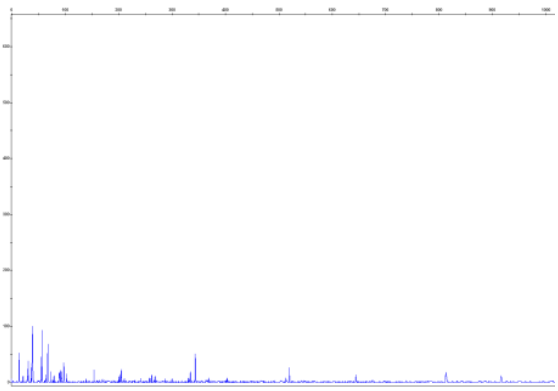

B10.1HhaI

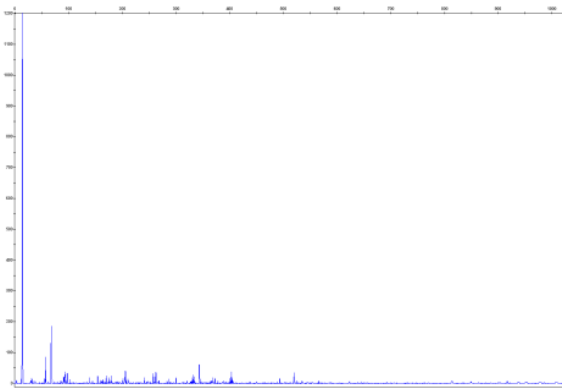

B10.4HhaI

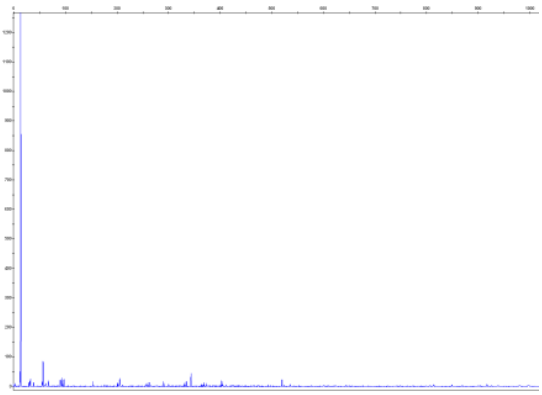

B10.2HhaI

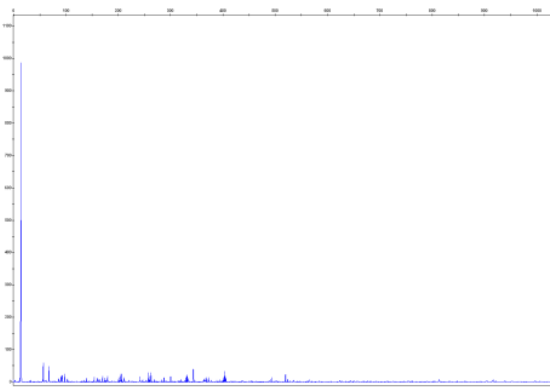

B10.5HhaI

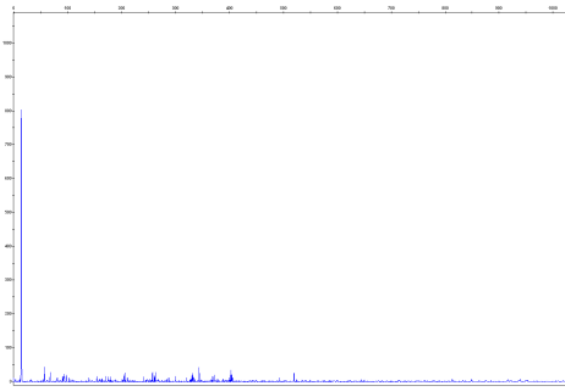

B10.3HhaI

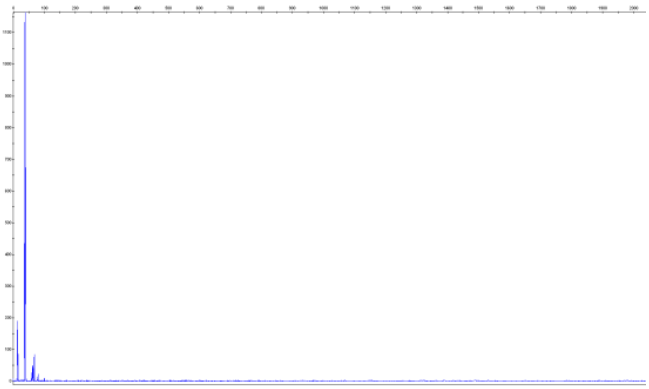

B10.6 HhaI

Figure 47. HhaI T-RFLP electropherograms for Site #10, samples 1-6, spring

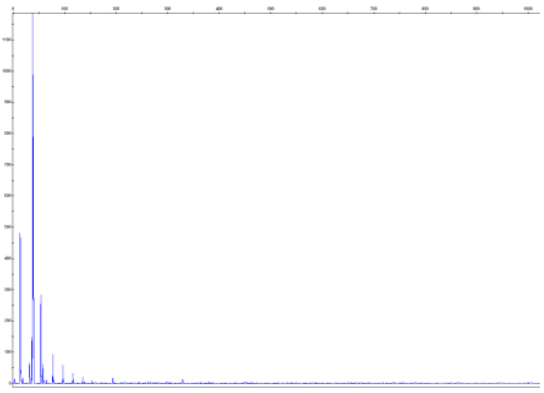

B1.1HaeIII

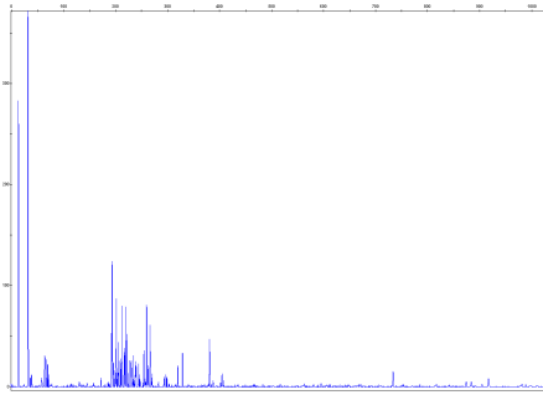

B1.4HaeIII

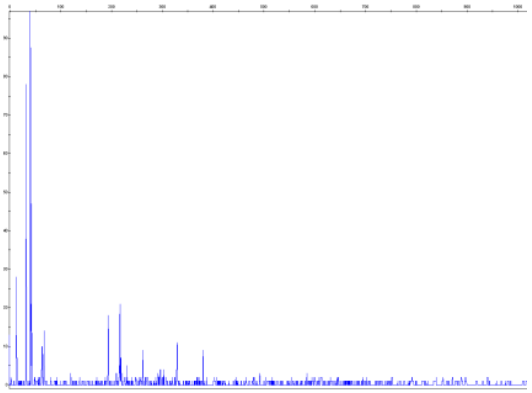

B1.2HaeIII

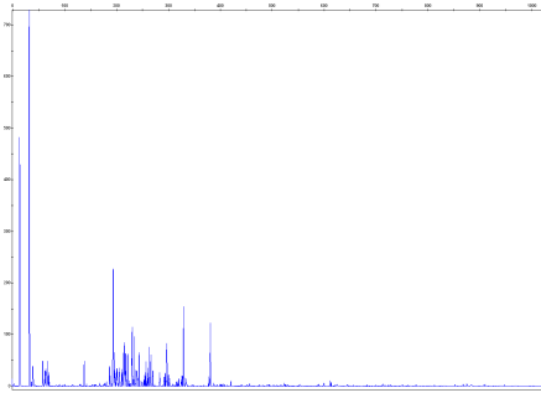

B1.5HaeIII

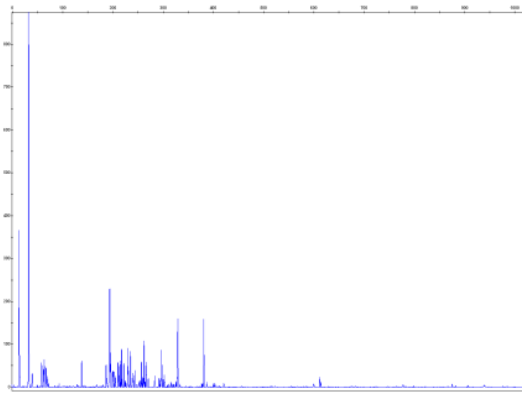

B1.3HaeIII

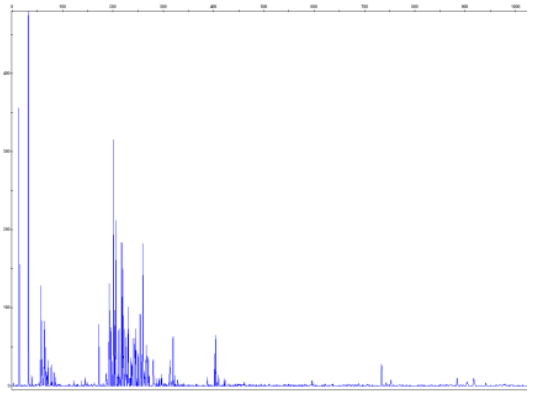

B1.6HaeIII

Figure 48. HaeIII T-RFLP electropherograms for Site #1, samples 1-6, spring

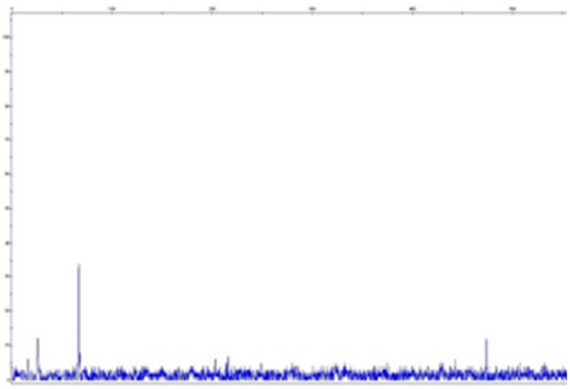

B2.1 HaeIII

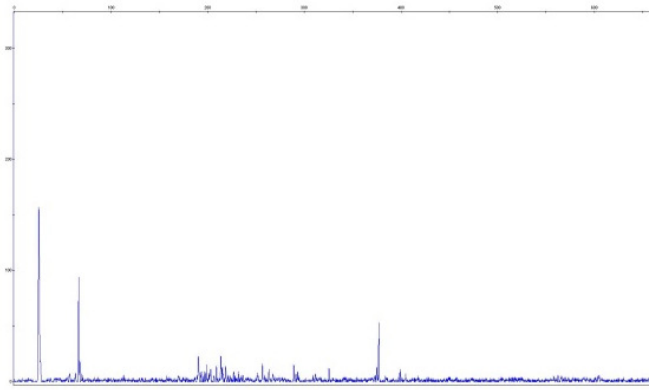

B2.4 HaeIII

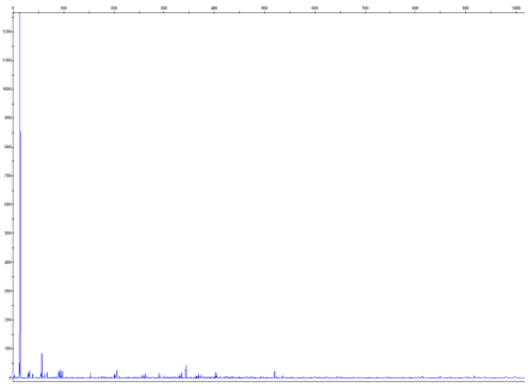

B2.2 HaeIII

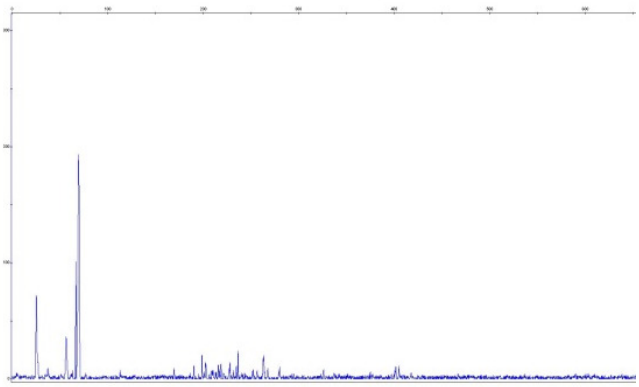

B2.5 HaeIII

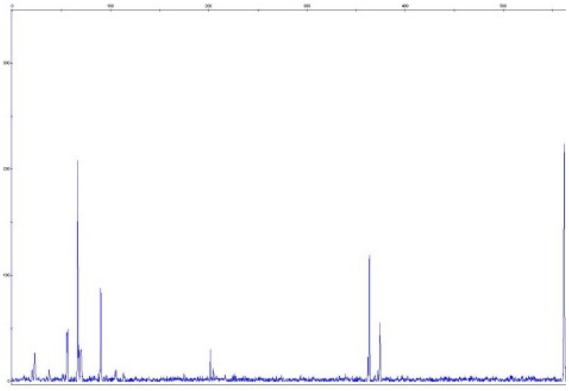

B2.3 HaeIII

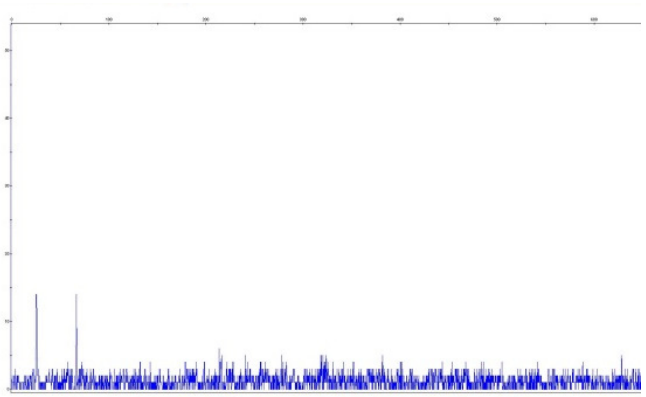

B2.6 HaeIII

Figure 49. HaeIII T-RFLP electropherograms for Site #2, samples 1-6, spring

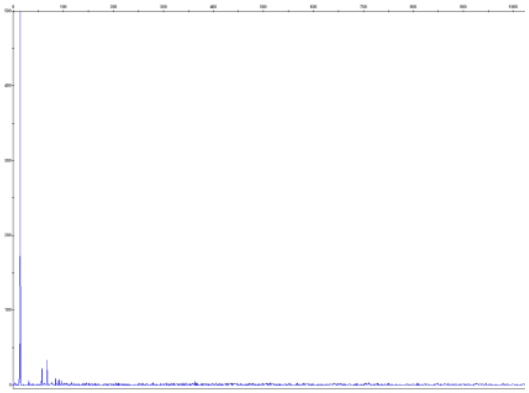

B3.1 HaeIII

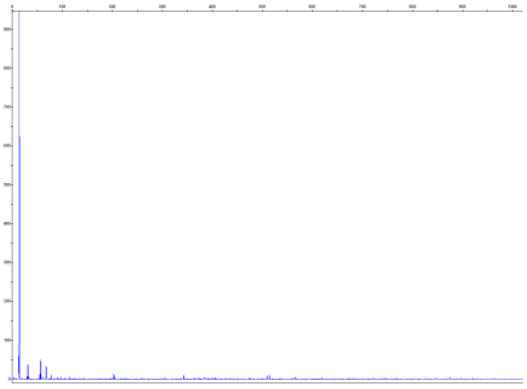

B3.4 HaeIII

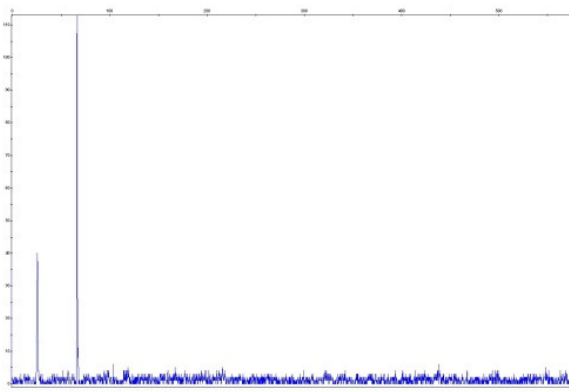

B3.2 HaeIII

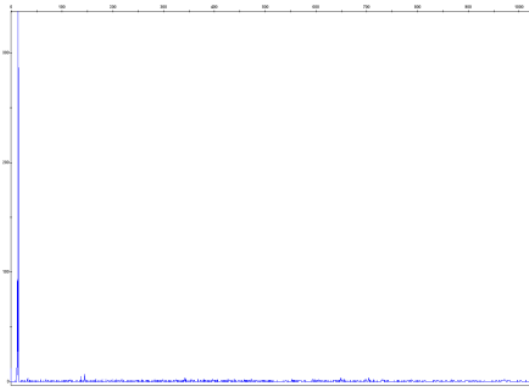

B3.5 HaeIII

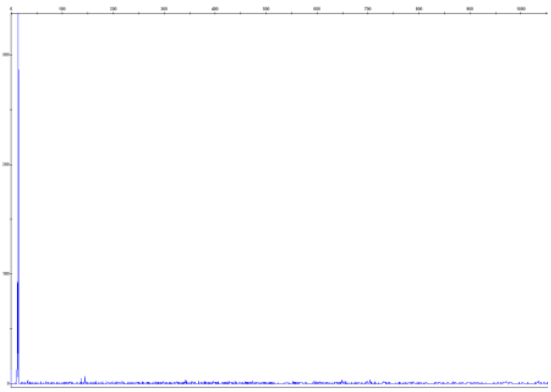

B3.3 HaeIII

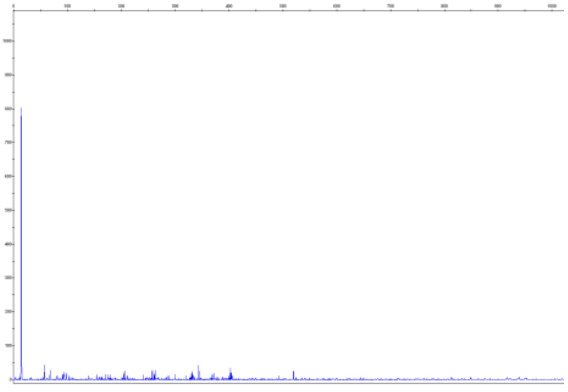

B3.6 HaeIII

Figure 50. HaeIII T-RFLP electropherograms for Site #3, samples 1-6, spring

B4.1HaeIII

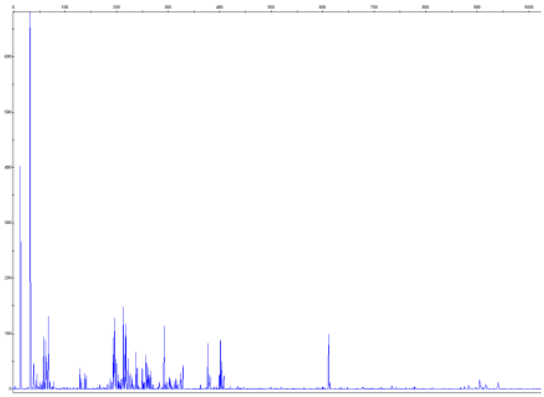

B4.4HaeIII

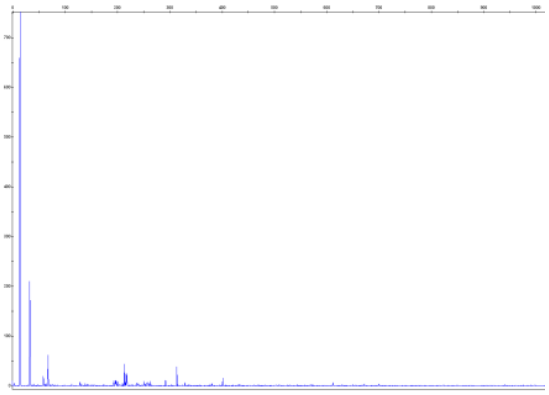

B4.2HaeIII

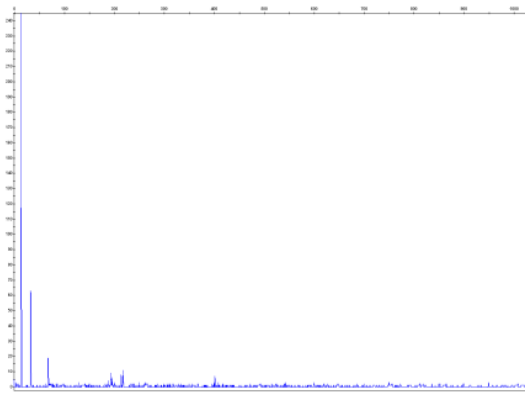

B4.5HaeIII

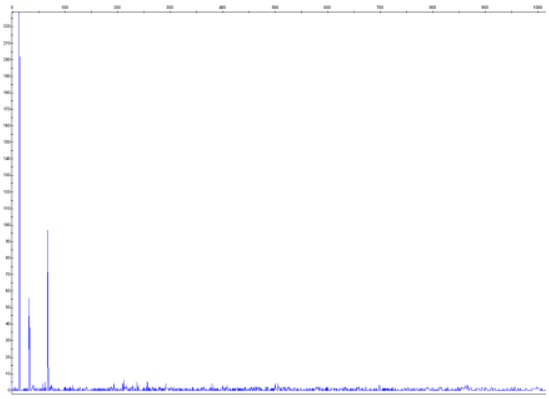

B4.3HaeIII

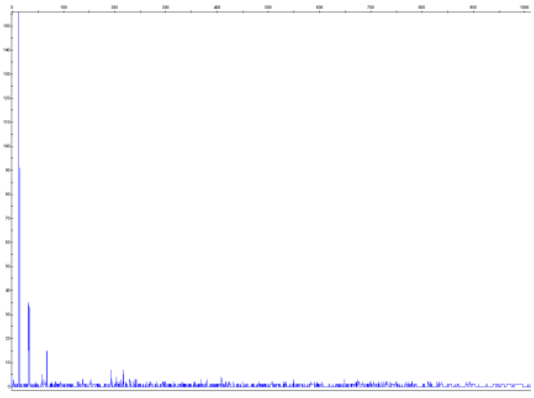

B4.6HaeIII

Figure 51. HaeIII T-RFLP electropherograms for Site #4, samples 1-6, spring

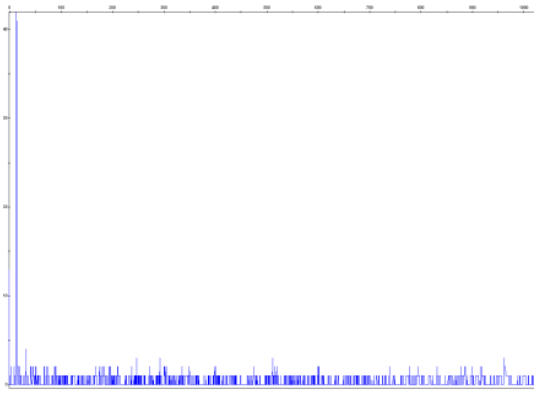

B5.1HaeIII

B5.4HaeIII

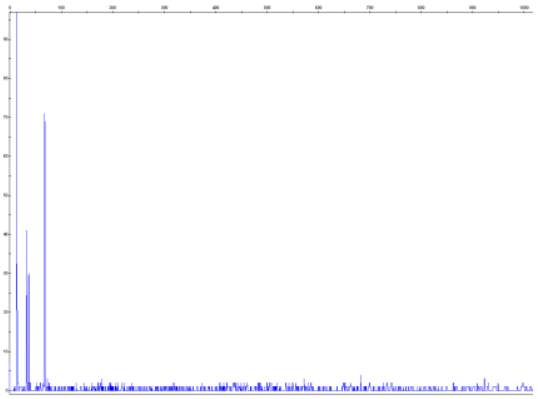

B5.2HaeIII

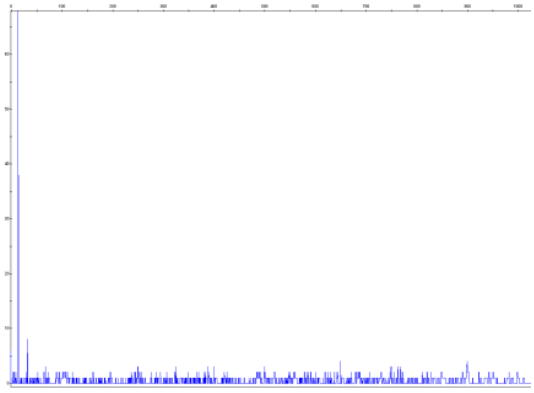

B5.5HaeIII

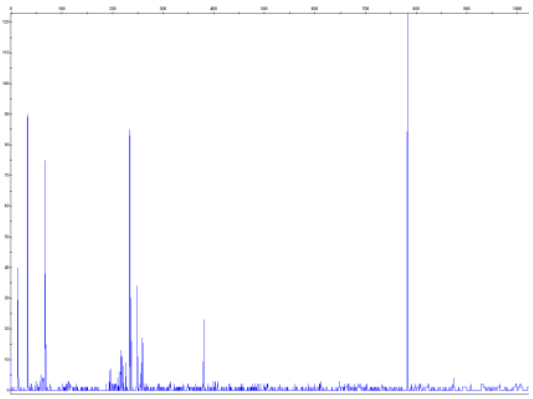

B5.3HaeIII

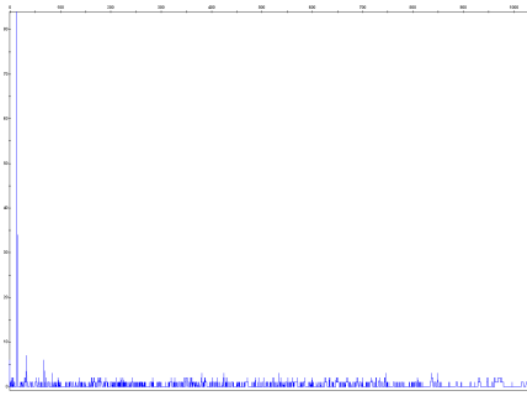

B5.6HaeIII

Figure 52. HaeIII T-RFLP electropherograms for Site #5, samples 1-6, spring

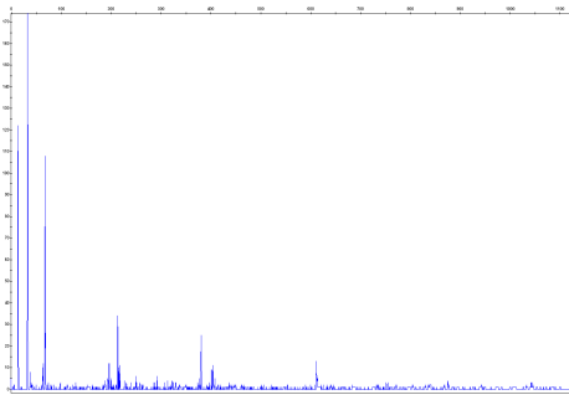

B6.1HaeIII

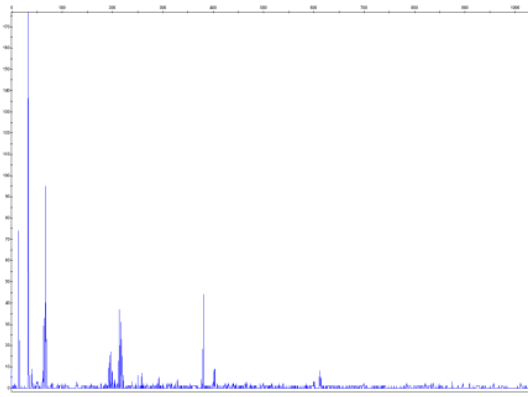

B6.4HaeIII

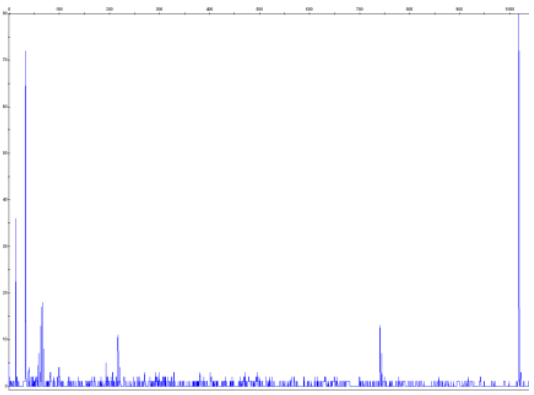

B6.2HaeIII

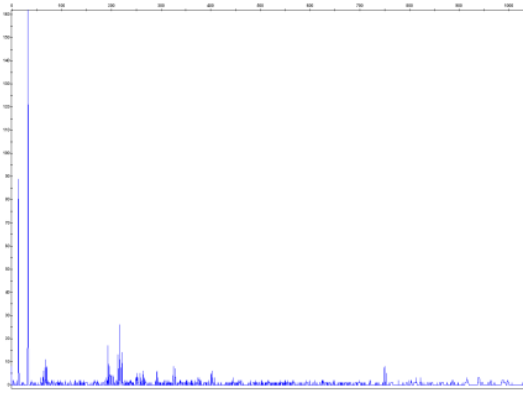

B6.5HaeIII

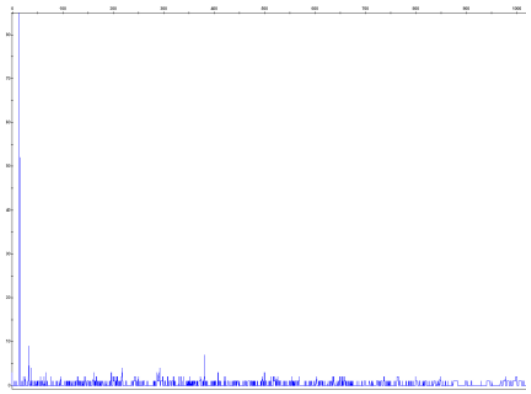

B6.3 HaeIII

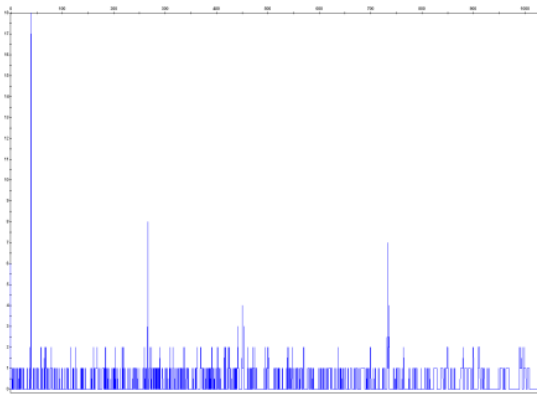

B6.6HaeIII

Figure 53. HaeIII T-RFLP electropherograms for Site #6, samples 1-6, spring

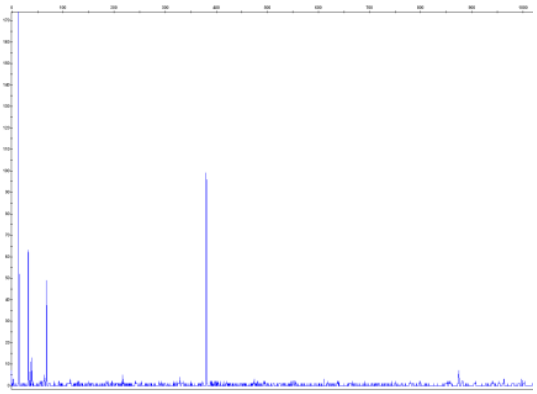

B7.1HaeIII

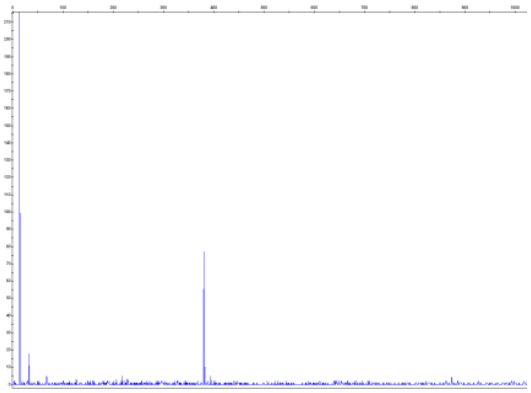

B7.4HaeIII

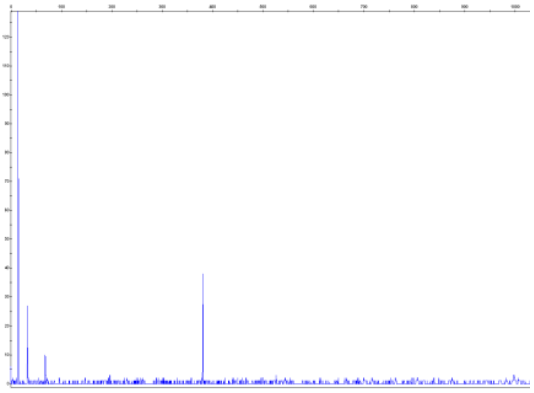

B7.2HaeIII

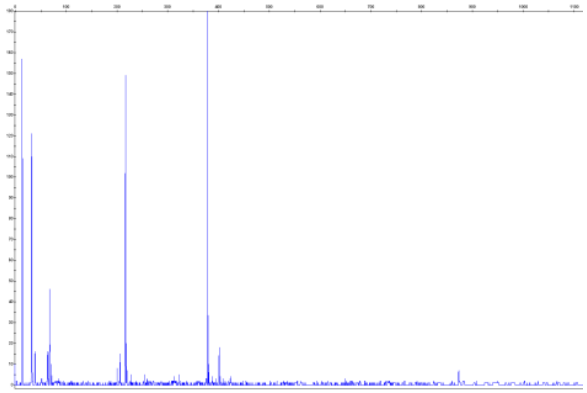

B7.5HaeIII

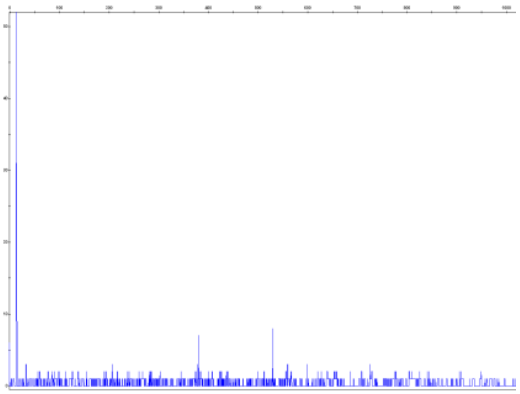

B7.3HaeIII

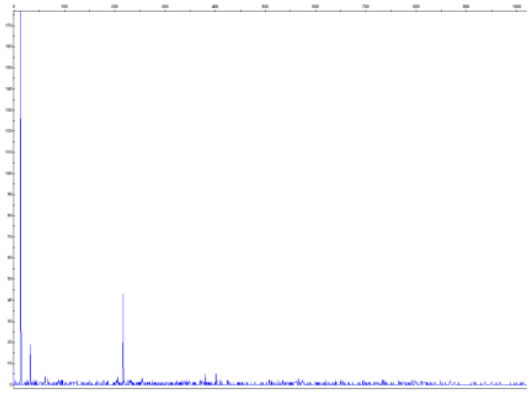

B7.6HaeIII

Figure 54. HaeIII T-RFLP electropherograms for Site #7, samples 1-6, spring

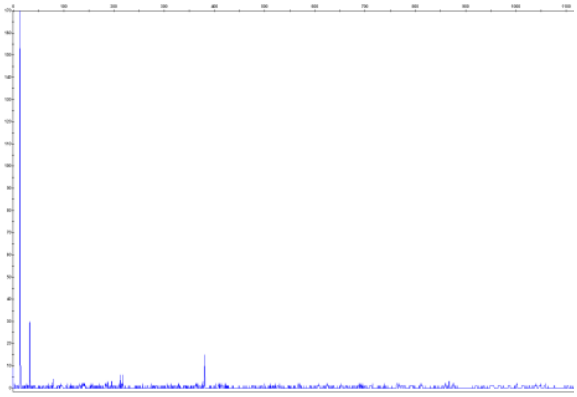

B8.1HaeIII

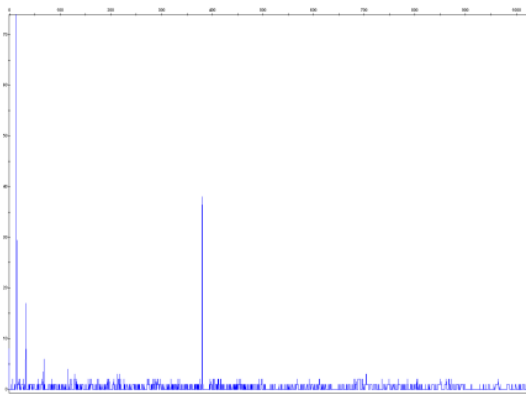

B8.4HaeIII

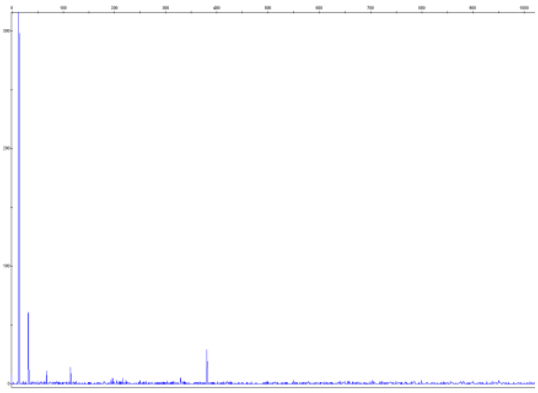

B8.2HaeIII

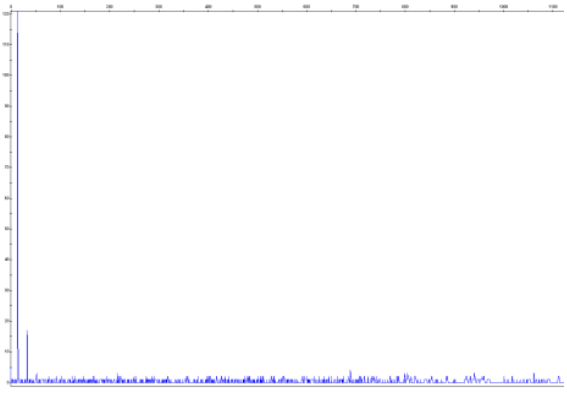

B8.5HaeIII

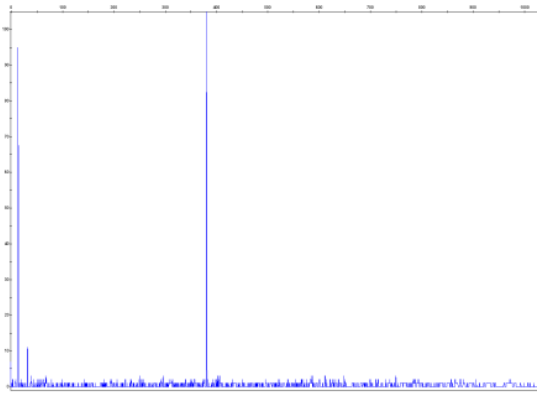

B8.3HaeIII

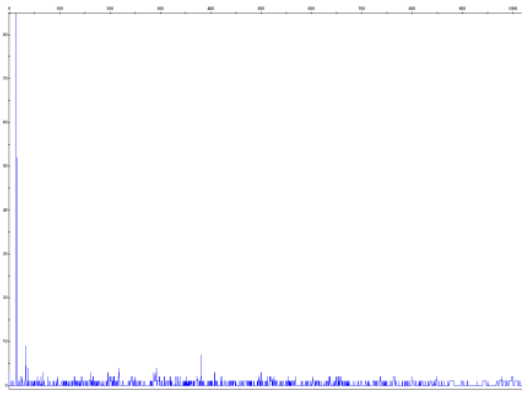

B8.6HaeIII

Figure 55. HaeIII T-RFLP electropherograms for Site #8, samples 1-6, spring

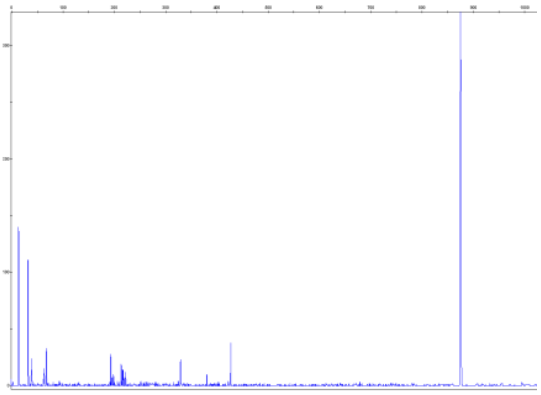

B9.1HaeIII

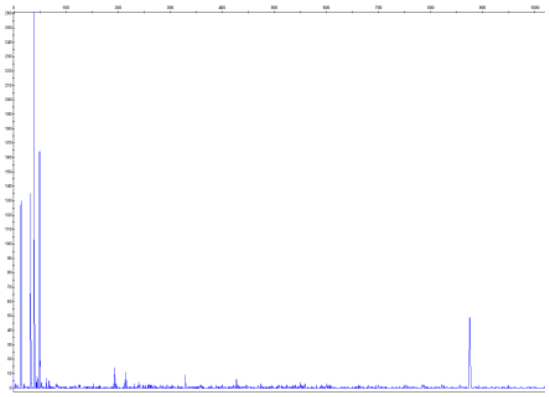

B9.4HaeIII

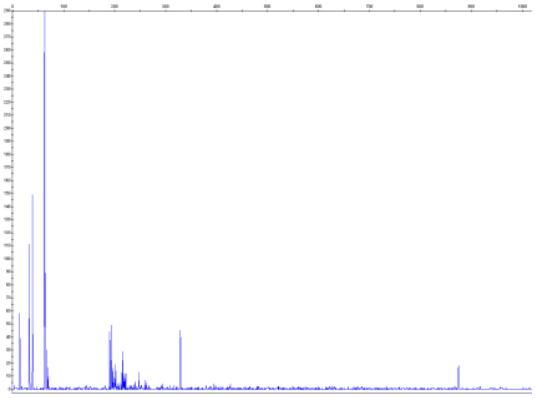

B9.2HaeIII

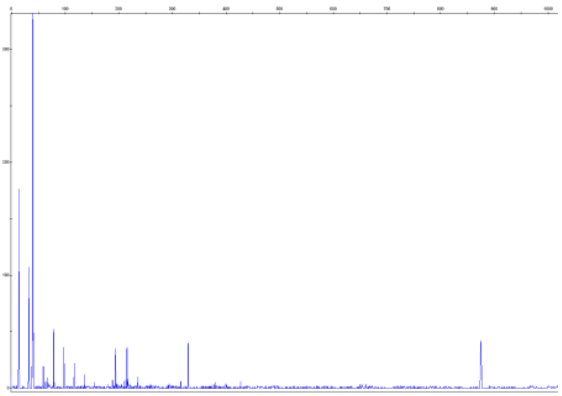

B9.5HaeIII

B9.3HaeIII

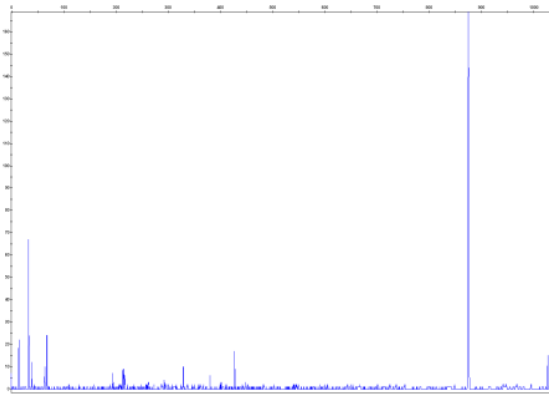

B9.6HaeIII

Figure 56. HaeIII T-RFLP electropherograms for Site #9, samples 1-6, spring

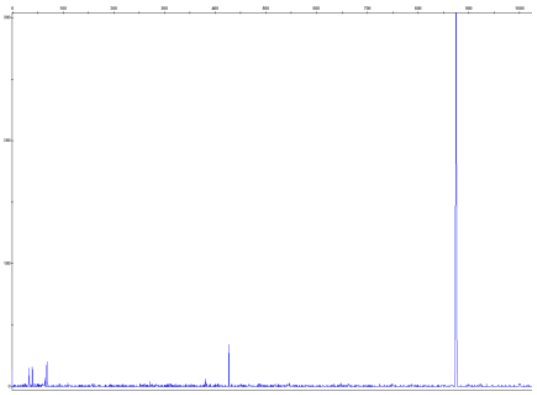

B10.1HaeIII

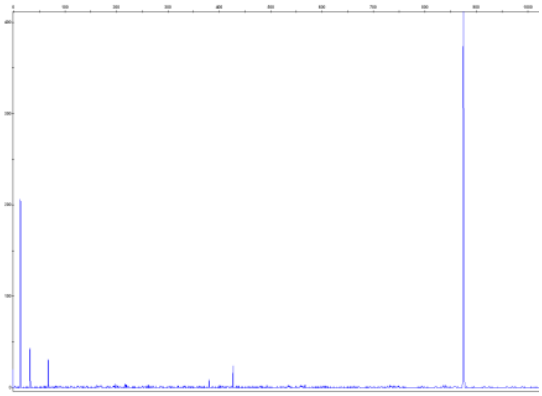

B10.4HaeIII

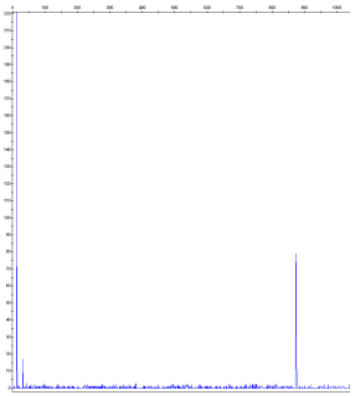

B10.2HaeIII

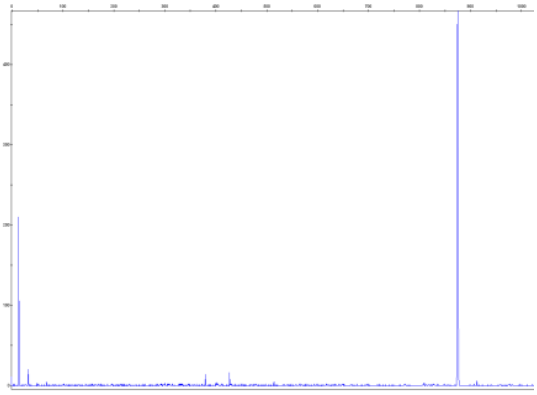

B10.5HaeIII

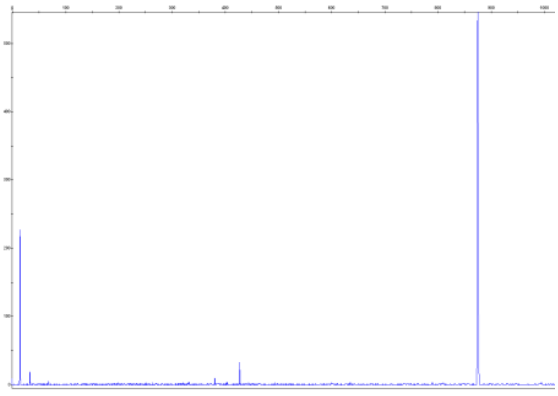

B10.3HaeIII

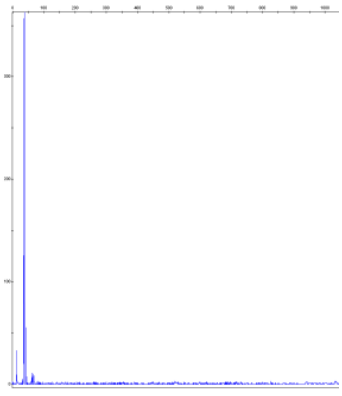

B10.6 HaeIII

Figure 57. HaeIII T-RFLP electropherograms for Site #10, samples 1-6, spring

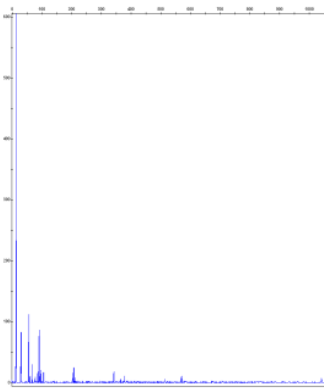

C1.1HhaI

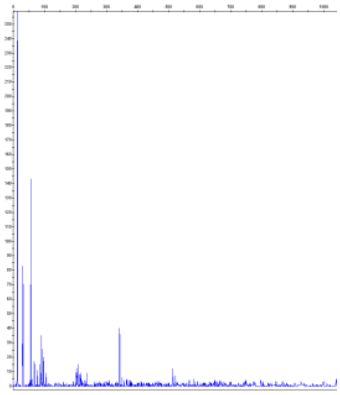

C1.4HhaI

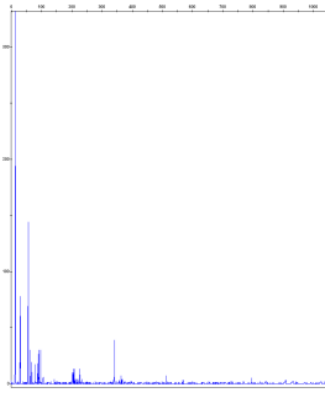

C1.2HhaI

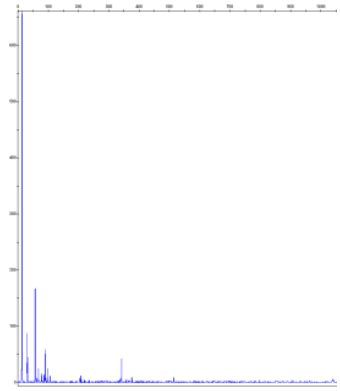

C1.5HhaI

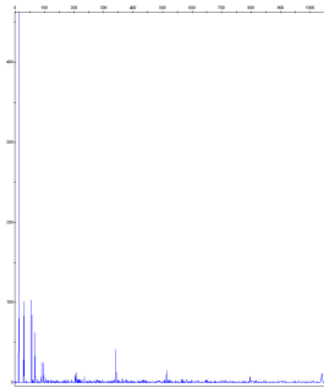

C1.3HhaI

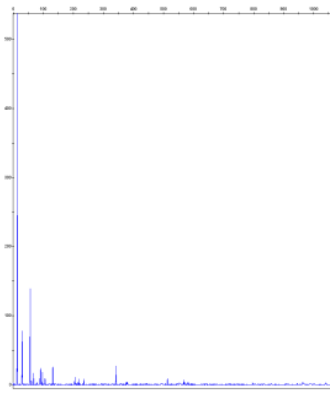

C1.6HhaI

Figure 58. HhaI T-RFLP electropherograms for Site #1, samples 1-6, fall

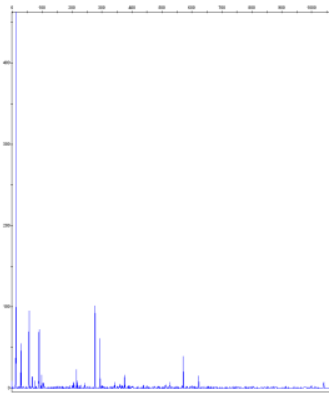

C2.1HhaI

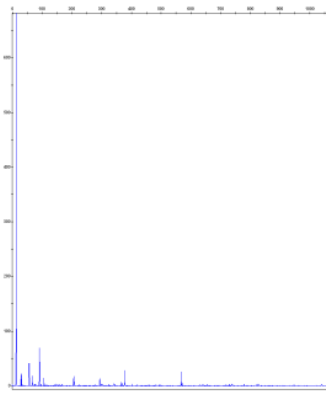

C2.4HhaI

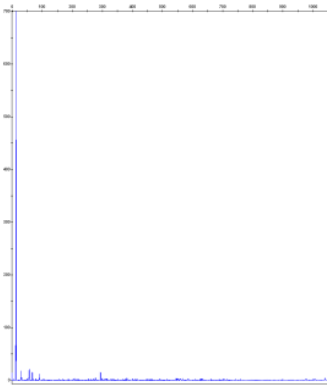

C2.2HhaI

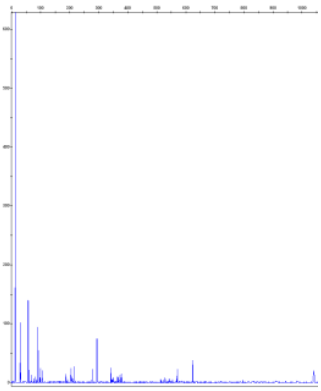

C2.5HhaI

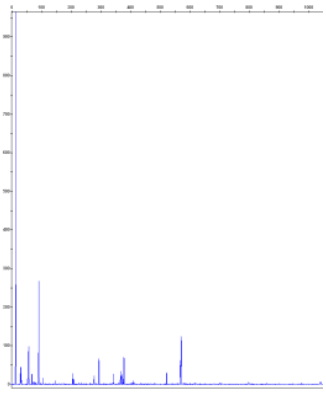

C2.3HhaI

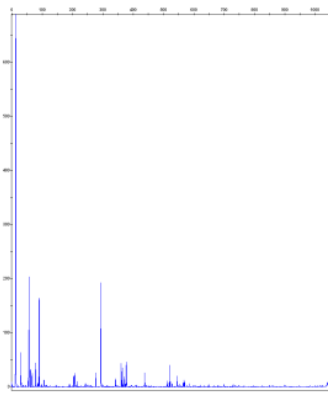

C2.6HhaI

Figure 59. HhaI T-RFLP electropherograms for Site #2, samples 1-6, fall

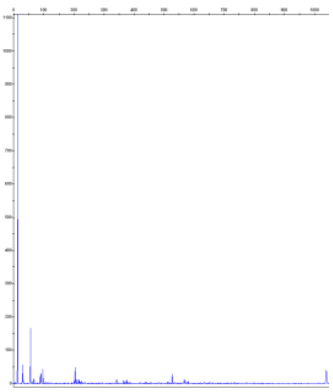

C3.1HhaI

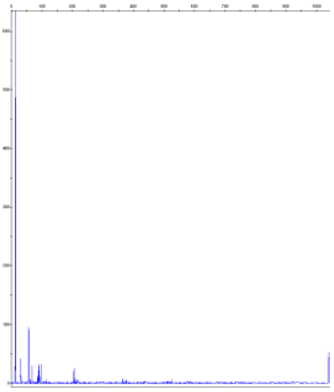

C3.4HhaI

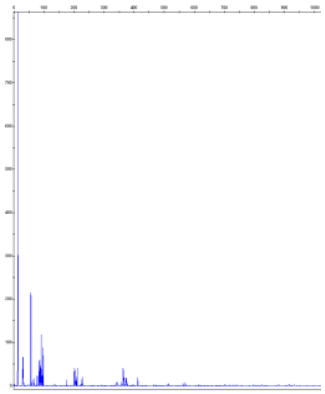

C3.2HhaI

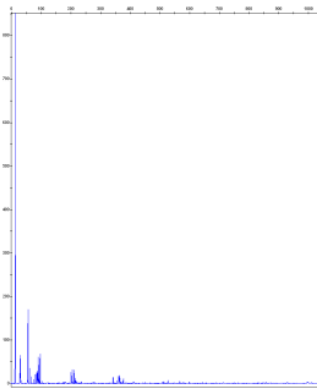

C3.5HhaI

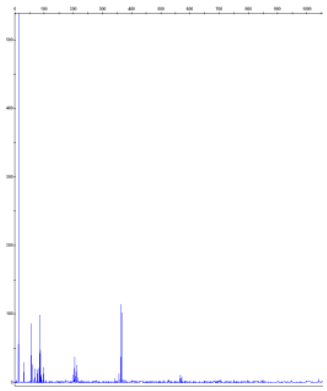

C3.3HhaI

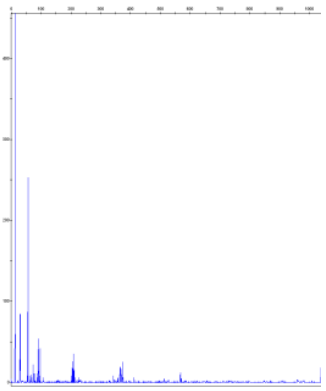

C3.6Hha

Figure 60. HhaI T-RFLP electropherograms for Site #3, samples 1-6, fall

C4.1HhaI

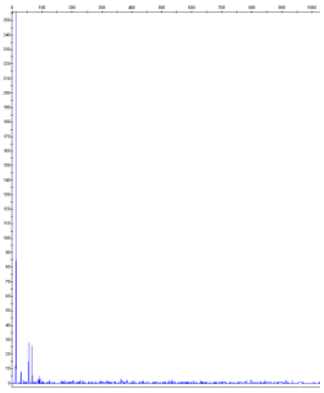

C4.4HhaI

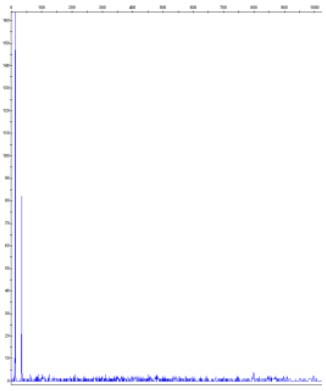

C4.2HhaI

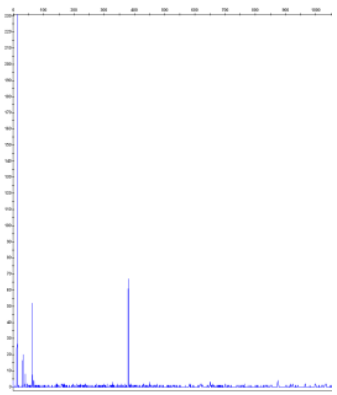

C4.5HaeIII

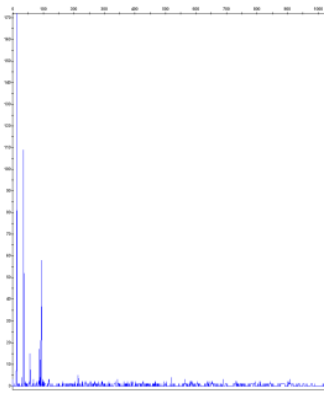

C4.3HhaI

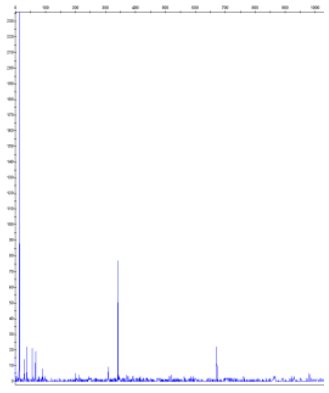

C4.6HhaI

Figure 61. HhaI T-RFLP electropherograms for Site #4, samples 1-6, fall

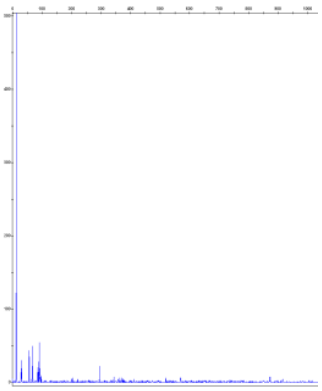

C5.1HhaI

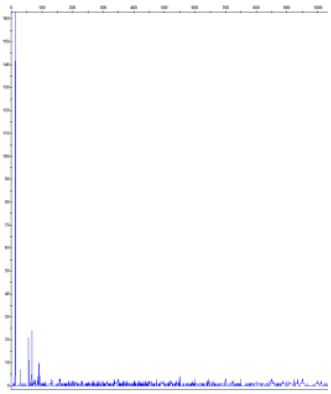

C5.4HhaI

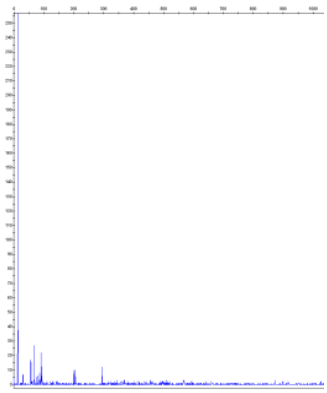

C5.2HhaI

C5.5HhaI

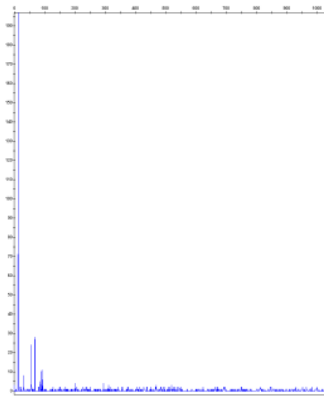

C5.3HhaI

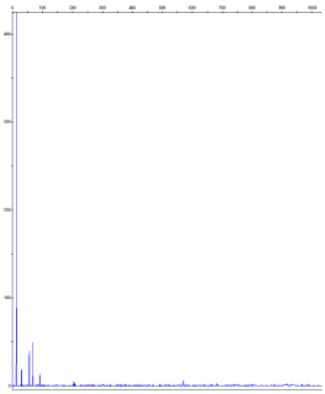

C5.6HhaI

Figure 62. HhaI T-RFLP electropherograms for Site #5, samples 1-6, fall

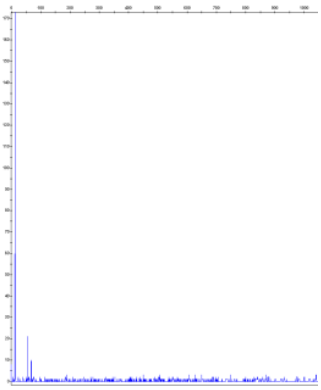

C6.1HhaI

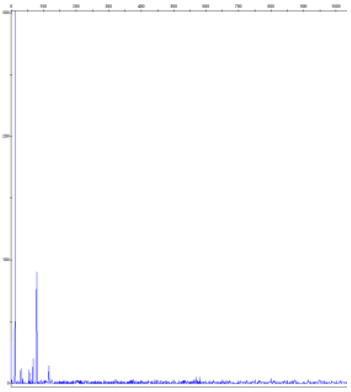

C6.4HhaI

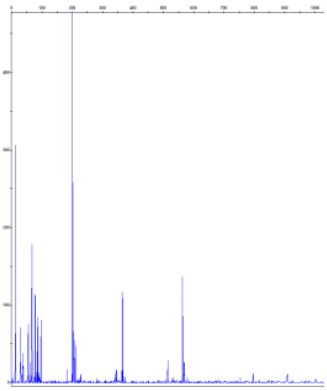

C6.2HhaI

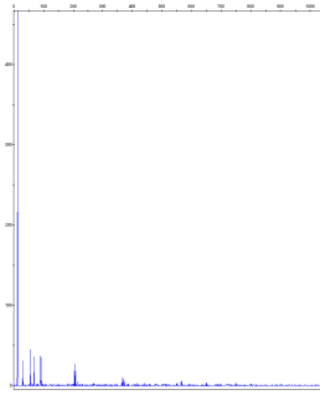

C6.5HhaI

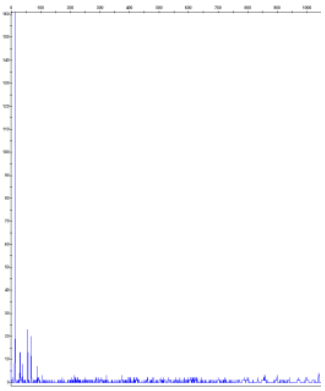

C6.3HhaI

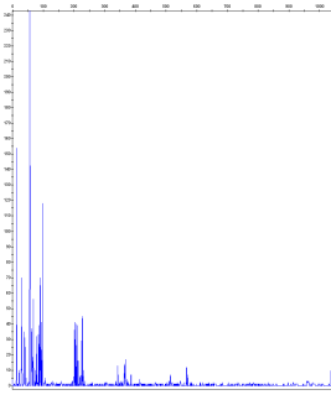

C6.6HhaI

Figure 63. HhaI T-RFLP electropherograms for Site #6, samples 1-6, fall

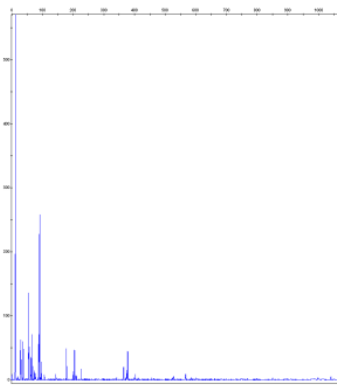

C7.1 HhaI

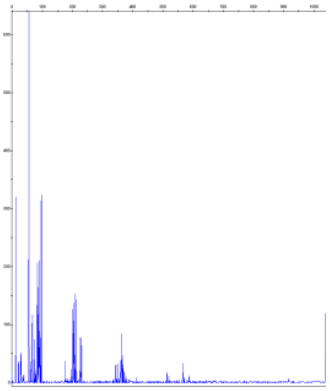

C7.4Hha

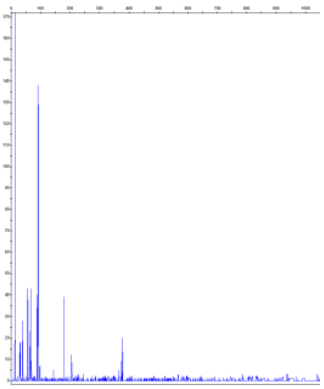

C7.2HhaI

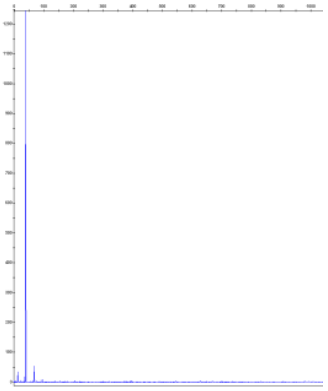

C7.5HhaI

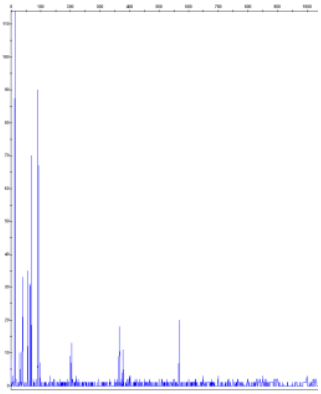

C7.3HhaI

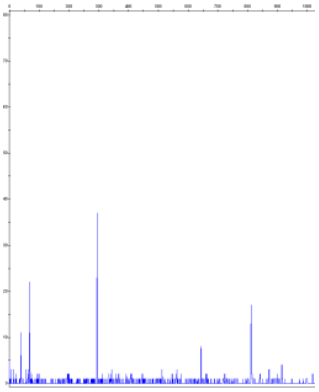

C7.6Hha

Figure 64. HhaI T-RFLP electropherograms for Site #7, samples 1-6, fall

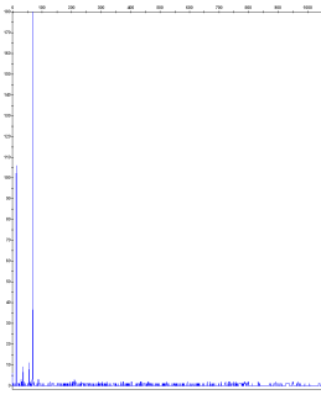

C8.1HhaI

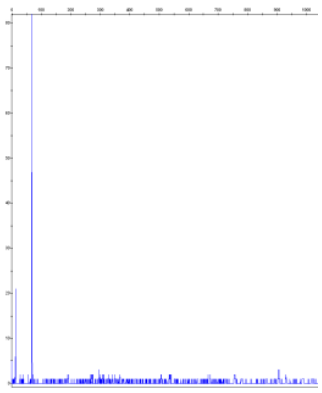

C8.4HhaI

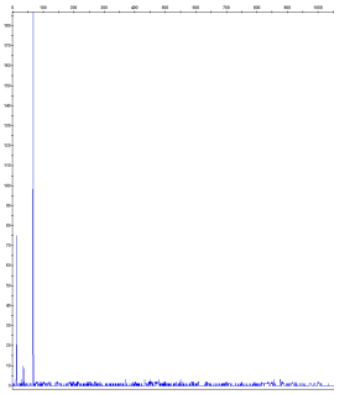

C8.2HhaI

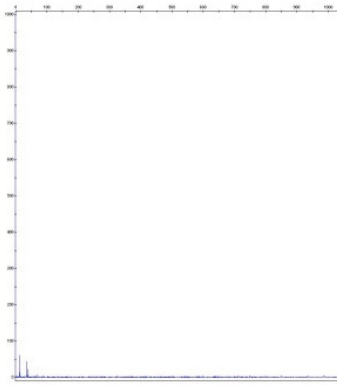

C8.5 HhaI

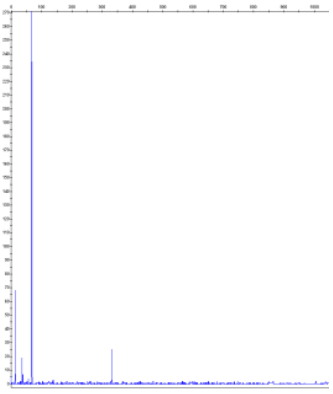

C8.3HhaI

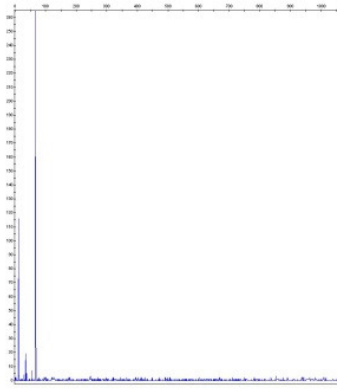

C8.6 HhaI

Figure 65. HhaI T-RFLP electropherograms for Site #8, samples 1-6, fall

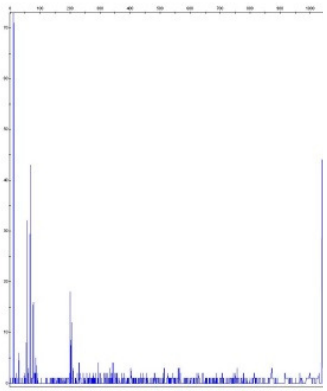

C9.1 HhaI

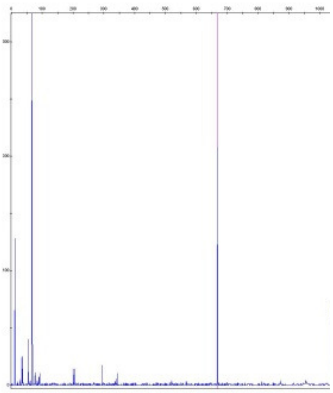

C9.4 HhaI

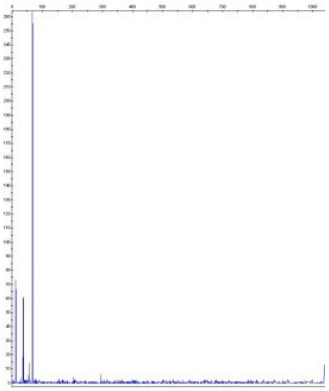

C9.2 HhaI

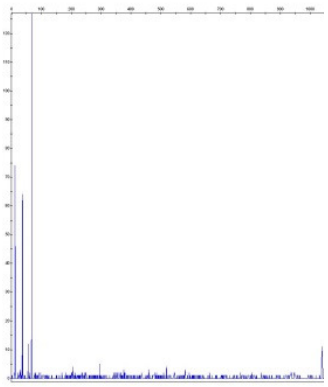

C9.5 HhaI

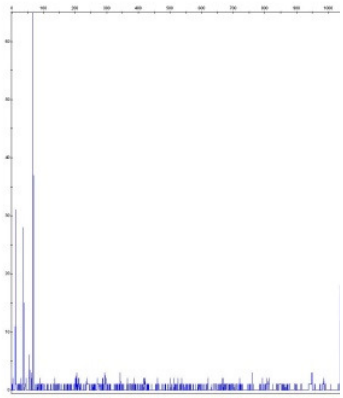

C9.3 HhaI

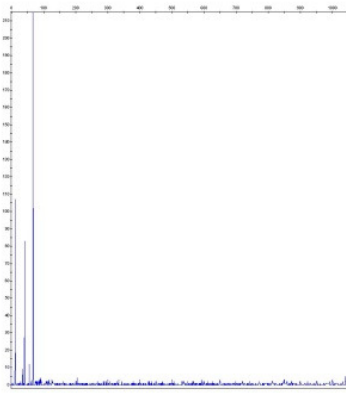

C9.6 HhaI

Figure 66. HhaI T-RFLP electropherograms for Site #9, samples 1-6, fall

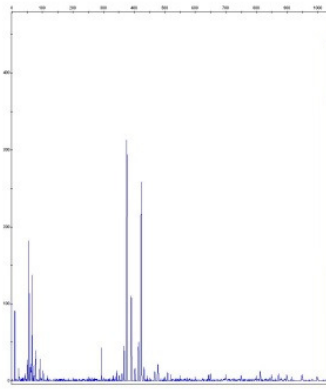

C10.1 HhaI

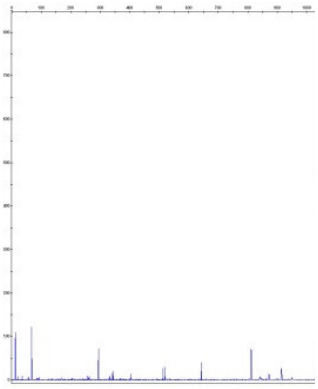

C10.4 HhaI

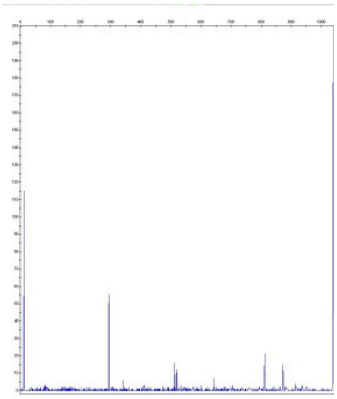

C10.2 HhaI

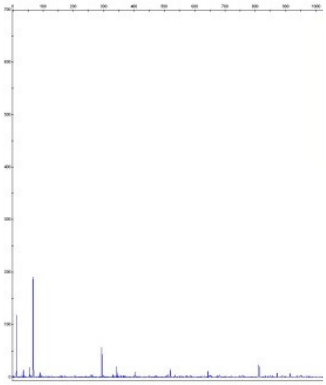

C10.5 HhaI

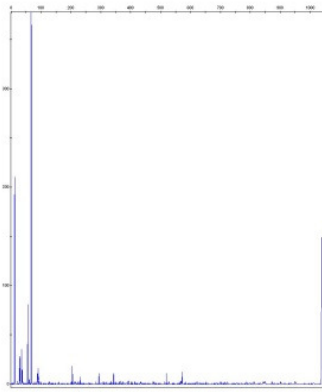

C10.3 HhaI

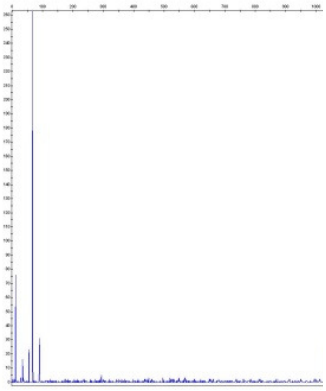

C10.6 HhaI

Figure 67. HhaI T-RFLP electropherograms for Site #10, samples 1-6, fall

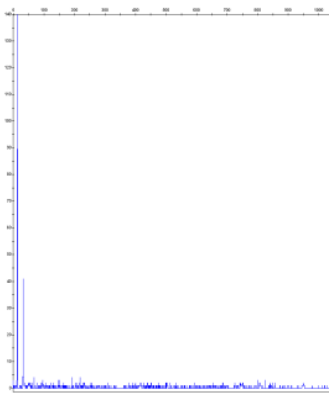

C1.1HaeIII

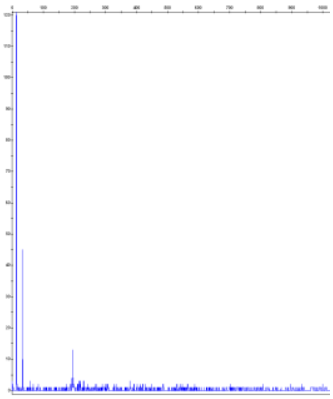

C1.4HaeIII

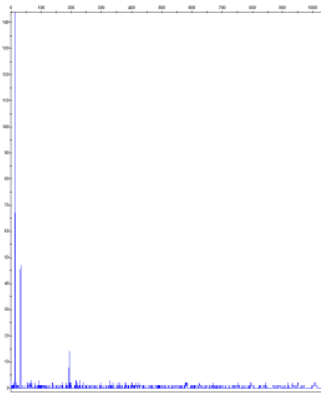

C1.2HaeIII

C1.5HaeIII

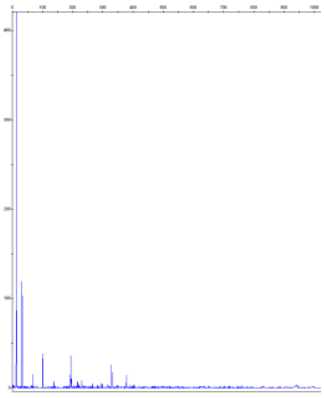

C1.3HaeIII

C1.6HaeIII

Figure 68. HaeIII T-RFLP electropherograms for Site #1, samples 1-6, fall

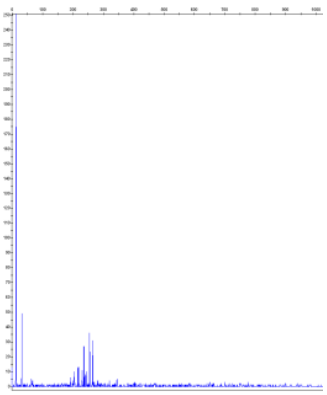

C2.1HaeIII

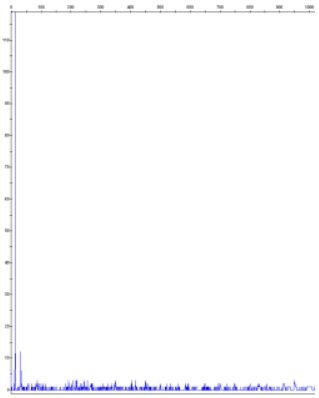

C2.4HaeIII

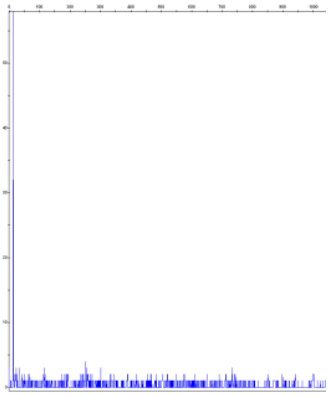

C2.2HaeIII

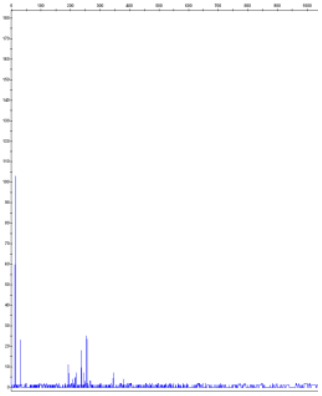

C2.5HaeIII

C2.3HaeIII

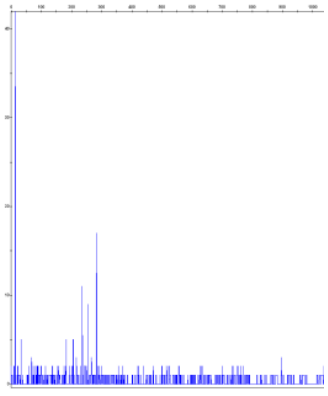

C2.6HaeIII

Figure 69. HaeIII T-RFLP electropherograms for Site #2, samples 1-6, fall

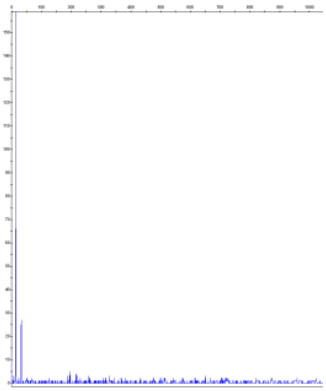

C3.1HaeIII

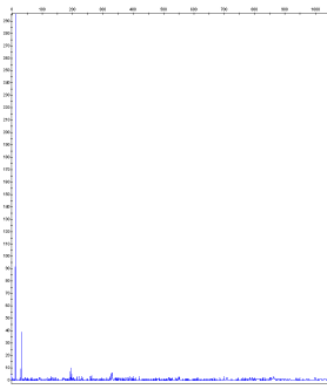

C3.4 HaeIII

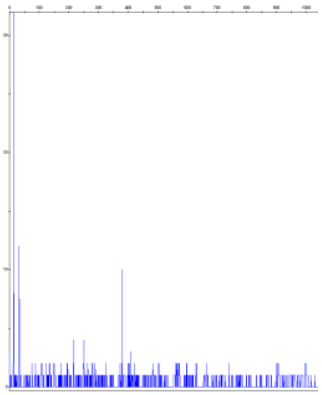

C3.2HaeIII

C3.5HaeIII

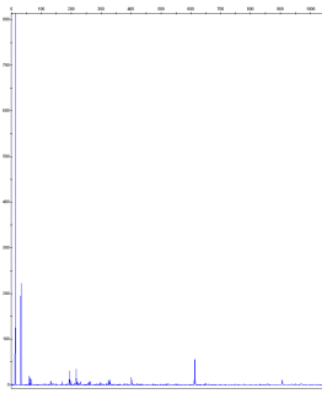

C3.3HaeIII

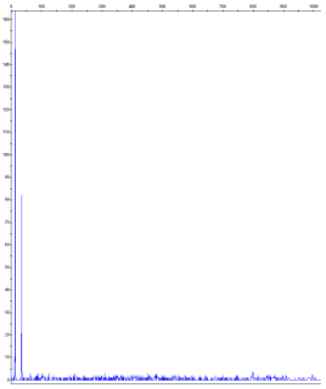

C3.6 HaeIII

Figure 70. HaeIII T-RFLP electropherograms for Site #3, samples 1-6, fall

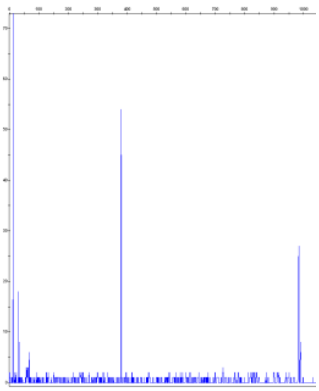

C4.1HaeIII

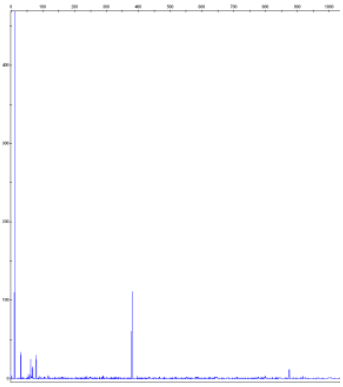

C4.4 HaeIII

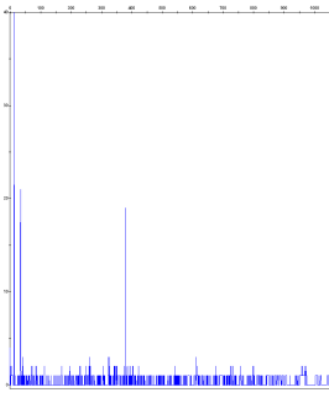

C4.2HaeIII

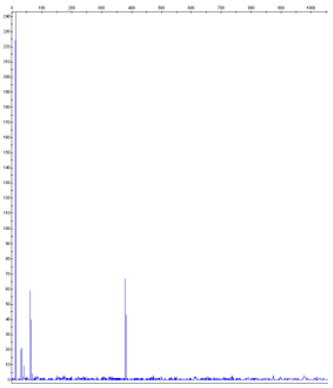

C4.5 HaeIII

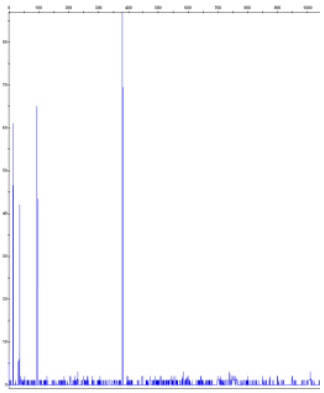

C4.3HaeIII

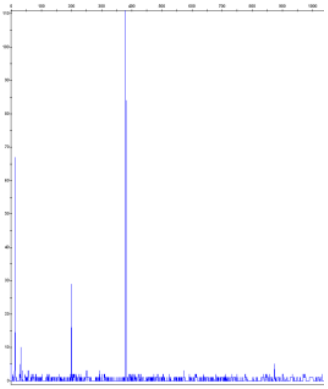

C4.6HaeIII

Figure 71. HaeIII T-RFLP electropherograms for Site #4, samples 1-6, fall

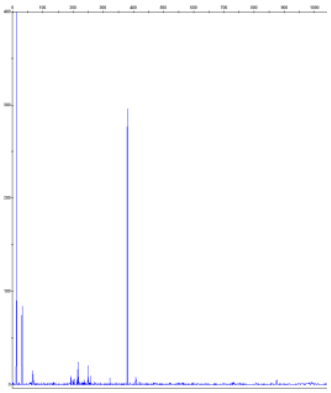

C5.1HaeIII

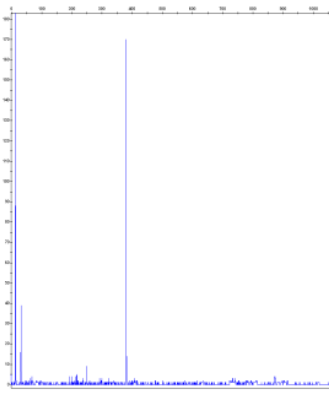

C5.4HaeIII

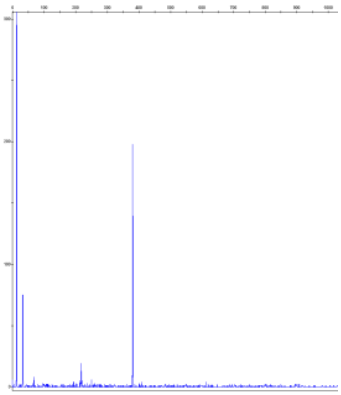

C5.2HaeIII

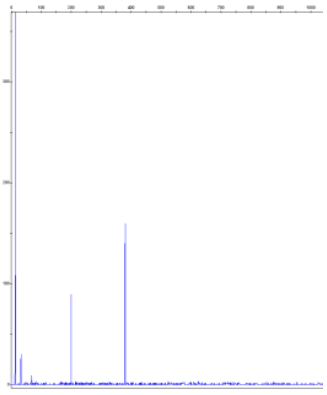

C5.5HaeIII

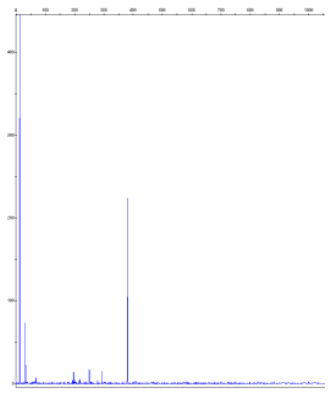

C5.3HaeIII

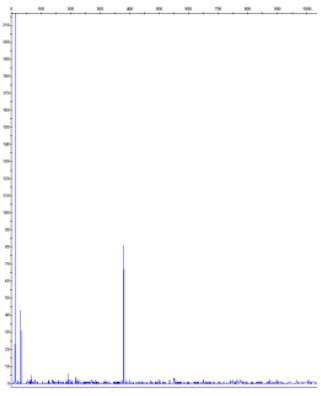

C5.6HaeIII

Figure 72. HaeIII T-RFLP electropherograms for Site #5, samples 1-6, fall

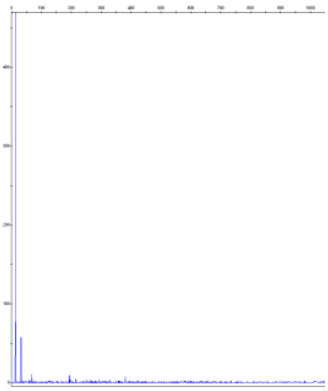

C6.1HaeIII

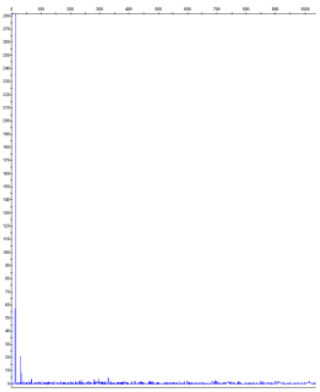

C6.4HaeIII

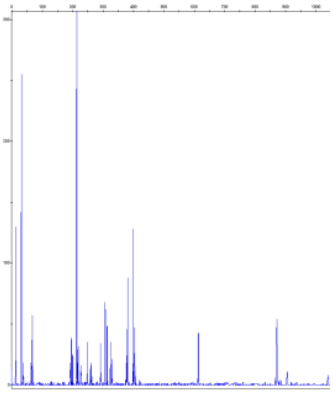

C6.2HaeIII

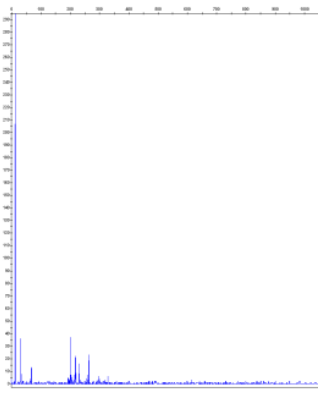

C6.5HaeIII

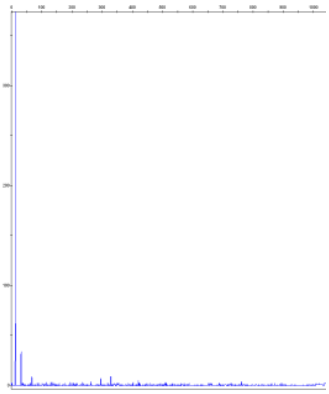

C6.3HaeIII

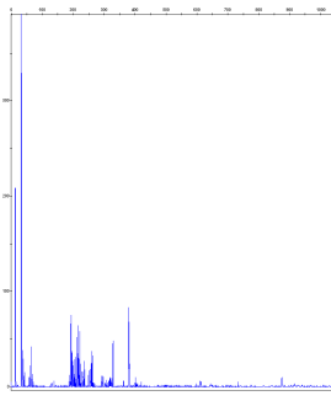

C6.6HaeIII

Figure 73. HaeIII T-RFLP electropherograms for Site #6, samples 1-6, fall

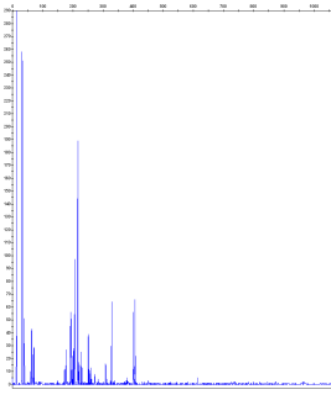

C7.1HaeIII

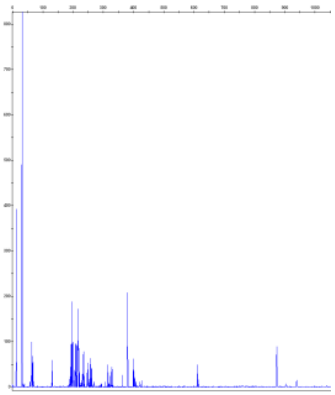

C7.4HaeIII

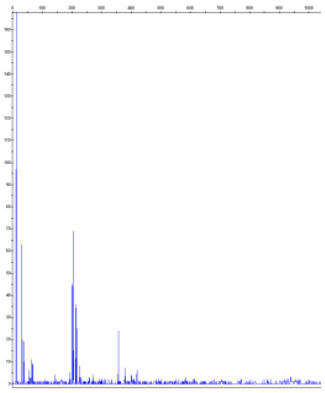

C7.2HaeIII

C7.5HaeIII

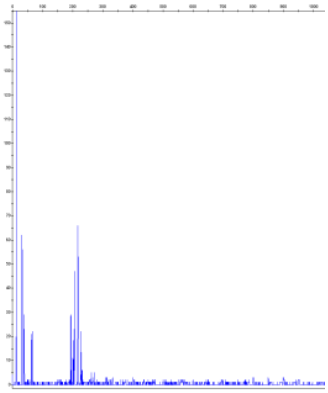

C7.3HaeIII

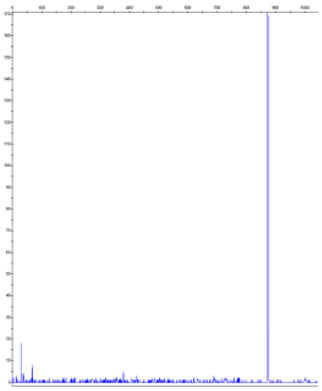

C7.6HaeIII

Figure 74. HaeIII T-RFLP electropherograms for Site #7, samples 1-6, fall

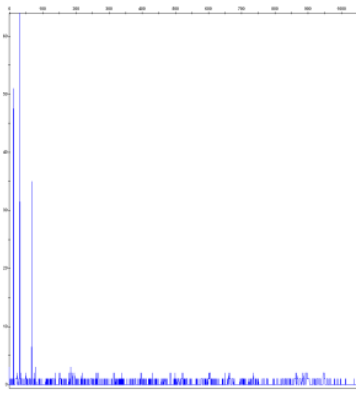

C8.1HaeIII

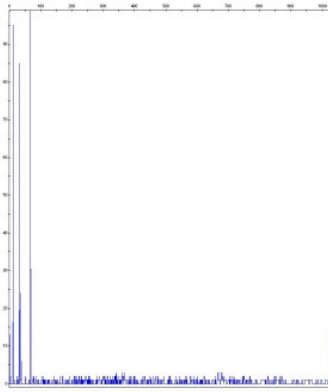

C8.4 HaeIII

C8.2HaeIII

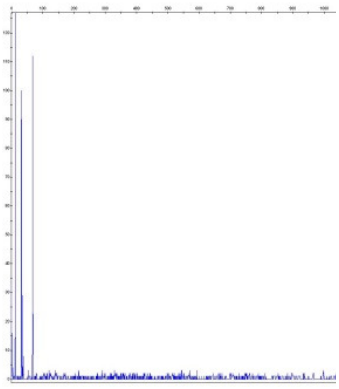

C8.5 HaeIII

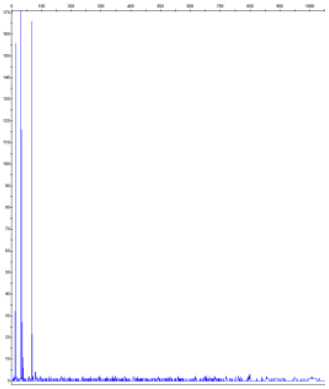

C8.3HaeIII

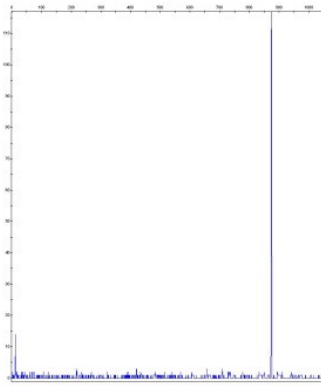

C8.6 HaeIII

Figure 75. HaeIII T-RFLP electropherograms for Site #8, samples 1-6, fall

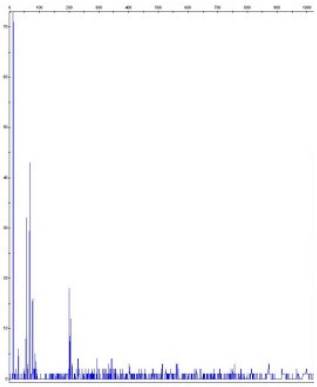

C9.1 HaeIII

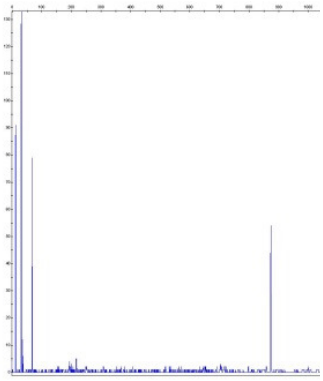

C9.4 HaeIII

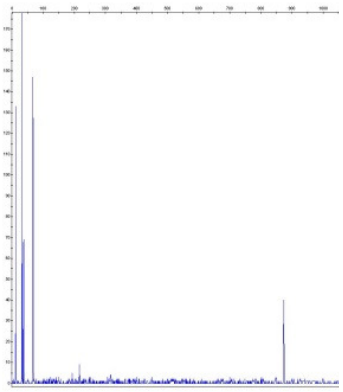

C9.2 HaeIII

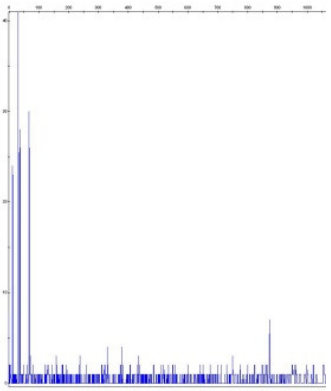

C9.5 HaeIII

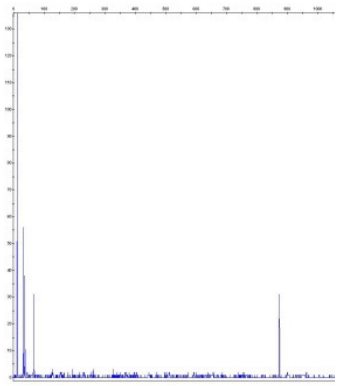

C9.3 HaeIII

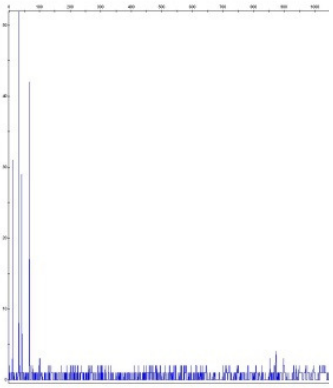

C9.6 HaeIII

Figure 76. HaeIII T-RFLP electropherograms for Site #9, samples 1-6, fall

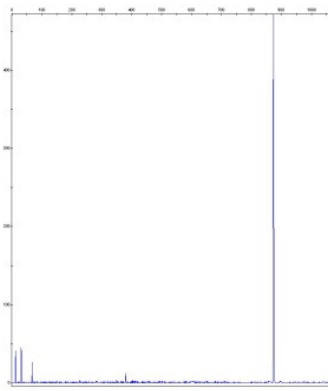

C10.1 HaeIII

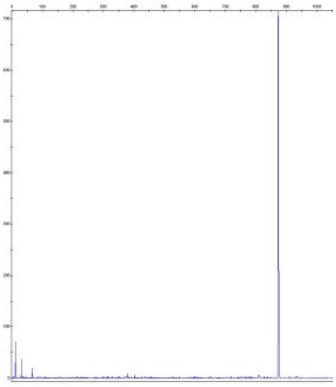

C10.4 HaeIII

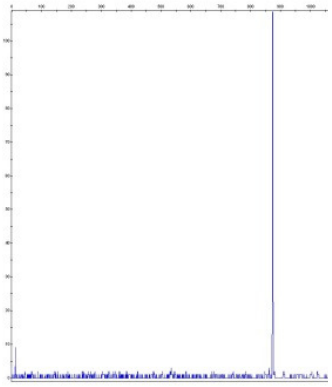

C10.2 HaeIII

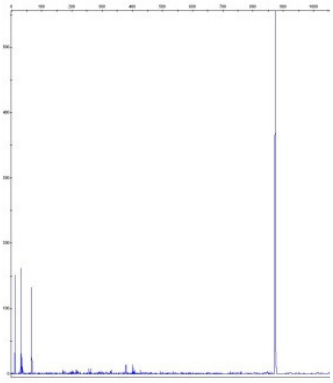

C10.5 HaeIII

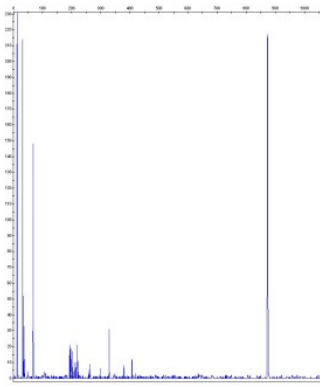

C10.3 HaeIII

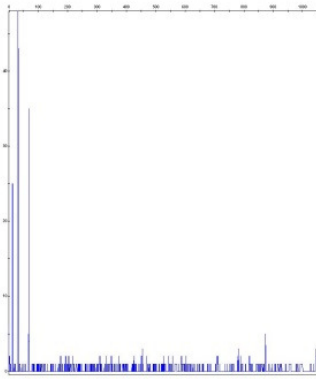

C10.6 HaeIII

Figure 77. HaeIII T-RFLP electropherograms for Site #10, samples 1-6, fall

VITA

Author: Cristine McIntyre Schucker

Place of Birth: Flagstaff, Arizona

Undergraduate Schools Attended: Arizona State University
Spokane Falls Community College
Eastern Washington University

Degrees Awarded: Associate of Arts, 2008, Spokane Falls Community College
Bachelor of Science in Biology, Minor in Chemistry, 2011,
Eastern Washington University

Honors and Awards: Cum laude, EWU, 2011
Graduate Student Fellowship, Biology, EWU, 2011 – 2013
American Water Resources Association Award, 2012
J. Herman and Jean Swartz Biotechnology Award, EWU, 2012
Outstanding Graduate Student Award, Biology, EWU, 2015

Professional Experience: Field Biologist - Pollinator Partnership;
Lincoln County, WA (2012 – 2014)

Project Manager, Wireless Communication Antenna Sites –
JM Consulting, Brookstone Telecom and Northwest Wireless
Consulting; AZ, CA, ID and WA (1996 – 2005)